A Review of Reaction Rates and Thermodynamic and Transport Properties for an 11-Species Air Model for Chemical and Thermal Nonequilibrium Calculations to 30 000 K

Roop N. Gupta
Scientific Research and Technology, Inc.
Tabb, Virginia

Jerrold M. Yos
Textron Defense Systems
Subsidiary of Textron, Inc.
Wilmington, Massachusetts

Richard A. Thompson
Langley Research Center
Hampton, Virginia

Kam-Pui Lee
Scientific Research and Technology, Inc.
Tabb, Virginia

Contents

Summary

Reaction-rate coefficients and thermodynamic and transport properties are reviewed and supplemented for an 11-species air model. These coefficients and properties can be used for analyzing flows in chemical and thermal nonequilibrium up to temperatures of 30 000 K. Such flows will likely occur around currently planned and future hypersonic vehicles. Guidelines for determining the state of the surrounding environment are provided. Curve fits are given for the various species properties for their efficient computation in flow-field codes. Approximate and more exact formulas are provided for computing the properties of partially ionized air mixtures in a high-energy environment. Limitations of the approximate mixing laws are discussed for a mixture of ionized species. An electron number-density correction for the transport properties of the charged species is given. This correction has generally been ignored in the aerospace literature.

Tabulated values of the curve-fit coefficients and computer subroutines to evaluate the various species properties using these coefficients are available from the NASA Computer Software Management and Information Center (COSMIC).

Introduction

Currently envisaged transatmospheric and aeroassist missions (refs. 1 to 4) have created a resurgence of interest in the aerothermodynamic design of hypersonic vehicles. However, the velocities and altitudes at which these proposed craft would operate are different, and sometimes more severe, than those experienced in the past. As a result, the nonequilibrium flow environment that will surround these vehicles will considerably impact the vehicle aerodynamics, thermal loads, and propulsion-system efficiency. Since such an environment is difficult to simulate in current ground-based test facilities, the design of these future vehicles will rely heavily on numeric calculations. In turn, these calculations will require a good understanding of the physical modelling required to simulate these phenomena.

Under hypersonic flight conditions, a vehicle travelling through the atmosphere will excite the air that flows around the body to very high temperatures as the kinetic energy of the vehicle is dissipated to the gas. Depending on the flight velocity, various chemical reactions will be produced behind a shock wave as shown in figure 1 (which is adapted from ref. 5) for the stagnation region of a sphere with a radius of 30.5 cm. These reactions will affect the properties of air and cause considerable deviation from those of a thermally and calorifically perfect gas. A vehicle flying through the higher reaches of the atmosphere at high velocities may also experience thermal nonequilibrium (fig. 1), since the lower density reduces the collision frequency, and the high velocity results in smaller transit times for the air molecules. Both of these processes create a delay in the equilibration of translational, rotational, vibrational, and electronic modes of the thermal energy. Under these conditions, the modelling of the air chemistry requires a multitemperature approach in contrast to classical single-temperature formulations.

Four regions (I to IV) are delineated in figure 1. These regions show when the various chemical activities are initiated at a given altitude and velocity. The initiation of chemical and thermal nonequilibrium processes for different velocity and altitude conditions is similarly depicted through regions A, B, and C. This figure clearly shows that the set of chemical reactions and thermodynamic and transport properties would change continuously for a given flight trajectory. For example, in regions A and B (i.e., before initiation of thermal nonequilibrium), the specific heat at constant pressure C_p would change as follows:

C_p = Constant in region I before the excitation of vibrational energy mode

$C_p = C_p(T)$ in region I after the excitation of vibrational energy mode and
before the dissociation of oxygen

$C_p = C_p(C_i, T)$ after the dissociation of oxygen

Similarly, the equation of state changes along the flight trajectory as the thermal equilibrium and thermal nonequilibrium regions (ref. 6) are traversed:

$$p = \rho \frac{R_{\text{univ}}}{\overline{M}} T \quad \text{(in regions A and B)}$$

$$p = \rho \frac{R_{\text{univ}}}{\overline{M}} T_{\text{tr}} \quad \text{(in region C)}$$

where T_{tr} is the translational temperature in an environment of thermal nonequilibrium.

In numerical simulations, the thermodynamic and transport properties and reaction-rate coefficients (in the case of finite-rate chemistry) are usually required. It is obvious from the previous discussion that these properties and the equation of state should be evaluated carefully when chemical and thermal nonequilibrium conditions exist in the flow field around a hypersonic vehicle. Under chemical and thermal equilibrium conditions, the transport and thermodynamic properties of high-temperature air and its components are well documented in the literature (refs. 7 to 12). However, for flows with finite-rate chemistry, the individual species properties and appropriate mixing laws that are required are not as well established. For example, in a partially ionized gas mixture, the conventional mixing laws (refs. 13 and 14) developed for nonionized mixtures cannot be extended to higher temperatures without considerable error (ref. 15).

The purpose of this report is to review the thermodynamic and transport properties and the reaction-rate coefficients of the most important reactions for the 11 constituent species of air (N, O, N_2, O_2, NO, N^+, O^+, N_2^+, O_2^+, NO^+, e^-) for temperatures up to 30 000 K. Those species properties that are not available in the literature for this 11-species model are provided, and curve fits are obtained for all properties to permit their efficient computation in flow-field codes. Tabulated values of the curve-fit coefficients and computer subroutines to evaluate the various species properties using these coefficients are provided in reference 16. These values and codes may be obtained for a fee from:

COSMIC
Computer Services Annex
University of Georgia
Athens, GA 30602
(404) 542-3265

Request the code by the designation LAR 14447. This code is written in FORTRAN 77 for use on computer with a FORTRAN compiler.

Approximate and more exact mixing laws for the various species properties are also provided for partially ionized gas mixtures. The limitations of the approximate mixing laws are pointed out, especially for a mixture of ionized species. An electron number-density correction for the transport properties of the ionized species, which has been generally neglected in the aerospace literature, is provided. Sources of the input data used in the calculation of various flow-field properties are identified. Appropriate formulas are provided for using these properties in computations of flows with thermal nonequilibrium.

Symbols

$A_{B_{ij}^*}, B_{B_{ij}^*}, C_{B_{ij}^*}$	curve-fit coefficients for collision cross section ratio B_{ij}^* (eq. (47))
$A_{b,r}$	coefficient in modified Arrhenius form of backward reaction-rate constant (eq. (3b))

$A_{\overline{D}_{ij}}, B_{\overline{D}_{ij}}, C_{\overline{D}_{ij}}, D_{\overline{D}_{ij}}$	curve-fit coefficients for diffusion coefficient $\overline{D}_{ij}$ (eq. (42c))
$A_{f,r}$	coefficient in modified Arrhenius form of forward reaction-rate constant (eq. (3a))
A_{ij}	matrix elements of first Chapman-Enskog formula
A_{ij}^*	ratio of collision cross sections, $\overline{\Omega}_{ij}^{(2,2)} \big/ \overline{\Omega}_{ij}^{(1,1)}$
$A_{K_{eq,r}}, B_{K_{eq,r}}, C_{K_{eq,r}},$ $D_{K_{eq,r}}, E_{K_{eq,r}}, F_{K_{eq,r}}$	curve-fit coefficients for equilibrium constants $K_{eq,r}$ (eqs. (5c) and (5d))
$A_{K_{f,i}}, B_{K_{f,i}}, C_{K_{f,i}},$ $D_{K_{f,i}}, E_{K_{f,i}}$	curve-fit coefficients for frozen thermal conductivity of species i, $K_{f,i}$ (eq. (26))
A_n	coefficients of polynomial curve fits for thermodynamic properties, $n = 1, 2, \ldots, 7$ (eqs. (10a) to (10c))
$A_{\mu_i}, B_{\mu_i}, C_{\mu_i}$	curve-fit coefficients for viscosity of species i, μ_i (eq. (25))
$A_{\overline{\Omega}_{ij}^{(1,1)}}, B_{\overline{\Omega}_{ij}^{(1,1)}}, C_{\overline{\Omega}_{ij}^{(1,1)}}, D_{\overline{\Omega}_{ij}^{(1,1)}}$	curve-fit coefficients for collision cross sections $\overline{\Omega}_{ij}^{(1,1)}$ (eq. (45))
$A_{\overline{\Omega}_{ij}^{(2,2)}}, B_{\overline{\Omega}_{ij}^{(2,2)}}, C_{\overline{\Omega}_{ij}^{(2,2)}}, D_{\overline{\Omega}_{ij}^{(2,2)}}$	curve-fit coefficients for collision cross sections $\overline{\Omega}_{ij}^{(2,2)}$ (eq. (46))
a_0	first Bohr radius, 0.52918×10^{-8} cm
$B_{b,r}$	temperature exponent for backward reaction-rate constant
$B_{f,r}$	temperature exponent for forward reaction-rate constant
B_{ij}^*	ratio of collision cross sections, $(5\overline{\Omega}_{ij}^{(1,2)} - 4\overline{\Omega}_{ij}^{(1,3)}) \big/ \overline{\Omega}_{ij}^{(1,1)}$
Δb_{il}	mass diffusion parameter defined by equation (A10)
C_p	specific heat at constant pressure, $\left(\frac{\partial h}{\partial T}\right)_p$, cal/g-mole-K
C_{p_r}	reactive specific heat at constant pressure, $\left(\sum\limits_{i=1}^{NS} h_i \frac{\partial C_i}{\partial T}\right)_p$, cal/g-mole-K
C_{p_f}	frozen specific heat at constant pressure, $C_{p_f} = \sum\limits_{i=1}^{NS} C_i C_{p,i} \left(\frac{\partial h}{\partial T} - \sum\limits_{i=1}^{NS} h_i \frac{\partial C_i}{\partial T}\right)_p$, cal/g-mole-K
$C_{p,i}$	specific heat at constant pressure of species i, $\left(\frac{\partial h_i}{\partial T}\right)_p$, cal/g-mole-K
$(C_{p,i})_{el}$	electronic component of $C_{p,i}$, cal/g-mole-K
$(C_{p,i})_{int}$	internal component of $C_{p,i}$, cal/g-mole-K
$(C_{p,i})_{rot}$	rotational component of $C_{p,i}$, cal/g-mole-K

$(C_{p,i})_{tr}$	translational component of $C_{p,i}$, cal/g-mole-K
$(C_{p,i})_{vib}$	vibrational component of $C_{p,i}$, cal/g-mole-K
C_v	specific heat at constant volume, $\left(\frac{\partial e}{\partial T}\right)_v$, cal/g-mole-K
$C_{v,i}$	specific heat at constant volume of species i, $\left(\frac{\partial e_i}{\partial T}\right)_v$, cal/g-mole-K
$(C_{v,i})_{int}$	internal component of $C_{v,i}$, cal/g-mole-K
$(C_{v,i})_{tr}$	translational component of $C_{v,i}$, cal/g-mole-K
D_{ii}	coefficient of self diffusion, cm^2/sec
D_{ij}	binary diffusion coefficient, cm^2/sec
$\overline{D}_{ij}$	$= pD_{ij}$, cm^2-atm/sec
$\tilde{D}_{ij}$	multicomponent diffusion coefficient, cm^2/sec
$E_{b,r}$	activation energy for backward reaction r, erg/g-mole
$E_{f,r}$	activation energy for forward reaction r, erg/g-mole
e	internal energy of mixture, cal/g-mole
e_i	internal energy of species i, cal/g-mole
F_i	free energy of species i, cal/g-mole
F_i^0	free energy of species i at the standard state of 1 atm pressure (1 atm = 101.3 kPa), cal/g-mole
h	enthalpy of mixture $\sum\limits_{i=1}^{NS} C_i h_i$, cal/g-mole
$\overline{h}$	Planck constant, 6.6261×10^{-27} erg-sec
h_i	enthalpy of species i, cal/g-mole
$\hat{h}_i$	specific-heat function for species i, cal/g-mole-K
$(\Delta h_i^f)_{T_{ref}}$	standard heat of formation of species i at temperature T_{ref}, cal/g-mole
J	conversion factor from calories to ergs, 4.184×10^7 ergs/calorie
J_i^k	kth component of diffusion mass flux of species i, $k = 1$ to 3, g/cm^2-sec
K	total effective thermal conductivity of mixture in thermodynamic equilibrium, $K_f + K_r$, cal/cm-sec-K
K_e	thermal conductivity of electrons, cal/cm-sec-K
K_{el}	component of thermal conductivity of mixture due to electron excitation, cal/cm-sec-K
$K_{eq,r}$	equilibrium constant for reaction r, $k_{f,r}/k_{b,r}$
K_f	frozen thermal conductivity of mixture in thermo-dynamic equilibrium, $K_{tr} + K_{int}$, cal/cm-sec-K

4

$K_{f,i}$	frozen thermal conductivity of species i in thermodynamic equilibrium, $K_{\text{tr},i} + K_{\text{int},i}$, cal/cm-sec-K
K_{int}	internal component of frozen thermal conductivity of a mixture in thermodynamic equilibrium, $K_{\text{rot}} + K_{\text{vib}} + K_{\text{el}}$, cal/cm-sec-K
$K_{\text{int},i}$	internal component of frozen thermal conductivity of species i in thermodynamic equilibrium, cal/cm-sec-K
K_r	reaction component of thermal conductivity of a mixture (eqs. (A19) and (A20)), cal/cm-sec-K
$K_{\text{tr}}, K_{\text{tr}}^{(1)}$	translational thermal conductivity of mixture from first Chapman-Enskog approximation, cal/cm-sec-K
K_{tr}^*	translational thermal conductivity of mixture without contributions caused by electron-heavy particle collisions, $K_{\text{tr}} - K_e$, cal/cm-sec-K
$K_{\text{tr},i}$	translational component of thermal conductivity of species i, cal/cm-sec-K
K_{vib}	vibrational component of thermal conductivity of mixture, cal/cm-sec-K
k	Boltzmann's constant, 1.38066×10^{-16} erg/K
$k_{b,r}$	backward reaction-rate coefficient for reaction r, $\text{cm}^3/\text{mole-sec}$ or $\text{cm}^6/\text{mole}^2\text{-sec}$
$k_{f,r}$	forward reaction-rate coefficient for reaction r, $\text{cm}^3/\text{mole-sec}$
Le_i	Lewis number, defined by equation (A9)
$Le_{f,ij}$	frozen binary Lewis number, $\rho C_{p_f} D_{ij}/K_f$
Le_{ij}	total binary Lewis number, $\rho C_p D_{ij}/K$
$L_{f,ij}$	multicomponent Lewis number, $\rho C_{p_f} \widetilde{D}_{ij}/K_f$
$\overline{M}$	molecular weight of mixture, g/g-mole
M_i	molecular weight of species i, g/g-mole
m_i	mass of particle i, g
N_A	Avogadro's number, 6.0221×10^{23} molecules/g-mole
N_{Pr}	total Prandtl number, $C_p \mu/K$
$N_{Pr,f}$	frozen Prandtl number, $C_{p_f} \mu/K_f$
n	number density, particles/cm^3
n_i	number density of species i, particles/cm^3
p	pressure, atm
p_e	electron pressure, atm
p_{em}	limiting value of electron pressure, atm

$Q_{\text{tr},i}$	translational partition function per unit volume, $1/\text{cm}^3$
q^k	kth component of overall heat-flux vector, $k = 1$ to 3, $\text{cal}/\text{cm}^2\text{-sec}$
R_{univ}	universal gas constant, $1.987 \, \text{cal}/\text{g-mole-K}$
r_a	radius of electron orbit from solution of Schrödinger equation, cm
r_c	Coulomb cutoff (or Debye shielding) radius, cm
r_d	density cutoff radius, cm
S_i	entropy of species i at temperature T, $\text{cal}/\text{g-mole-K}$
T	temperature under thermodynamic equilibrium, K
$T_{D_{b,r}}$	characteristic reaction temperature for backward reaction r, $E_{b,r}/k$, K
$T_{D_{f,r}}$	characteristic reaction temperature for forward reaction r, $E_{f,r}/k$, K
T_e	electron temperature, K
T_{el}	electronic excitation temperature, K
T_{ref}	reference temperature, 298.15 K
T_{rot}	rotational temperature, K
T_{tr}	translational temperature, K
T_{ve}	vibrational-electron-electronic excitation temperature, K
T_{vib}	vibrational temperature, K
t	time, sec
u_i	mean molecular velocity of species i, cm/sec
V_i^k	kth component of diffusion velocity of species i, $k = 1$ to 3, cm/sec
$\dot{w}_i$	mass rate of formation of species i, $\text{g}/\text{cm}^3\text{-sec}$
X_i	concentration of species i, moles/volume
x_i	mole fraction of species i
x^k	kth component of general orthogonal coordinate system, $k = 1$ to 3, cm
$Z_{(j-\text{NS}),i}$	constants (used in eq. (2c)) given in table I
$\alpha_{i,r}$	stoichiometric coefficient for reactant i in reaction r
$\beta_{i,r}$	stoichiometric coefficient for product i in reaction r
γ	ratio of specific heats, C_p/C_v
γ_j	mole mass ratio of species j, X_j/ρ
$\Delta_{ij}^{(1)}$	defined by equation (34), cm-sec

6

$\Delta_{ij}^{(2)}$	defined by equation (35), cm-sec
λ_i	mean-free path of pure species i, cm
$\overline{\lambda}_i$	modified mean-free path of species i in a mixture, cm
λ_i^*	mean-free path of species i in a mixture, cm
$\mu^{(1)}, \mu$	viscosity of mixture from first Chapman-Enskog approximation, g/cm-sec
μ_i	viscosity of species i, g/cm-sec
ρ	density of mixture, g/cm^3
ρ_i	density of species i, g/cm^3
$\overline{\Omega}_{ij}^{(1,1)}$	average collision cross section (used for diffusion, viscosity, translational, internal, and reaction components of thermal conductivity) for collisions between species i and j, Å^2 (1 Å= 10^{-8} cm)
$\overline{\Omega}_{ij}^{(2,2)}$	average collision cross section (used for viscosity and translational component of thermal conductivity) for collisions between species i and j, Å^2
$\overline{\Omega}_{ij}^{(1,2)}, \overline{\Omega}_{ij}^{(1,3)}$	average collision cross sections (used for translational component of thermal conductivity) for collisions between species i and j, Å^2

Subscripts:

b	backward reaction
e	electron
el	electronic excitation
i	species i
j	species j
l	species l
p	constant pressure
r	reaction
rot	rotational energy mode
tr	translational energy mode
ve	vibrational-electron-electronic energy mode
ν	$\equiv$ NS, total number of species

Abbreviations:

ASTV	Aeroassisted Space Transfer Vehicle
mol.	molecules
NASP	National Aero-Space Plane
NATA	Nonequilibrium Arc Tunnel Analysis

NIR	total number of independent reactions
NJ	sum of reacting species (NS) plus number of catalytic bodies
NR	total number of reactions
NS	total number of species

Chemical Kinetic Model and Reaction Rates

Thermal Equilibrium

When chemical reactions proceed at a finite rate, the rate-of-production terms appear in the energy equation, when formulated in terms of temperature, and in the species continuity equations (refs. 17 to 19). For a multicomponent gas with NS reacting chemical species and NR chemical reactions, the stoichiometric relations for the overall change from reactants to products are

$$\sum_{i=1}^{NJ} \alpha_{i,r} X_i \underset{k_{b,r}}{\overset{k_{f,r}}{\rightleftarrows}} \sum_{i=1}^{NJ} \beta_{i,r} X_i \tag{1}$$

where $r = 1, 2, ..., NR$ and NJ is equal to the sum of the reacting species (NS) plus the number of catalytic bodies. The quantities $\alpha_{i,r}$ and $\beta_{i,r}$ are the stoichiometric coefficients for reactants and products, respectively, and $k_{f,r}$ and $k_{b,r}$ are the forward and backward rate constants. The quantities X_i denote the concentrations of the chemical species and catalytic bodies in moles per unit volume. The catalytic bodies (NJ – NS) may be chemical species or linear combinations of species that do not undergo a chemical change during the reaction.

The net mass rate of production of the ith species per unit volume resulting from all the reactions NR may be obtained (ref. 18) from

$$\dot{w}_i = M_i \sum_{r=1}^{NR} \left(\frac{dX_i}{dt}\right)_r = \sum_{r=1}^{NR} \left(\frac{d\rho_i}{dt}\right)_r \tag{2a}$$

or

$$\dot{w}_i = M_i \sum_{r=1}^{NR} (\beta_{i,r} - \alpha_{i,r})(R_{f,r} - R_{b,r}) \tag{2b}$$

where

$$R_{f,r} = k_{f,r} \prod_{j=1}^{NJ} (\gamma_j \rho)^{\alpha_{j,r}} \tag{2c}$$

$$R_{b,r} = k_{b,r} \prod_{j=1}^{NJ} (\gamma_j \rho)^{\beta_{j,r}} \tag{2d}$$

Here, the mole-mass ratio γ_j (also known as the mole number) is defined as

$$\gamma_j = \left\{ \begin{array}{ll} \frac{X_j}{\rho} = \frac{C_j}{M_j} & (j = 1, 2, ..., NS) \\ \sum_{i=1}^{NS} Z_{(j-NS),i} \, \gamma_i & (j = NS+1, ..., NJ) \end{array} \right\} \tag{2e}$$

The constants $Z_{(j-\text{NS}),i}$ are functions of the catalytic efficiencies of the NS species and are determined from the linear dependence of the catalytic bodies upon the NS species. Values of these constants for the 11-species air model are given in table I.

The reaction rates in equation (1) or equations (2c) and (2d) are expressed in the modified Arrhenius form as

$$k_{f,r} = A_{f,r}T^{B_{f,r}}\exp(-T_{D_{f,r}}/T), \quad \frac{1}{\text{sec}}\left(\frac{\text{mole}}{\text{cm}^3}\right)^{-\alpha_r} \tag{3a}$$

$$k_{b,r} = A_{b,r}T^{B_{b,r}}\exp(-T_{D_{b,r}}/T), \quad \frac{1}{\text{sec}}\left(\frac{\text{mole}}{\text{cm}^3}\right)^{-\beta_r} \tag{3b}$$

where

$$\alpha_r = \sum_{i=1}^{\text{NJ}} \alpha_{i,r} - 1 \tag{4a}$$

$$\beta_r = \sum_{i=1}^{\text{NJ}} \beta_{i,r} - 1 \tag{4b}$$

and where $T_{D_{f,r}}$ and $T_{D_{b,r}}$ are the characteristic reaction temperatures for the forward and backward reactions, respectively. Values for the reaction rates $k_{f,r}$ and $k_{b,r}$ are tabulated in table II for the 11-species air model. For a specified temperature, density, and species composition, equations (2) to (4) can be used to obtain the production rate of a species i in a multicomponent gas by employing the catalytic body efficiencies and reaction rates from tables I and II. The first seven reactions and reaction rates in table II are taken from reference 20 and were employed in reference 17 for the 7-species air model (N, O, N_2, O_2, NO, NO^+, e^-). Reaction rates for reactions 8 to 20 of table II are taken from reference 21. Some of these reactions have been regrouped here (and in ref. 22) through the use of third bodies M_1 to M_4, which is similar to the approach used in reference 17.

The reaction rates given in table II are appropriate for flow velocities of about 8 km/sec (i.e., up to the Shuttle-type reentry velocities). For higher flow velocities, the backward reaction rates can be obtained from the forward reaction rates[1] by using the following relation:

$$k_{b,r} = \frac{k_{f,r}(T)}{K_{\text{eq},r}(T)} \tag{5a}$$

The equilibrium constants $K_{\text{eq},r}$ have been obtained by using the atomic partition functions and the molecular partition functions provided in reference 23. The electronic partition function for the atomic species and internal partition functions of molecular species are tabulated in reference 23. The internal partition functions of the molecular species were obtained using existing data on molecular constants augmented by solving the Schrödinger equation. The translational component required for obtaining the total partition function (which is used to compute the equilibrium constant) is obtained from

$$Q_{\text{tr},i} = (2\pi m_i kT/\bar{h}^2)^{3/2} \tag{5b}$$

where $Q_{\text{tr},i}$ is the translational partition function per unit volume and $\bar{h}$ is the Planck constant.

The computed values of $K_{\text{eq},r}$ have been curve-fitted here by the least-squares curve-fit method as a function of temperature using the expression

$$K_{\text{eq},r} = \left\{\exp\left(F_{K_{\text{eq},r}}\right)\right\}(10^4/T)^{\left(A_{K_{\text{eq},r}}Z^4 + B_{K_{\text{eq},r}}Z^3 + C_{K_{\text{eq},r}}Z^2 + D_{K_{\text{eq},r}}Z + E_{K_{\text{eq},r}}\right)} \tag{5c}$$

or,

$$\ln(K_{\text{eq},r}) = A_{K_{\text{eq},r}}Z^5 + B_{K_{\text{eq},r}}Z^4 + C_{K_{\text{eq},r}}Z^3 + D_{K_{\text{eq},r}}Z^2 + E_{K_{\text{eq},r}}Z + F_{K_{\text{eq},r}} \tag{5d}$$

---

[1] The high-temperature data for the forward reaction rates are not well-defined.

where

$$Z = \ln \left(10^4/T\right) \tag{5e}$$

The curve-fit coefficients in equations (5c) and (5d) are given in table III. Caution should be exercised in evaluating the equilibrium constant $K_{\mathrm{eq},r}$ from the coefficients given in table III. All the six significant digits for the coefficients should be used. Equation (5d) is preferred to equation (5c) in computing the equilibrium constant for reasons of accuracy, because the exponent of the exponential term in equation (5c) is a large number. Since the electronic partition functions of atomic species (tabulated in ref. 23) are significantly affected at high temperatures and low densities, the curve-fit coefficients are given for 6 different values of the total number density. These number densities cover the range of practical interest for aerospace applications. Figure 2(a) shows the variation of the equilibrium constant with temperature for different values of the total number density. The equilibrium constant clearly exhibits a number-density dependence at very high temperatures and low total number densities. Figure 2(b) gives a comparison of the present curve fit with the exact values calculated from the partition functions. Values obtained from Park's curve fits (ref. 23) and from table II by employing the relation $K_{\mathrm{eq},r} = k_{f,r}/k_{b,r}$ are also shown. Park's five curve-fit coefficients were obtained by using five discrete temperatures (2000, 4000, 6000, 8000, and 10 000 K); thus, they are in disagreement with the exact values and the present curve fits at the higher temperatures. Comparison of the exact values with those obtained from table II also gives an indication of the temperature range beyond which the backward reaction rates of table II should not be employed.

The equilibrium constant $K_{\mathrm{eq},r}$ is usually given as a function of temperature only. Figure 2(a) and table III indicate, however, that under low-density and high-temperature conditions $K_{\mathrm{eq},r}$ is also a function of the total number density n. This dependence arises because the electronic partition functions of nitrogen and oxygen atoms and ions are dependent upon the total number density under those conditions. In reality, there is a finite (as opposed to infinite) number of electronic states that contribute to the electronic partition function. This finite number of states is obtained because (a) the orbits of electrons cannot extend beyond the distance to the nearest neighboring particle (a phenomenon known as the density cutoff) and (b) the Coulomb field is truncated due to the perturbation of the field by the electrons and ions in the neighborhood (a phenomenon known as the charge shielding). On the average, the distance to the nearest particle is given in centimeters as

$$r_d = 1/n^{1/3} \tag{5f}$$

where n is the total number density in particles/cm^3 and r_d is the radius of an electron orbit as the result of density cutoff. In the hypersonic flight regime of interest, this radius prevails over the Coulomb cutoff radius r_c, (or Debye shielding) defined in centimeters by

$$r_c = 6.90 \left(\frac{T}{n_e}\right)^{1/2} \tag{5g}$$

Further, the quantum theory gives the allowable radius r_a of an electron orbit as follows:

$$r_a = a_0 N^2 \tag{5h}$$

where $a_0 = 0.52918 \times 10^{-8}$ cm and is known as the first Bohr radius, and N (which is an eigenvalue in the solution of the Schrödinger equation) is called the principal quantum number. Equating the smaller of the two radii given by equations (5f) and (5g) with equation (5h) yields the cutoff quantum number N_{max} as

$$N_{\mathrm{max}} = \sqrt{\frac{r_c}{a_0}} \quad \text{or} \quad \sqrt{\frac{r_d}{a_0}} \tag{5i}$$

Only electronic states with principal quantum numbers up through N_{max} contribute to the electronic partition function. Since the contribution from the highly excited states with quantum numbers near

N_{max} is proportional to $N_{max}^3 \exp(-E/kT)$, where E is the ionization energy, these highly excited states dominate the overall partition function at sufficiently high temperatures or low total number densities, and the partition function then becomes strongly dependent on number density (eqs. (5f), (5g), and (5i)). Under these conditions, most of the atoms present in the gas are in the highly excited electronic states near N_{max} rather than in the ground state. Since these highly excited atoms have very different properties than ground-state atoms, the reaction-rate data given in table II, which were determined for primarily ground-state atoms, are no longer appropriate for the low-density, high-temperature conditions at which the number-density dependence of the partition function becomes significant. Therefore, more general models, which account explicitly for the behavior of the excited atoms, are required. This regime lies outside the range of primary interest for aerospace applications, however, and is not covered in this study.

Park (ref. 24) has recently presented a new set of reaction rates for use in computing highly ionized flow in the hypersonic environment. In particular, the power of the preexponential temperature of the rate coefficients for the associative ionization and dissociative recombination reactions (reactions 7, 10, and 13 in table II) is assigned a value of zero at temperatures greater than 6000 K to keep the rate coefficients from becoming unrealistically large at very high temperatures, for which no experimental data are available. Since the power of the preexponential temperature of the rate coefficients is negative and zero for reactions 10 and 13, respectively, in table II, Park's suggestion is already implemented in the reaction rates for these reactions. The preexponential power of the rate coefficient for reaction 7 may need to be reexamined when the temperatures become excessively large. Further, for extremely high temperatures, such as those encountered with earth reentry velocities greater than 12 km/sec, much slower reaction rates have been recommended (refs. 25 and 26) for electron-impact ionization reactions 8 and 9 given in table II. Also, the reaction rates given in reactions 8 and 9 in table II are from expansion flow data, which tend to be lower than data obtained under compressive flow conditions.

Thermal Nonequilibrium

The reaction rates given in table II were originally used by Blottner (ref. 17) and Dunn and Kang (ref. 21) in the context of a single temperature assuming thermal equilibrium. Park's (ref. 25) guidelines (in the context of his two-temperature model) may be used for defining the rate-controlling temperature in dissociation and the electron-impact ionization reactions under thermal nonequilibrium conditions. These guidelines were used in reference 27, for example.

Based on the preferential dissociation concept, Park has suggested the use of a temperature weighted with the vibrational temperature to characterize dissociation reactions (ref. 25). The reaction rates in Park's model are assumed to be dictated by the geometric average temperature

$$T_{av} = \sqrt{T_{tr}T_{vib}} \tag{6a}$$

and the dissociation reaction rates are given by

$$k_{f,r} = A_{f,r}T_{av}^{B_{f,r}} \exp(-T_{D_{f,r}}/T_{av}) \tag{6b}$$

The recombination (or backward) reaction rate, however, depends only on the temperature of the impacting particles and may, therefore, be evaluated from

$$k_{b,r} = k_{f,r}(T_{tr})/K_{eq,r}(T_{tr}) \tag{6c}$$

Treanor and Marrone (refs. 28 and 29) suggested a more rational (but slightly more difficult) way than Park's method to account for the effect of vibrational relaxation on dissociative reactions with the preferential dissociation concept. They suggested the use of a vibrational coupling factor (refs. 27 to 29) with the dissociation reaction rates obtained under the assumption of thermal equilibrium.

Recent work of Jaffe (ref. 30), based on collision theory and using methods of statistical mechanics, yielded no evidence of preferential weighting to any particular energy mode in obtaining the total energy available in a collision, whether it is an elastic, inelastic, or reactive encounter. Jaffe found that the multitemperature effects on the reaction rates were small for dissociation. These findings were supported by those of Moss et al. (ref. 31), who carried out flow-field analyses with the Direct Simulation Monte Carlo (DSMC) approach. Thus, a weaker dependence of $k_{f,r}$ on T_{vib} (such as the one suggested by Sharma et al. (ref. 32) as $T_{\text{av}} = T_{\text{tr}}^{0.6} T_{\text{vib}}^{0.4}$) might be more realistic, especially for highly energetic flows.

It is obvious that the multitemperature kinetic models for high-energy flows based on both preferential and nonpreferential dissociation assumptions employ a considerable degree of empiricism. They exemplify the degree of uncertainty that exists in modelling the multitemperature kinetics. Quantum mechanical studies of the type in reference 30, supplemented by nonobtrusive laser diagnostic studies, would be desirable for establishing these models on a sounder basis.

Species Thermodynamic Properties and Mixture Formulas

Thermal Equilibrium

Thermodynamic properties (i.e., $C_{p,i}$ and h_i) are required for each species considered in a finite-rate flow-field calculation. For calculations with chemical equilibrium, the free energies F_i are also required. Since the multicomponent gas mixtures are considered to be mixtures of thermally perfect gases, the thermodynamic properties for each species are calculated by using the local static temperature. Then, properties for the gas mixture are determined in terms of the individual species properties through the following relations:

$$h = \sum_{i=1}^{\text{NS}} C_i h_i \tag{7a}$$

where

$$h_i = \int_{T_{\text{ref}}}^{T} C_{p,i} \; dT + (\Delta h_i^f)_{T_{\text{ref}}} \tag{7b}$$

and

$$C_{p_f} = \sum_{i=1}^{\text{NS}} C_i C_{p,i} \tag{8a}$$

where

$$C_{p,i} = \left(\frac{\partial h_i}{\partial T} \right)_p \tag{8b}$$

The mixture C_{p_f} as defined by equation (8a) is the "frozen" specific heat. This definition does not account for species production or conversion due to chemical reactions. Frozen specific heat is commonly used in defining the Prandtl and Lewis numbers[2] for a mixture and is related to the mixture enthalpy h through the relation

$$C_{p_f} = \left(\frac{\partial h}{\partial T} - \sum_{i=1}^{\text{NS}} h_i \frac{\partial C_i}{\partial T} \right)_p = \sum_{i=1}^{\text{NS}} C_i C_{p,i} \tag{9}$$

Expressions for $C_{p,i}$ using the partition-function approach were obtained in reference 33, whereas a virial coefficient method was used in references 34 and 35. If the effects of nonrigidity of the rotor

---

[2] See appendix A for various definitions.

and anharmonicity of the oscillator are included in these two methods, the two formulations are equivalent (see section 3.1 of ref. 36) and can be used interchangeably. Using the virial formulation, Browne (refs. 34 and 35) obtained the thermodynamic properties as corrections to those of the monatomic gas in terms of the first and second virial coefficients and their temperature derivatives.

Reference 33 provides curve fits for $C_{p,i}$ and h_i, whereas references 34 and 35 provide tabulations of these data. Since the use of curve fits reduces the expense of computing the original functional relations, the tabulated thermodynamic properties of references 34 and 35 have been curve-fitted here as a function of temperature for the temperature range of $300 \text{ K} \leq T \leq 30\,000 \text{ K}$. The following polynomial equations are employed for these curve fits:

Specific heat:

$$\frac{C_{p,i}}{R_{\text{univ}}} = A_1 + A_2 T + A_3 T^2 + A_4 T^3 + A_5 T^4 \tag{10a}$$

Specific enthalpy:

$$\frac{h_i}{R_{\text{univ}} T} = A_1 + \frac{A_2 T}{2} + \frac{A_3 T^2}{3} + \frac{A_4 T^3}{4} + \frac{A_5 T^4}{5} + \frac{A_6}{T} \tag{10b}$$

For equilibrium calculations, the following curve fit for the free energies F_i may be used:

$$\frac{F_i^0}{R_{\text{univ}} T} = A_1[1 - \ln(T)] - \frac{A_2 T}{2} - \frac{A_3 T^2}{6} - \frac{A_4 T^3}{12} - \frac{A_5 T^4}{20} + \frac{A_6}{T} - A_7 \tag{10c}$$

where F_i^0 is the free energy of species i at a pressure of 1 atm (standard state). The specific-heat data are easily curve-fitted to the polynomial form of equation (10a). Other polynomial forms are based on the following thermodynamic relations at constant pressure:

$$dh_i = C_{p_i} \, dT \tag{11a}$$

$$dS_i = C_{p_i} \, \frac{dT}{T} \tag{11b}$$

$$dh_i = T \, dS_i \tag{11c}$$

and

$$dF_i = -S_i \, dT \tag{11d}$$

where F_i is the free energy and S_i is the entropy of species i at temperature T.

The polynomial coefficients have been evaluated by using the least-squares curve-fit technique. In particular, the following polynomial for the specific enthalpy has been curve-fitted to the tabulated values of references 34 and 35:

$$\frac{h_i - A_6 R_{\text{univ}}}{R_{\text{univ}} T} = \overline{A}_1 + \overline{A}_2 T + \overline{A}_3 T^2 + \overline{A}_4 T^3 + \overline{A}_5 T^4 \tag{12a}$$

Constants A_1 to A_5 in equations (10a) to (10c) are then obtained from

$$A_n = n\overline{A}_n \qquad\qquad (n = 1, 2, 3, 4, 5) \tag{12b}$$

The constant A_6 in equations (10b) and (10c) is computed separately. This constant is related to the heat of formation through the relation

$$A_6 R_{\text{univ}} = (h_i)_{T=0} = (\Delta h_i^f)_{T_{\text{ref}}} - [(h_i)_{T_{\text{ref}}} - (h_i)_{T=0}] \tag{12c}$$

In equation (12c), $[(h_i)_{T_{\text{ref}}} - (h_i)_{T=0}]$ is available from the tabulated data to be fitted. Sources giving tabulated values of specific enthalpy and free energy generally use 0 K as the reference temperature.

To transform this reference temperature to the reference of 298.15 K employed here, it is necessary to know the heat of reaction at the new reference. Appendix B gives the method used for calculating $(\Delta h_i^f)_{T=298.15}$.

It is sometimes useful to define a specific-heat function $\hat{h}_i$ such that

$$\hat{h}_i = \frac{h_i - (\Delta h_i^f)_{T_{\text{ref}}}}{T} \tag{12d}$$

This relation may be used to obtain T from $\hat{h}_i$ in an iterative manner. Equation (12d) may be expressed in a polynomial form by using equations (12a) and (12c) as follows:

$$\hat{h}_i = (\overline{A}_1 + \overline{A}_2 T + \overline{A}_3 T^2 + \overline{A}_4 T^3 + \overline{A}_5 T^4) R_{\text{univ}} - \frac{[(h_i)_{T_{\text{ref}}} - (h_i)_{T=0}]}{T} \tag{12e}$$

or, with the approximation $\int_0^{T_{\text{ref}}} C_{p,i}\, dT \approx C_{p,i} T_{\text{ref}}$,

$$\hat{h}_i = (\overline{A}_1 + \overline{A}_2 T + \overline{A}_3 T^2 + \overline{A}_4 T^3 + \overline{A}_5 T^4) R_{\text{univ}} - \frac{C_{p,i} T_{\text{ref}}}{T} \tag{12f}$$

The constant A_7 has been obtained by subtracting the remaining terms of the free-energy polynomial (eq. (10c)), evaluated with the other known constants, from the tabulated free-energy data as follows:

$$A_7 = A_1[1 - \ln(T)] - \frac{A_2}{2}T - \frac{A_3 T^2}{6} - \frac{A_4 T^3}{12} - \frac{A_5 T^4}{20} - \left[\frac{F_i^0 - (h_i)_{T=0}}{R_{\text{univ}} T} \right] \tag{13}$$

Table IV is a listing of the polynomial constants (A_1 to A_7) for the 11-species air model. The polynomial coefficients have been obtained for five temperature ranges between 300 and 30 000 K. To assure a smooth variation of thermodynamic properties over the entire temperature range, values of A_1 to A_7 should be linearly averaged across the curve-fit boundaries (i.e., $800 < T < 1200, 5500 < T < 6500, 14\,500 < T < 15\,500$, and $24\,500 < T < 25\,500$), because the curves are not continuous at the boundaries. A sample subroutine that evaluates the polynomial curve fits and performs the linear averaging is presented in appendix C. This routine may be easily modified to suit the user's requirements.

Temperature T in equations (10) to (12) is in kelvins. With the universal gas constant in cal/g-mole-K, the specific heat and enthalpies have the units of cal/g-mole-K and cal/g-mole, respectively.

Figure 3 is a comparison of the values of specific heat obtained from the polynomial curve fit (eqs. (10)) with the data of Browne (ref. 35). Values provided by Hansen (ref. 37) are also included for comparison. Hansen's values begin to deviate from those of references 33 and 35 beyond 4000 K for O_2 (fig. 3(a)), beyond 8000 K for N_2 (fig. 3(b)), and beyond 6000 K for NO (fig. 3(c)). This deviation may be a result of the rigid-rotor and harmonic-oscillator partition function employed by Hansen and of the neglect of electronic contribution. At higher temperatures, the population of levels corresponding to the nonparabolic regions of the potential-energy curve are no longer negligible, and it becomes necessary to introduce the nonrigidity and anharmonicity corrections into the energy levels of the molecules as was done in reference 35.

Reference 38 has provided tabulated values for specific heats, enthalpies, and internal energies for the 11-species air model up to temperatures of 6000 K. These values are nearly identical to those given in references 33 to 35. The minor differences that do exist may be due to different forms of the partition function, different spectroscopic data, inclusion of excited-state data, inclusion of isotopic effects, different heats of formation, or other factors.

14

Thermal Nonequilibrium

The thermodynamic property data of references 33 to 35 can be used to separate the contributions of different internal energy modes to the specific heat, as is required in the case of multitemperature flow-field models. For example, in a two-temperature model (refs. 25 and 27), advantage may be taken of the fact that the translational and rotational energy modes are fully excited and equilibrated at room temperature; therefore, the heat capacities for these modes are independent of temperature. The combined vibrational-electronic specific heat for species i, $(C_{p,i})_{ve}$, can then be evaluated by using the value for the total specific heat $C_{p,i}$ evaluated at temperature T_{ve} and by subtracting out the constant contribution from the translational and rotational specific heats. This can be described (see fig. 4 for the various contributions) by

$$[(C_{p,i})_{ve}]_{T_{ve}} = (C_{p,i})_{T_{ve}} - (C_{p,i})_{tr} - (C_{p,i})_{rot} \tag{14}$$

where the translational component of the specific heat $(C_{p,i})_{tr}$ is $\frac{5}{2} R_{univ}$ for all species, while the rotational component $(C_{p,i})_{rot}$ is R_{univ} for diatomic species and 0 for monatomic species.

The enthalpy h_i for a two-temperature model can be evaluated similarly, since contributions from the translational and rotational modes are linear with temperature. Therefore, the vibrational-electronic enthalpy for species i, $(h_i)_{ve}$, can be obtained from the specific enthalpy h_i evaluated at temperature T_{ve} by subtracting the contribution from the translational and rotational enthalpies evaluated at T_{ve} as well as the enthalpy of formation as follows:

$$[(h_i)_{ve}]_{T_{ve}} = [h_i]_{T_{ve}} - [(C_{p,i})_{tr} + (C_{p,i})_{rot}](T_{ve} - T_{ref}) - (\Delta h_i^f)_{T_{ref}} \tag{15}$$

The specific enthalpy from all the contributions of internal energy modes can then be obtained by adding the contributions of translational and rotational enthalpies (evaluated at the translational-rotational temperature) and the enthalpy of formation to the vibrational-electronic enthalpy as follows:

$$h_i(T, T_{ve}) = [(h_i)_{ve}]_{T_{ve}} + [(C_{p,i})_{tr} + (C_{p,i})_{rot}](T - T_{ref}) + (\Delta h_i^f)_{T_{ref}} \tag{16}$$

The procedure outlined here for obtaining the specific heats and enthalpies for different internal energy modes can be used only with one- or two-temperature models. This approach may be used for a three-temperature model only if one of the energy modes is partially excited and the rest are fully excited. If more than one internal energy mode is only partially excited, the partition-function approach (with appropriate corrections for the rotor nonrigidity and oscillator anharmonicity) would be needed to obtain the thermodynamic properties of different energy modes.

Species Transport Properties and Mixture Formulas

Thermal Equilibrium

The transport properties required in flow-field calculations are viscosity, thermal conductivity, and diffusion coefficients. The collision cross sections required for these properties have been recomputed herein using the same molecular data used previously by Yos (refs. 7 to 9). The computational techniques employed in the calculations are described in references 39 to 41; these references give details of the NATA (Nonequilibrium Arc Tunnel Analysis) code. In NATA, the average collision cross sections $\pi\overline{\Omega}_{ij}^{(l,s)}$ for the collisions between species i and j are calculated from basic cross-section data as functions of temperature and gas composition for each pair of species in the mixture[3]. The basic data are either in tabular form or are given as simple analytical functions of temperature or composition. NATA contains 12 methods or options for calculating the cross sections $\pi\overline{\Omega}_{ij}^{(1,1)}$, $\pi\overline{\Omega}_{ij}^{(2,2)}$, and B_{ij}^* (the ratio of cross sections). The options include using the Coulomb cross

---

[3] Different combinations of the indices l and s are required for higher order terms of the Chapman-Enskog theory.

section for the electrons and ions plus using exponential potential (ref. 42) and Lennard-Jones (6–12) potential (ref. 36) for neutral species in high and low temperature ranges, respectively. The formulas used in NATA to compute the transport properties from the collision cross sections are obtained from an approximation (ref. 43) to the first-order Chapman-Enskog expressions. These formulas are provided in subsequent sections.

Transport properties of single species. The viscosity μ_i and frozen[4] thermal conductivity $K_{f,i}$ of a gas containing a single molecular species are given, to a good approximation, by the formulas in chapters VII and VIII of reference 36. First, the viscosity is

$$\mu_i = \frac{5}{16} \frac{\sqrt{\pi m_i k T}}{\pi \overline{\Omega}_{ii}^{(2,2)}} \times 10^{16} \tag{17a}$$

or

$$\mu_i = \left(2.6693 \times 10^{-5}\right) \frac{\pi \sqrt{M_i T}}{\pi \overline{\Omega}_{ii}^{(2,2)}} \tag{17b}$$

Further, the viscosity can be written in terms of the mean free path λ_i as

$$\mu_i = \frac{5\pi}{32} \rho u \lambda_i \tag{17c}$$

where the gas density is

$$\rho \equiv \rho_i = m_i n_i \tag{17d}$$

the mean molecular velocity is

$$u \equiv u_i = \sqrt{\frac{8kT}{\pi m_i}} \tag{17e}$$

and the mean free path is

$$\lambda_i = \left[\sqrt{2} n_i \pi \overline{\Omega}_{ii}^{(2,2)}\right]^{-1} \times 10^{16} \tag{17f}$$

Next, the frozen thermal conductivity can be written in the modified Eucken approximation (ref. 36) as

$$K_{f,i} = K_{\text{tr},i} + K_{\text{int},i} \tag{18a}$$

Here, $K_{\text{tr},i}$ is the translational component of the thermal conductivity and $K_{\text{int},i}$ is the component of thermal conductivity resulting from the diffusion of internal excitation energy of the molecules. The translational component may be written as

$$K_{\text{tr},i} = \frac{75}{64} \frac{k\sqrt{\pi kT/m_i}}{\pi \overline{\Omega}_{ii}^{(2,2)}} \times 10^{16}/J \tag{18b}$$

$$= \left(1.9891 \times 10^{-4}\right) \frac{\pi \sqrt{T/M_i}}{\pi \overline{\Omega}_{ii}^{(2,2)}} \tag{18c}$$

$$= \frac{15}{4} \frac{\mu_i R_{\text{univ}}}{M_i} \tag{18d}$$

$$= \frac{3}{2} \frac{\mu_i (C_{p,i})_{\text{tr}}}{M_i} \tag{18e}$$

---

[4] See appendix A for various definitions.

$$= \frac{5}{2} \frac{\mu_i}{M_i} (C_{v,i})_{\text{tr}} \tag{18f}$$

or, in terms of the mean free path λ_i, as

$$K_{\text{tr},i} = \frac{5\pi}{32} \frac{\rho u \lambda_i}{M_i} \left[\frac{5}{2} (C_{v,i})_{\text{tr}} \right] \tag{18g}$$

The internal component of thermal conductivity may be written as

$$K_{\text{int},i} = \frac{3}{8} \left(\frac{C_{p,i}}{R_{\text{univ}}} - \frac{5}{2} \right) \frac{k\sqrt{\pi k T / m_i}}{\pi \overline{\Omega}_{ii}^{(1,1)}} \times 10^{16} / J \tag{18h}$$

$$= \left(6.3605 \times 10^{-5} \right) \frac{\pi \sqrt{T/M_i}}{\pi \overline{\Omega}_{ii}^{(1,1)}} \left(\frac{C_{p,i}}{R_{\text{univ}}} - \frac{5}{2} \right) \tag{18i}$$

$$= \frac{\mu_i}{M_i} \left(\frac{\rho D_{ii}}{\mu_i} \right) (C_{p,i})_{\text{int}} \tag{18j}$$

$$= \frac{5\pi}{32} \frac{\rho_i u_i \lambda_i (C_{v,i})_{\text{int}}}{M_i} \left(\frac{\rho_i D_{ii}}{\mu_i} \right) \tag{18k}$$

where the internal specific heat has been introduced from the relation

$$(C_{p,i})_{\text{int}} \equiv (C_{v,i})_{\text{int}} = C_{p,i} - \frac{5}{2} R_{\text{univ}} = C_{v,i} - \frac{3}{2} R_{\text{univ}} \tag{18l}$$

and the coefficient of self diffusion D_{ii} from the first Chapman-Enskog approximation is as follows:

$$D_{ii} = \frac{3}{8} \frac{\sqrt{\pi m_i k T}}{\pi \overline{\Omega}_{ii}^{(1,1)}} \left(\frac{1}{\rho} \right) \times 10^{16} \tag{18m}$$

$$= \left(2.6280 \times 10^{-3} \right) \frac{\pi \sqrt{T^3 / M_i}}{\pi \overline{\Omega}_{ii}^{(1,1)} p} \tag{18n}$$

The coefficient of self diffusion D_{ii} must be regarded as somewhat artificial. It is more correct to regard it as a limiting form of the coefficient of binary diffusion.

Using equations (18a), (18d), (18j), and (18l), the frozen thermal conductivity may now be expressed as

$$K_{f,i} = \frac{R_{\text{univ}} \mu_i}{M_i} \left[\frac{15}{4} + \left(\frac{\rho D_{ii}}{\mu_i} \right) \left(\frac{C_{p,i}}{R_{\text{univ}}} - \frac{5}{2} \right) \right] \tag{19a}$$

or, from equations (18a), (18e), and (18j),

$$K_{f,i} = \frac{\mu_i}{M_i} \left[\frac{3}{2} (C_{p,i})_{\text{tr}} + \left(\frac{\rho D_{ii}}{\mu_i} \right) (C_{p,i})_{\text{int}} \right] \tag{19b}$$

$$= \frac{\mu_i}{M_i} \left[\frac{5}{2} (C_{v,i})_{\text{tr}} + \left(\frac{\rho D_{ii}}{\mu_i} \right) (C_{v,i})_{\text{int}} \right] \tag{19c}$$

From equations (17a) and (18m) the factor $(\rho D_{ii}/\mu_i)$ is related to the collision cross sections $\pi\overline{\Omega}_{ii}^{(l,l)}$ through the following relation

$$\frac{\rho D_{ii}}{\mu_i} = \frac{6}{5}\frac{\pi\overline{\Omega}_{ii}^{(2,2)}}{\pi\overline{\Omega}_{ii}^{(1,1)}} \qquad (20)$$

The ratio $\pi\overline{\Omega}_{ii}^{(2,2)}/\pi\overline{\Omega}_{ii}^{(1,1)}$ in equation (20) is a very slowly varying function of temperature T; hence, $\rho D_{ii}/\mu_i$ is very nearly constant. This factor, appearing in equations (18j), (18k), (19a), (19b), and (19c), has a value close to 1.32 for the Lennard-Jones potential over a wide temperature range (ref. 44). If this factor is approximated by unity, equations (19b) and (19c) for the frozen thermal conductivity reduce to the form

$$K_{f,i} = \frac{\mu_i}{M_i}\left[\frac{3}{2}(C_{p,i})_{\text{tr}} + (C_{p,i})_{\text{int}}\right] \qquad (21a)$$

$$= \frac{\mu_i}{M_i}\left(C_{p,i} + \frac{5}{4}R_{\text{univ}}\right) \qquad (21b)$$

$$= \frac{\mu_i}{M_i}\left(C_{v,i} + \frac{9}{4}R_{\text{univ}}\right) \qquad (21c)$$

or, using equation (17c) to express the results in terms of the mean free path,

$$K_{f,i} = \frac{5\pi}{32}\left(\frac{\rho u \lambda_i}{M_i}\right)\left(C_{v,i} + \frac{9}{4}R_{\text{univ}}\right) \qquad (21d)$$

This is the form for the thermal conductivity derived originally by Eucken. It differs from the modified Eucken approximation (eq. (19)) used in the present work by the ratio

$$\left[1 + \frac{4}{15}\frac{(C_{v,i})_{\text{int}}}{R_{\text{univ}}}\left(\frac{\rho_i D_{ii}}{\mu_i}\right)\right]\Bigg/\left[1 + \frac{4}{15}\frac{(C_{v,i})_{\text{int}}}{R_{\text{univ}}}\right]$$

which is about 6 percent in the case of a diatomic gas near room temperature, where the only internal energy excited is the rotational energy.

The modified Eucken approximation (eqs. (19)) neglects the effects of inelastic collisions on the thermal conductivity. Such collisions introduce a coupling between the translational and internal components of the thermal conductivity; this coupling tends to reduce the total frozen thermal conductivity below the value (eqs. (19)) predicted by the modified Eucken approximation. The effects have been treated in detail for various polyatomic gases near room temperature. It has been found (refs. 45 to 47) that the errors in equations (19) may approach 10 to 20 percent when there is a rapid exchange of energy between the internal and translational states through inelastic collisions, as is normally the case for rotational excitation in low-temperature polyatomic gases. However, the errors become smaller when the exchange is less rapid, and are negligible when 20 or more collisions are required for the exchange of energy between internal excitation and translation.

The effects of inelastic collisions on the thermal conductivity of high-temperature air have apparently never been treated in detail. However, it appears that the inelastic cross sections should, in general, be small enough to make errors in the modified Eucken approximation (eqs. (19)) negligible for air at temperatures greater than about 1000 K. At temperatures below 1000 K, it may be desirable for more accurate calculations to correct equations (19) for the effects of inelastic rotational-translational energy transfer using the analysis of references 45 to 47. However, this correction has not been included in the values presented here.

18

The collision cross sections $\pi\overline{\Omega}_{ii}^{(l,l)}$ or $\pi\overline{\Omega}_{ij}^{(l,s)}$[5] are, in general, the weighted averages of the cross sections for collisions between species i and j. These collisions have been defined (refs. 7 to 9) as

$$\pi\overline{\Omega}_{ij}^{(l,s)} = \frac{\int_0^\infty \int_0^\pi \exp(-\gamma^2)\gamma^{2s+3}(1-\cos^l\chi)4\pi\sigma_{ij}\sin\chi\ d\chi\ d\gamma}{\int_0^\infty \int_0^\pi \exp(-\gamma^2)\gamma^{2s+3}(1-\cos^l\chi)\sin\chi\ d\chi\ d\gamma} \tag{22}$$

where $\sigma_{ij} = \sigma_{ij}(\chi, g)$ is the differential-scattering cross section for the pair (i, j), χ is the scattering angle in the center-of-mass system, g is the relative velocity of the colliding particles, and $\gamma = \left([m_i m_j/2(m_i+m_j)kT]^{1/2}\right)g$ is the reduced velocity. For collisions between the similar species, equation (22) yields $\pi\overline{\Omega}_{ii}^{(l,l)}$ required in equations (17) and (18). Various combinations of the indices l and s are required for higher order terms of the Chapman-Enskog theory. For the order considered here, only $\pi\overline{\Omega}_{ij}^{(1,1)}$, $\pi\overline{\Omega}_{ij}^{(1,2)}$, $\pi\overline{\Omega}_{ij}^{(1,3)}$, and $\pi\overline{\Omega}_{ij}^{(2,2)}$ are needed.

The collision cross sections $\pi\overline{\Omega}_{ii}^{(1,1)}$ and $\pi\overline{\Omega}_{ii}^{(2,2)}$ employed here are the same as those used by Yos (refs. 7 to 9). The cross sections for the neutral species N, N_2, NO, O, and O_2 were taken from the tabulations of Yun, Weissman, and Mason (ref. 48) for temperatures up to $15\,000$ K. Above $15\,000$ K, the cross sections for atomic N were obtained by extending Yun's calculations to $30\,000$ K using the same input data and techniques that were used in his work. The cross sections for the remaining species N_2, NO, O, and O_2 were extrapolated to $30\,000$ K assuming the same temperature dependence as calculated for N.

For the ionized species, the calculations used effective Coulomb cross sections that were chosen to make the computed transport properties for a fully ionized gas agree with the correct theoretical results (ref. 49) discussed in references 7 and 9. The specific formulas used in the calculations are

$$\pi\overline{\Omega}_{ee}^{(2,2)} = 1.29Q_c \times 10^{16} \qquad \text{(for electrons)} \tag{23a}$$

$$\pi\overline{\Omega}_{II}^{(2,2)} = 1.36Z^4 Q_c \times 10^{16} \qquad \text{(for ions)} \tag{23b}$$

$$\pi\overline{\Omega}_{ee}^{(1,1)} = \pi\overline{\Omega}_{II}^{(1,1)} = 0.795Z^4 Q_c \times 10^{16} \qquad \text{(for electrons and ions)} \tag{23c}$$

where $Z = 1$ for singly ionized species and

$$Q_c = \frac{e^4}{(kT)^2}\ln\Lambda\ \ \mathrm{cm}^2 \tag{23d}$$

The shielding parameter Λ is defined as

$$\Lambda = \left[\frac{9(kT)^3}{4\pi e^6 n_e} + \frac{16(kT)^2}{e^4 n_e^{2/3}}\right]^{1/2} \tag{23e}$$

$$= \left[2.09 \times 10^{-2}\left(\frac{T^4}{10^{12}p_e}\right) + 1.52\left(\frac{T^4}{10^{12}p_e}\right)^{2/3}\right]^{1/2} \tag{23f}$$

where T is the temperature in kelvins and $p_e = n_e kT$ is the electron pressure in atmospheres.[6] In equation (23d), $e = 4.8 \times 10^{-10}$ esu is the electron charge. Equations (23a) to (23f) are applicable

---

[5] The collision cross sections designated here as $\pi\overline{\Omega}_{ij}^{(l,s)}$ are the same as $\pi\sigma^2\Omega_{ij}^{(l,s)*}$ given in reference 36 and as $\overline{\Omega}_{ij}^{(l,s)}$ given in reference 39.

[6] For flows with thermal nonequilibrium, $p_e = n_e kT_e$ should be used to obtain the electron pressure.

only for electron pressures below the limiting value given by

$$p_{\text{em}} = 0.0975 \left(\frac{T}{10^3} \right)^4 \tag{23g}$$

for which the shielding factor $\ln \Lambda$ is equal to 1 in equation (23d) (ref. 49), and should not be used for electron pressures above this limit. The limiting electron pressure, p_{em}, from equation (23g) is plotted as a function of temperature in figure 5. The electron pressures encountered in typical aerospace applications should fall well below this limit.

In the present report, the transport properties of the charged species (i.e., ions and electrons) are provided for the limiting electron pressure $p_e = p_{\text{em}}$ at which the shielding factor $\ln \Lambda = 1$. For any other electron pressure, it is necessary to correct the tabulated transport properties of the charged species according to the formula

$$\frac{\mu_i(p_e)}{\mu_i(p_{\text{em}})} = \frac{K_{f,i}(p_e)}{K_{f,i}(p_{\text{em}})} = \frac{K_{\text{tr},i}(p_e)}{K_{\text{tr},i}(p_{\text{em}})} = \frac{K_{\text{int},i}(p_e)}{K_{\text{int},i}(p_{\text{em}})} = \frac{1}{\ln \Lambda(p_e)}$$

$$= \frac{2}{\ln \left[2.09 \times 10^{-2} \left(\dfrac{T}{1000 p_e^{1/4}} \right)^4 + 1.52 \left(\dfrac{T}{1000 p_e^{1/4}} \right)^{8/3} \right]} \tag{24a}$$

Similarly, the collision cross sections $\pi \overline{\Omega}_{ij}^{(l,s)}$ (for the pair of species for which both are ions or electrons or a combination of the two) for any other electron pressure p_e may be obtained from the values provided herein for $p_e = p_{\text{em}}$ by employing the relation

$$\frac{\pi \overline{\Omega}_{ij}^{(l,s)}(p_e)}{\pi \overline{\Omega}_{ij}^{(l,s)}(p_{\text{em}})} = \ln \Lambda(p_e)$$

$$= \frac{1}{2} \ln \left[2.09 \times 10^{-2} \left(\frac{T}{1000 p_e^{1/4}} \right)^4 + 1.52 \left(\frac{T}{1000 p_e^{1/4}} \right)^{8/3} \right] . \tag{24b}$$

Equation (24b) is also applicable for $i = j$ (single species).

In calculating the contribution $K_{\text{int},i}$ of the internal energy states to the thermal conductivity for the atomic species N and O, the diffusion cross section $\pi \overline{\Omega}_{ii}^{(1,1)}$ in equation (18h) or (18i) has been set equal to the corresponding charge-exchange cross section for the atom and atomic ion (refs. 8 and 50). As discussed in reference 7, this approximation allows for the effects of excitation exchange in reducing the contribution of internal energy states to the thermal conductivity in a gas of identical atoms. For consistency, the same approximation has also been employed in the tabulated cross sections and self-diffusion coefficients for these species.

The individual species viscosities and thermal conductivities computed using equations (17) and (18) have been curve-fitted herein as a function of temperature by employing the following relations:

$$\mu_i = [\exp(C_{\mu_i})] T^{[A_{\mu_i} \ln T + B_{\mu_i}]} \tag{25}$$

$$K_{f,i} = [\exp(E_{K_{f,i}})] T^{[A_{K_{f,i}} (\ln T)^3 + B_{K_{f,i}} (\ln T)^2 + C_{K_{f,i}} \ln T + D_{K_{f,i}}]} \tag{26}$$

The curve-fit coefficients in equations (25) and (26) are given in tables V and VI for the 11 chemical species. These coefficients yield values of the viscosity and frozen thermal conductivity

of ionic species at the limiting electron pressure (eq. (23g)) and should be corrected for any other electron pressure (or number density) by using equation (24a).

Similar to the equilibrium constant calculations from equation (5d), the thermal conductivity should be evaluated from the logarithmic form of equation (26). Also, all the five significant digits for the coefficients appearing in table VI should be used.

Figure 6 displays typical results from the viscosity curve fit (eq. (25)) of equations (17) for some of the neutral and charged species. The frozen thermal conductivity curve fit (eq. (26)) of equations (18) is shown in figure 7 for the same species. Figure 7 and table V show that fourth-order curve fits are needed for the thermal conductivity.

Transport properties of multicomponent mixtures. Rigorous kinetic theory formulas that have been derived directly from a solution of the Boltzmann equation using the classical Chapman-Enskog procedure (refs. 36 and 51) are available for obtaining the transport properties of a gas mixture from the molecular constituent species. In the first Chapman-Enskog approximation, formulas for both the viscosity and translational component of thermal conductivity K_{tr} of a gas mixture are of the general form

$$\mu^{(1)} \text{ or } K_{tr}^{(1)} = - \begin{vmatrix} A_{11} & \cdots & A_{1\nu} & | & x_1 \\ & & \cdot & | & \cdot \\ & & \cdot & | & \cdot \\ & & \cdot & | & \cdot \\ A_{\nu 1} & \cdots & A_{\nu\nu} & | & x_\nu \\ - & - & - & - & - \\ x_1 & \cdots & x_\nu & | & 0 \end{vmatrix} \Big/ |A_{ij}| \tag{27}$$

where x_i is the mole fraction of the ith species, $\nu(\equiv NS)$ is the total number of species present in the mixture, and the matrix elements A_{ij} can be expressed in the form

$$A_{ij} = A_{ji} = -x_i x_j a_{ij} + \delta_{ij} \left(x_i A_i + \sum_{l=1}^{\nu} x_i x_l a_{il} \right) \tag{28}$$

where $a_{ij} = a_{ji}$ and δ_{ij} is the Kronecker delta. Elements A_i and a_{ij} are defined subsequently. The superscript 1 on μ or K_{tr} indicates that equation (27) is the first Chapman-Enskog approximation for the transport property. Further details for obtaining the transport properties by employing the first Chapman-Enskog approximation are given in reference 43. In principle, the problem of calculating the transport coefficients for a given mixture consists of two parts: first, the determination of the collision cross sections $\pi\overline{\Omega}_{ij}$ for all possible pairs of species (i, j); and second, the evaluation of the Chapman-Enskog formulas. The amount of computation required to evaluate the mixture transport properties is greatly reduced if approximations to the complete Chapman-Enskog formulas are employed. Reference 7 has provided approximate formulas for the transport properties based on the relations developed in references 52 to 54. References 13, 14, and 55, and more recently, references 15 and 56 have also provided approximations to the Chapman-Enskog formulas. These are apparently the most satisfactory of the many simplifying approximations for the mixture viscosity and thermal conductivity that have been suggested by various authors. However, effects of the elements a_{ij} in the Chapman-Enskog formula are completely neglected in Brokaw's approximation (ref. 53), so that this approximation always gives too large a value for the transport properties. In the Buddenberg-Wilke (refs. 13 and 55) and Mason-Saxena (ref. 14) formulas, the effects of these elements are accounted for by means of a single empirical constant, which is assumed to be the same for all gas mixtures. The approximation used by Peng and Pindroh (ref. 52) represents an attempt to take account of the nondiagonal elements explicitly to the first order at the expense of a somewhat increased calculational effort. Armaly and Sutton (refs. 15 and 56) neglected the nondiagonal matrix

elements A_{ij} in a manner similar to Brokaw (ref. 53). However, they did not force the value of A_{ij}^*, defined as

$$A_{ij}^* = \frac{\overline{\Omega}_{ij}^{(2.2)}}{\overline{\Omega}_{ij}^{(1.1)}} \tag{29}$$

to be equal to 5/3 and 5/2 in their approximations for viscosity and thermal conductivity, respectively.[7] They assigned different values to A_{ij}^* for ion-atom and neutral atom-molecule interactions. From the computer time, storage, and simplicity point of view, references 13 and 14 appear to be adequate for nonionized gas mixtures, whereas references 15 and 56 are useful for computing the viscosity and translational component of thermal conductivity for an ionized gas mixture.

In all the approximations to the Chapman-Enskog formulas for viscosity and translational thermal conductivity discussed thus far, the transfer of momentum or energy from one species to another by collisions has been either neglected or has been accounted for by an empirical constant. This transfer process, which is represented by the nondiagonal elements a_{ij} in the Chapman-Enskog formula (eq. (28)), has the effect of making the less conductive species in the mixture carry a larger fraction of the transport. This process, therefore, reduces the overall conductivity of the mixture below the value it would have if the transfer process were neglected.

In reference 43, Yos obtained approximations to the Chapman-Enskog formulas that account for the effects of the aforementioned transfer process between different species. These approximations reproduce the results of the first Chapman-Enskog formula (eqs. (27) and (28)) to within a fraction of a percent for air at 6000 K and for other cases considered in reference 43 and are simpler to use than the latter. Based on the relations developed by Yos (ref. 43), the following formulas may be used to compute the mixture viscosity and translational component of thermal conductivity:

$$\mu^{(1)} \text{ or } K_{\text{tr}}^{(1)} = \frac{\sum\limits_{i=1}^{\text{NS}} x_i/(A_i + a_{\text{av}})}{1 - a_{\text{av}} \sum\limits_{i=1}^{\text{NS}} x_i/(A_i + a_{\text{av}})} \tag{30}$$

Here, NS is the number of species in the gas, x_i is the mole fraction of the ith species, and a_{av} is an average value of the nondiagonal matrix elements contained in equation (28) and is defined as

$$a_{\text{av}} = \frac{\sum\limits_{i,j=1}^{\text{NS}} x_i x_j \left(\frac{1}{A_i} - \frac{1}{A_j}\right)^2 a_{ij}}{\sum\limits_{i,j=1}^{\text{NS}} x_i x_j \left(\frac{1}{A_i} - \frac{1}{A_j}\right)^2} \tag{31a}$$

where

$$A_i = \sum_{l=1}^{\text{NS}} x_l B_{il} \tag{31b}$$

For the viscosity, the quantities a_{ij} and B_{ij} in equations (31a) and (31b) are defined as

$$a_{ij} = \frac{N_A}{(M_i + M_j)} \left[2\Delta_{ij}^{(1)} - \Delta_{ij}^{(2)}\right] \tag{32a}$$

$$B_{il} = \frac{N_A}{M_i} \Delta_{il}^{(2)} \tag{32b}$$

---

[7] With $A_{ij}^* = 5/3$ and 5/2, A_{ij} becomes identical to zero in the Chapman-Enskog formula.

For translational thermal conductivity, the above quantities are defined as

$$a_{ij} = (4.184 \times 10^7) \left(\frac{2}{15k}\right) \frac{M_i M_j}{(M_i + M_j)^2} \left[\left(\frac{33}{2} - \frac{18}{5} B_{ij}^*\right) \Delta_{ij}^{(1)} - 4\Delta_{ij}^{(2)}\right] \tag{33a}$$

and

$$B_{il} = (4.184 \times 10^7) \frac{2}{15k(M_i + M_l)^2}$$

$$\times \left[8M_i M_l \Delta_{il}^{(2)} + (M_i - M_l)\left(9M_i - \frac{15}{2} M_l + \frac{18}{5} B_{il}^* M_l\right) \Delta_{il}^{(1)}\right] \tag{33b}$$

In these equations, M_i is the molecular weight of the ith species, N_A is the Avogadro number, and k is the Boltzmann constant. The remaining quantities are defined

$$\Delta_{ij}^{(1)} = \frac{8}{3}(1.5460 \times 10^{-20}) \left[\frac{2M_i M_j}{\pi R_{\text{univ}} T(M_i + M_j)}\right]^{1/2} \pi \overline{\Omega}_{ij}^{(1,1)} \tag{34}$$

$$\Delta_{ij}^{(2)} = \frac{16}{5}(1.5460 \times 10^{-20}) \left[\frac{2M_i M_j}{\pi R_{\text{univ}} T(M_i + M_j)}\right]^{1/2} \pi \overline{\Omega}_{ij}^{(2,2)} \tag{35}$$

$$B_{ij}^* = \frac{5\overline{\Omega}_{ij}^{(1,2)} - 4\overline{\Omega}_{ij}^{(1,3)}}{\overline{\Omega}_{ij}^{(1,1)}} \tag{36}$$

and the collision integrals $\pi \overline{\Omega}_{ij}^{(l,s)}$ are weighted averages of the cross sections defined in equation (22).

The mixture frozen thermal conductivity K_f employed in defining the frozen Prandtl and Lewis numbers[8] can be obtained from the modified Eucken approximation (ref. 54)

$$K_f = K_{\text{tr}} + K_{\text{int}} \tag{37}$$

where K_{tr} is the translational component of the thermal conductivity given by equations (30) to (36) and K_{int} is the component of thermal conductivity resulting from the internal excitation energy of the molecules, (ref. 7) given by

$$K_{\text{int}} = 2.3901 \times 10^{-8} k \sum_{i=1}^{\text{NS}} \left[\frac{\left(\frac{C_{p,i}}{R_{\text{univ}}} - \frac{5}{2}\right) x_i}{\sum_{j=1}^{\text{NS}} x_j \Delta_{ij}^{(1)}}\right] \tag{38a}$$

$$= 2.3901 \times 10^{-8} k \sum_{i=1}^{\text{NS}} \left[\frac{\left[\frac{(C_{p,i})_{\text{int}}}{R_{\text{univ}}}\right] x_i}{\sum_{j=1}^{\text{NS}} x_j \Delta_{ij}^{(1)}}\right] \tag{38b}$$

If the approximations of references 52 to 54 are employed in place of the more exact formulas given by equations (30) to (36), the following approximate formulas for the mixture viscosity and

---

[8] See appendix A for various definitions.

thermal conductivity may be used (ref. 7). For the mixture viscosity,

$$\mu^{(1)} = \sum_{i=1}^{\text{NS}} \left(\frac{\frac{M_i}{N_A} x_i}{\sum_{j=1}^{\text{NS}} x_j \, \Delta_{ij}^{(2)}} \right) \tag{39}$$

For the translational component of thermal conductivity in a mixture,

$$K_{\text{tr}}^{(1)} = 2.3901 \times 10^{-8} \frac{15}{4} k \sum_{i=1}^{\text{NS}} \left(\frac{x_i}{\sum_{j=1}^{\text{NS}} \alpha_{ij} x_j \Delta_{ij}^{(2)}} \right) \tag{40a}$$

where $\Delta_{ij}^{(2)}$ is given by equation (35) and α_{ij} is defined as

$$\alpha_{ij} = 1 + \frac{[1 - (M_i/M_j)][0.45 - 2.54(M_i/M_j)]}{[1 + (M_i/M_j)]^2} \tag{40b}$$

The approximations of equations (39) and (40) may be valid only for the range of conditions for which they have been developed and not for general application because of the approximate analysis of the nondiagonal matrix elements A_{ij} of equation (27). Generally, these approximate formulas give good results for nonionized or weakly ionized flows with a savings of about a factor of two in computation time compared with the more accurate formulation of equations (30) to (33), since it is no longer necessary to evaluate the nondiagonal matrix element a_{av} in equation (31a).

A further savings of about another factor of two in the transport property calculations may be obtained if α_{ij} in equation (40b) and the factor

$$\frac{6}{5} \frac{\pi \overline{\Omega}_{ij}^{(2,2)}}{\pi \overline{\Omega}_{ij}^{(1,1)}}$$

in equation (20) are approximated by unity, so that all three of the properties μ, K_{tr}, and K_{int} in equations (38) to (40) depend on the same parameter $\sum_{j}^{\text{NS}} x_j \, \Delta_{ij}^{(2)}$ in the denominator. With these approximations, equations (38) to (40) may be written in the form

$$\mu^{(1)} = \frac{5\pi}{32} \sum_{i=1}^{\text{NS}} \rho_i u_i \overline{\lambda}_i \tag{41a}$$

$$K_{\text{tr}}^{(1)} = \frac{5\pi}{32} \sum_{i=1}^{\text{NS}} \frac{\rho_i u_i \overline{\lambda}_i}{M_i} \left[\frac{5}{2} (C_{v,i})_{\text{tr}} \right] \tag{41b}$$

and

$$K_{\text{int}} = \frac{5\pi}{32} \sum_{i=1}^{\text{NS}} \frac{\rho_i u_i \overline{\lambda}_i}{M_i} (C_{v,i})_{\text{int}} \tag{41c}$$

24

where the partial gas density of the ith component is

$$\rho_i = m_i n_i \tag{41d}$$

the mean molecular velocity of the ith component is

$$u_i = \sqrt{8kT/\pi m_i} \tag{41e}$$

and the modified mean-free path of the ith component in the mixture is

$$\bar{\lambda}_i = \left[2n \sum_{j=1}^{NS} \frac{x_j \pi \bar{\Omega}_{ij}^{(2,2)}}{\sqrt{1 + m_i/m_j}} \right]^{-1} \times 10^{16} \tag{41f}$$

In the above equations, n is the total particle density in particles/cm^3 and $(C_{v,i})_{\text{int}} = (C_{p,i})_{\text{int}}$. The modified mean-free path $\bar{\lambda}_i$ given by equation (41f) is not the mean distance between molecular collisions. It differs from the actual mean-free path λ_i^* of the ith component in a mixture defined in reference 6 as

$$\lambda_i^* = \left[n \sum_{j=1}^{NS} x_j \pi \bar{\Omega}_{ij}^{(2,2)} \sqrt{1 + m_i/m_j} \right]^{-1} \times 10^{16} \tag{41g}$$

by the factor $2(1 + m_i/m_j)^{-1}$ in each term of the summation. The modified mean-free path $\bar{\lambda}_i$ represents the mean distance travelled by species i before losing its average excess momentum relative to the surrounding gas medium through head-on collisions with species j. (See Hansen, ref. 57.) From equations (37), (41b), and (41c), the expression for the frozen thermal conductivity, K_f, of the mixture can be written as

$$K_f = \frac{5\pi}{32} \sum_{i=1}^{NS} \frac{\rho_i u_i \bar{\lambda}_i}{M_i} \left[\frac{5}{2}(C_{v,i})_{\text{tr}} + (C_{v,i})_{\text{int}} \right] \tag{41h}$$

$$= \frac{5\pi}{32} \sum_{i=1}^{NS} \frac{\rho_i u_i \bar{\lambda}_i}{M_i} \left[C_{v,i} + \frac{9}{4}(R_{\text{univ}}) \right] \tag{41i}$$

in close analogy to the Eucken expression (eq. (21d)) for a single-component gas. Equations (41a) to (41i) represent the predictions of the elementary kinetic theory for the viscosity and thermal conductivity of a gas mixture. (See refs. 36 and 58.) Although less accurate than the approximation given by equations (37) to (40), they may still be adequate for many applications, particularly in view of the current uncertainty in our knowledge of the collision cross sections for high-temperature gases.

The binary diffusion coefficient D_{ij} needed to obtain the binary and multicomponent Lewis numbers (refs. 17, 18, and 36) is obtained from the complete first Chapman-Enskog approximation (ref. 36):

$$D_{ij} = \frac{\bar{D}_{ij}}{p} = \frac{kT}{p\Delta_{ij}^{(1)}} \tag{42a}$$

with

$$\bar{D}_{ij} = \frac{kT}{\Delta_{ij}^{(1)}} \tag{42b}$$

Here, p is the pressure in atmospheres. Equation (42b) for $\overline{D}_{ij}$ has been curve fitted in the present work by using the expression

$$\overline{D}_{ij} = \left[\exp(D_{\overline{D}_{ij}})\right] \, T^{\left[A_{\overline{D}_{ij}}(\ln T)^2 + B_{\overline{D}_{ij}}\ln T + C_{\overline{D}_{ij}}\right]} \tag{42c}$$

where T is the temperature in kelvins. The curve-fit coefficients of equation (42c) are given in table VII for the different interactions in the 11-species air model.

The values of $\overline{D}_{ij}$ obtained from equation (42c) with the curve-fit coefficients given in table VII are for the limiting electron pressure p_{em} (eq. (23g)).[9] If the pair of interacting species are both ions, both electrons, or any combination of the two, then $\overline{D}_{ij}$ must be corrected for the given electron pressure as follows:

$$\overline{D}_{ij}(p_e) = \overline{D}_{ij}(p_{em}) \, \frac{2}{\ln\left[2.09 \times 10^{-2}\left(\dfrac{T}{1000p_e^{1/4}}\right)^4 + 1.52\left(\dfrac{T}{1000p_e^{1/4}}\right)^{8/3}\right]} \tag{42d}$$

To obtain the viscosity μ and the frozen component of thermal conductivity K_f of a gas mixture either from the more exact equations (30) to (38) or from the approximate relations in equations (39) to (41), the binary collision cross sections $\pi\overline{\Omega}_{ij}^{(l,s)}$ and their ratios are needed in equations (34) to (36). These cross sections, defined by equation (22), are the same as those used by Yos (refs. 7 to 9). In addition to the formulas given by equations (23) for the Coulomb collision integrals, the following relations are employed:

$$\pi\overline{\Omega}_{eI}^{(1,1)} = 0.795 Z^2 Q_c \times 10^{16} \tag{43a}$$

$$\pi\overline{\Omega}_{eI}^{(2,2)} = 1.29 Z^2 Q_c \times 10^{16} \tag{43b}$$

where the subscripts e and I represent electrons and ions, respectively, and $Z = 1$ for singly ionized species, and Q_c is defined in equation (23d).

The NATA (Nonequilibrium Arc Tunnel Analysis) code (refs. 39 to 41) employed to obtain the collision cross sections $\pi\overline{\Omega}_{ij}^{(l,s)}$ contains default provisions for estimating some cross sections if they are not specified explicitly in the built-in data base or the input. The defaults are summarized as follows:

1. If both species are ions, the Coulomb cross sections given by equations (23) and (43) are used.

2. If one species is neutral and the other is ionized, the formula

$$\pi\overline{\Omega}_{ij}^{(l,s)} = A^{(l,s)} T^{-0.4} \tag{44a}$$

is employed with the constants $A^{(l,s)}$ defined in the code.

3. If both species are neutral and are not alike, the cross sections are estimated using the simple mixing rule

$$\pi\overline{\Omega}_{ij}^{(l,s)} = \frac{1}{4}\left(\sqrt{\pi\overline{\Omega}_{ii}^{(l,s)}} + \sqrt{\pi\overline{\Omega}_{jj}^{(l,s)}}\right)^2 \tag{44b}$$

---

[9] For flows with thermal equilibrium, $p_e = n_e kT$ may be used to obtain the electron pressure. For thermal nonequilibrium conditions, the electron temperature T_e should be employed instead of T in the previous equation of state.

The built-in data in NATA specify steps for calculating the cross sections for the like-like interactions of ten species (e^-, N_2, O_2, N, O, NO, NO^+, N^+, O^+, and N_2^+) and for those unlike interactions for which experimental or theoretical cross sections are available in the literature. The cross sections for O_2^+ are the same as those for N_2^+ in these calculations. NATA contains 12 methods or options for calculating $\pi\overline{\Omega}_{ij}^{(1,1)}$, $\pi\overline{\Omega}_{ij}^{(2,2)}$, and B_{ij}^*; these methods are described in detail in references 39 to 41. Reference 59 provides a comparison between the theoretical calculations based on these cross sections and the experimental values for the thermal conductivity of nitrogen up to temperatures of 14000 K; fairly good agreement between the two is shown. The accuracy of the calculated transport properties is largely determined by the accuracy of the input data for the cross-section integrals. Reference 7 contains a detailed discussion of the values employed in the present study, and a brief review of these values is provided in the following paragraph.

Similar to the collision cross sections for single-species transport properties described previously, the values of $\pi\overline{\Omega}_{ij}^{(l,s)}$ for mixture transport properties for the atomic and molecular interactions have been obtained from the calculations of Mason (ref. 48) for temperatures up to 15000 K. The cross sections for the interactions not tabulated by Mason were assumed to be approximately the same as the other neutral-neutral interactions. For temperatures above 15000 K, the cross sections for the atomic and other neutral-neutral interactions were obtained by extending Mason's calculations up to 30000 K by using the same potential functions that were used in his work (ref. 60). Since neutral species are not important at high temperatures, the effect of this procedure on the overall transport properties should be negligible. Further, there appear to be insufficient data available on the ion-neutral interactions. These interactions have been calculated from the approximate potentials given by Peng and Pindroh (ref. 52). Those potentials were obtained by drawing a smooth curve joining the polarization potential at large intermolecular distances to a Morse potential obtained from spectroscopic data at short distances. Further details for obtaining the interactions between a neutral species and its own ion with resonant and nonresonant ion-neutral collisions are given in references 7 and 8. There has been a lot of experimental work on the electron-molecule cross sections, whereas the cross sections for electron-atom scattering are somewhat uncertain, as detailed in reference 7. For Coulomb collisions between the charged particles, effective collision integrals were chosen in reference 7 so as to make the calculated values of the electrical conductivity and the electronic contribution to the thermal conductivity agree as closely as possible with the results for a completely ionized gas.

Figures 8 and 9 show viscosity and frozen thermal conductivity values, respectively, of equilibrium air at 1 atm obtained by employing the collision cross sections computed here for the constituent species. The present calculations employ equation (39) for the mixture viscosity and equations (37), (38), and (40) for the mixture frozen thermal conductivity. Also, the collision cross sections used are nearly identical to those obtained in reference 9. The mixing laws employed for the viscosity and thermal conductivity shown in figures 8 and 9 are accurate for subionization temperatures (less than 9000 K at 1 atm) only. For ionized flows, more accurate mixing laws of the type given in equation (30) should be employed. Figures 8 and 9 also include viscosity and thermal conductivity values from other sources for comparison. In these figures, the predictions of Peng and Pindroh (ref. 52) and Esch et al. (ref. 61) are based on the Buddenberg-Wilke (ref. 55) type of mixture law and have the same level of approximation as the present calculations. The mixture laws employed by Hansen (ref. 37) and Svehla (ref. 44) contain a somewhat lower level of approximation. In Hansen's and Svehla's work, the viscosity is computed by using the simple summation formula for a mixture of hard-sphere molecules, whereas a linearized expression with Eucken's assumption (ref. 36) is used for the frozen thermal conductivity. The viscosity values obtained in the present work are in good agreement (fig. 8) with the values obtained by Peng and Pindroh (ref. 52) and Esch et al. (ref. 61), presumably because of the similar mixing laws. Hansen's (ref. 37) predictions, which are based on the Morse potential function, are lower, especially at higher temperatures. Svehla's (ref. 44) predictions, which are based on the Lennard-Jones potential, are also lower than the present results for temperatures

higher than 2500 K. Even with the beginning of dissociation of molecular nitrogen at about 4000 K (when the dissociation of molecular oxygen is almost complete), Hansen's values of viscosity are not much different from Sutherland's law. For the frozen thermal conductivity (fig. 9), the present values are in agreement with those obtained by Peng and Pindroh (ref. 52) up to temperatures of about 9000 K. The values obtained by Esch et al. (ref. 61) deviate from the present values beyond 6000 K. This deviation may be due to the constant cross-section values that are used for the ionized species in the 8000 to 15 000 K temperature range in reference 61. Hansen's predictions of thermal conductivity are lower than the other data and are closer to the Sutherland values up to temperatures of about 4000 K. Again, the differences between the present computations and those of Hansen are presumably due to the somewhat more rigorous mixing laws employed herein. Svehla (ref. 44) has not provided values of the frozen thermal conductivity for equilibrium air and, therefore, his values are not shown in figure 9.

There are 121 possible binary interactions for the dissociating air with 11 species. Therefore, 121 values of each of the collision cross sections $\pi \overline{\Omega}_{ij}^{(1,1)}$, $\pi \overline{\Omega}_{ij}^{(2,2)}$, and the collision cross-section ratio B_{ij}^* are required to evaluate the transport properties. If the symmetrical equality is used, i.e., $(i,j) = (j,i)$, only 66 values of each cross section and cross-section ratio are required. These values have been curve-fit in the present study as a function of temperature for the limiting electron pressure $p_{\rm em}$ (eq. (23g)) using the following relations

$$\pi \overline{\Omega}_{ij}^{(1,1)} = \left[\exp \left(D_{\overline{\Omega}_{ij}^{(1,1)}} \right) \right] T^{\left[A_{\overline{\Omega}_{ij}^{(1,1)}} (\ln\ T)^2 + B_{\overline{\Omega}_{ij}^{(1,1)}} \ln\ T + C_{\overline{\Omega}_{ij}^{(1,1)}} \right]} \tag{45}$$

$$\pi \overline{\Omega}_{ij}^{(2,2)} = \left[\exp \left(D_{\overline{\Omega}_{ij}^{(2,2)}} \right) \right] T^{\left[A_{\overline{\Omega}_{ij}^{(2,2)}} (\ln\ T)^2 + B_{\overline{\Omega}_{ij}^{(2,2)}} \ln\ T + C_{\overline{\Omega}_{ij}^{(2,2)}} \right]} \tag{46}$$

$$B_{ij}^{*}{}^{(2,2)} = \left[\exp \left(C_{B_{ij}^*} \right) \right] T^{\left[A_{B_{ij}^*} \ln\ T + B_{B_{ij}^*} \right]} \tag{47}$$

Curve-fit coefficients in equations (45) to (47) are given in tables VIII to X for all interactions in the 11-species air model. Similar to the calculations for the equilibrium constant and thermal conductivity, the collision cross sections should be evaluated from the logarithmic forms of equations (45) and (46) by keeping all four significant digits for the coefficients given in tables VIII to X. For electron pressures different from $p_{\rm em}$, the formula given by equation (24b) is used to correct the cross sections for the ionic species. No such correction is required for the cross-section-ratio parameter B_{ij}^*.

Figure 10 illustrates some typical curve-fits that were obtained by using equation (42c) and equations (45) to (47) with the associated constants. The figure compares the computed values of binary diffusion coefficient, collision integrals, and collision-integral ratio with the resulting curve-fit for different interaction pairs of neutral and ionized species, including electrons. The collision-integral ratio, B_{ij}^*, is almost constant with temperature as shown in the figure and was fitted with the lower order curve-fit when possible. The collision integrals $\pi \overline{\Omega}_{ij}^{(l,s)}$ for the charged species pairs show a simple T^{-2} dependence that requires only two curve-fit coefficients, as seen in equations (23).

Thermal Nonequilibrium

The transport properties of a multitemperature gas mixture may be obtained by following the approaches of references 27 and 62. These references have used equations (39) and (40) for the calculation of mixture viscosity and translational thermal conductivity. The collision integrals for heavy particles in these equations are evaluated by using the heavy-particle translational temperature, whereas those for electrons with any other partner are obtained by using the electron temperature. With these modifications, equations (39) and (40a) can be written for a gas mixture

as

$$\mu = \sum_{i=1}^{NS-1} \left[\frac{\frac{M_i}{N_A} x_i}{\sum\limits_{j=1}^{NS-1} x_j \, \Delta_{ij}^{(2)}(T) + x_e \, \Delta_{ie}^{(2)}(T_e)} \right] + \frac{\frac{M_e}{N_A} x_e}{\sum\limits_{j=1}^{NS} x_j \, \Delta_{ej}^{(2)}(T_e)} \tag{48}$$

$$K_{tr}^* = (2.3901 \times 10^{-8}) \frac{15}{4} k \sum_{i=1}^{NS-1} \left[\frac{x_i}{\sum\limits_{j=1}^{NS-1} \alpha_{ij} x_j \, \Delta_{ij}^{(2)}(T) + 3.54 x_e \, \Delta_{ie}^{(2)}(T_e)} \right] \tag{49}$$

where α_{ij} is still obtained from equation (40b). The above definition of K_{tr}^* does not include contributions due to electron–heavy-particle and electron–electron collisions. These contributions, defined by K_e, are given subsequently. The approach outlined here may also be used to obtain the mixture viscosity and thermal conductivity from the more exact expressions in equations (30) to (36). Equations (38) for the internal thermal conductivity need to be modified for the multitemperature formulation. The contributions resulting from the excitation of different internal energy modes cannot be lumped together into a single term K_{int} for such a formulation. Further, equation (37) can no longer be used to obtain a frozen thermal conductivity for the mixture. The relation given in equation (37) may be used to obtain a frozen thermal conductivity with only the rotational mode contributing to the internal energy at the translational temperature. In general, there are four components of the internal thermal conductivity, similar to the molecular specific heat (fig. 4). Using these components, the kth component of the overall heat-flux vector can be expressed as

$$q^k = -(K_{tr}^* + K_{rot}) \frac{\partial T}{\partial x^k} - K_{vib} \frac{\partial T_{vib}}{\partial x^k} - K_{el} \frac{\partial T_{el}}{\partial x^k} - K_e \frac{\partial T_e}{\partial x^k} + \sum_{i=1}^{NS} \rho_i h_i V_i^k \tag{50a}$$

where K_{tr}^* is the translational thermal conductivity defined previously by equation (49) and K_{rot}, K_{vib}, and K_{el} are the rotational, vibrational, and electronic thermal conductivities, respectively, associated with these internal energy modes (ref. 63). Also, K_e is the thermal conductivity of electrons, T is the translational-rotational temperature, T_{vib} is the vibrational temperature, T_{el} is the electronic excitation temperature, T_e is the electron temperature, x^k is the kth component in a general orthogonal coordinate system, and the last term is the diffusive component of the heat-flux vector. In the diffusive heat-flux component, ρ_i, h_i, and V_i^k are the density, enthalpy, and diffusion velocity of species i, respectively. Further details of the heat-flux vector q^k and other definitions are given in appendix A. For a two-temperature model, equation (50a) may be written (refs. 25 and 27) as

$$q^k = -(K_{tr}^* + K_{rot}) \frac{\partial T}{\partial x^k} - (K_{vib} + K_{el} + K_e) \frac{\partial T_{ve}}{\partial x^k} + \sum_{i=1}^{NS} \rho_i h_i V_i^k \tag{50b}$$

Different components of the internal thermal conductivity in equations (50) can be evaluated from equation (38a) or (38b) by appropriate modifications for these components. For example, K_{rot} can be obtained from

$$(K_{rot})_{\substack{partial \\ excitation}} = 2.3901 \times 10^{-8} k \sum_{i=mol.} \left\{ \frac{\left[\frac{C_{p,i}(T_{rot})}{R_{univ}} - \frac{5}{2} \right] x_i}{\sum\limits_{j=1}^{NS-1} x_j \, \Delta_{ij}^{(1)}(T) + x_e \, \Delta_{ie}^{(1)}(T_e)} \right\} \tag{51a}$$

$$= 2.3901 \times 10^{-8} k \sum_{i=\text{mol.}} \left\{ \frac{\left[\frac{(C_{p,i})_{\text{rot}}}{R_{\text{univ}}} \right] x_i}{\sum_{j=1}^{NS-1} x_j \, \Delta_{ij}^{(1)}(T) + x_e \, \Delta_{ie}^{(1)}(T_e)} \right\} \tag{51b}$$

for partial excitation of the rotational internal energy mode if the temperature is less than that needed to excite the vibrational energy mode (fig. 3). Values of specific heat at constant pressure $C_{p,i}$ in equation (51a) can be obtained from the curve-fit relation of equation (13) by employing the rotational temperature T_{rot} if different from the translational temperature T. In equation (51b), $(C_{p,i})_{\text{rot}}$ is the rotational component of the total $C_{p,i}$. When the vibrational mode begins to excite, the rotational mode is fully excited, and equation (51a) becomes

$$(K_{\text{vib}})_{\substack{\text{full} \\ \text{excitation}}} = 2.3901 \times 10^{-8} k \sum_{i=\text{mol.}} \left\{ \frac{x_i}{\sum_{j=1}^{NS-1} x_j \, \Delta_{ij}^{(1)}(T) + x_e \, \Delta_{ie}^{(1)}(T_e)} \right\} \tag{51c}$$

Similarly, expressions for K_{vib} with partial and full excitations of the vibrational energy mode may be written as

$$(K_{\text{vib}})_{\substack{\text{partial} \\ \text{excitation}}} = 2.3901 \times 10^{-8} k \sum_{i=\text{mol.}} \left\{ \frac{\left[\frac{C_{p,i}(T_{\text{vib}})}{R_{\text{univ}}} - \frac{7}{2} \right] x_i}{\sum_{j=1}^{NS-1} x_j \, \Delta_{ij}^{(1)}(T) + x_e \, \Delta_{ie}^{(1)}(T_e)} \right\} \tag{52a}$$

$$= 2.3901 \times 10^{-8} k \sum_{i=\text{mol.}} \left\{ \frac{\left[\frac{(C_{p,i})_{\text{vib}}}{R_{\text{univ}}} \right] x_i}{\sum_{j=1}^{NS-1} x_j \, \Delta_{ij}^{(1)}(T) + x_e \, \Delta_{ie}^{(1)}(T_e)} \right\} \tag{52b}$$

and

$$(K_{\text{vib}})_{\substack{\text{full} \\ \text{excitation}}} = 2.3901 \times 10^{-8} k \sum_{i=\text{mol.}} \left\{ \frac{x_i}{\sum_{j=1}^{NS-1} x_j \, \Delta_{ij}^{(1)}(T) + x_e \, \Delta_{ie}^{(1)}(T_e)} \right\} \tag{52c}$$

Once again, the value of $C_{p,i}$ in equation (52a) can be obtained from the curve-fit relation of equation (13) by employing T_{vib}; also, in equation (52b), $(C_{p,i})_{\text{vib}}$ is the vibrational component of the total $C_{p,i}$. The vibrational energy mode is fully excited when the electronic contribution becomes significant (as shown in fig. 4 for the specific heat at constant pressure).

The rotational and vibrational energy modes are almost fully excited at their respective characteristic temperatures. Therefore, for rotational and vibrational temperatures greater than these characteristic temperatures, equations (51b) and (52b) can be used to obtain K_{rot} and K_{vib}, respectively.

Expressions for K_{el} with the excitation of electronic energy mode can be written as

$$K_{el} = 2.3901 \times 10^{-8} k \sum_{i=1}^{NS-1} \left\{ \frac{\left[\frac{C_{p,i}(T_{el})}{R_{univ}} - \frac{9}{2} \right] x_i}{\sum_{j=1}^{NS-1} x_j \, \Delta_{ij}^{(1)}(T) + x_e \, \Delta_{ie}^{(1)}(T_e)} \right\} \tag{53a}$$

$$= 2.3901 \times 10^{-8} k \sum_{i=1}^{NS-1} \left\{ \frac{\left[\frac{(C_{p,i})_{el}}{R_{univ}} \right] x_i}{\sum_{j=1}^{NS-1} x_j \, \Delta_{ij}^{(1)}(T) + x_e \, \Delta_{ie}^{(1)}(T_e)} \right\} \tag{53b}$$

In equation (53a), higher electronic degeneracy levels begin to contribute to K_{el} (and $C_{p,i}$, etc.) as the characteristic temperatures for the electronic excitation of those degeneracy levels are reached. The term $(C_{p,i})_{el}$ in equation (53b) is the electronic contribution to the total $C_{p,i}$. The species that is left out in the outer summation in equations (53a) and (53b) is the electron.

Finally, the thermal conductivity for free electrons K_e in equations (50) may be obtained from the modified form of equation (40a) as follows:

$$K_e = (2.3901 \times 10^{-8}) \frac{15}{4} \frac{k x_e}{\sum_{j=1}^{NS-1} 1.45 x_j \, \Delta_{ej}^{(2)}(T_e) + x_e \, \Delta_{ee}^{(2)}(T_e)} \tag{54}$$

This thermal conductivity results from the collisions between electrons and other species, including other electrons.

In equations (51) to (53) for the partial conductivities in thermal nonequilibrium, the diffusion rates of the excited species are assumed to depend on the translational (or kinetic) temperature of the molecules rather than on the excitation temperature, because the collision frequency of the species is likely to depend strongly on the translational temperature. Therefore, the cross sections $\Delta_{ij}^{(1)}$ in the denominators of these equations are evaluated at the translational temperature T. Perhaps employing some averaged temperature, which would cover the effects of translational temperature and excitation on the cross sections, would be more desirable.

Concluding Remarks

The present work provides a review of the reaction-rate coefficients and thermodynamic and transport properties for an 11-species air model that are needed in analyzing the high-energy flow environment of currently proposed and future hypersonic vehicles. The properties not available in the literature have been provided for this set of species, and curve fits are given for the various species for their efficient computation in flow-field codes. Approximate and more exact formulas have been provided for computing the properties of partially ionized air mixtures in chemical and thermal nonequilibrium around such vehicles. Limitations of the approximate mixing laws for a mixture of ionized species are pointed out, and an electron number-density correction for the transport properties of the charged species is given. This correction has generally been ignored in the aerospace literature.

The work presented here uses the best estimates of available data needed to compute properties of the 11-species air model. However, there is need for improved data, especially for air in thermochemical nonequilibrium. There is a considerable degree of uncertainty about reaction-rate coefficients at high temperatures. For the multitemperature kinetic models, the theoretical basis needs to be

developed substantially and the experimental data base needs to be expanded considerably. The virial-coefficient and partition-function approaches for obtaining the thermodynamic properties are equally accurate at high temperatures if the effects of nonrigidity of the rotor and anharmonicity of the oscillator are included in the two methods. The curve fits provided here are for the thermodynamic properties based on the virial-coefficient formulation with these high-temperature corrections. These values seem adequate but need further verification. For transport properties, the input data for obtaining the collision cross sections at high temperatures require further study.

32

Appendix A

Heat Flux, Frozen and Total Prandtl and Lewis Numbers, and Associated Definitions

The kth component of the overall heat-flux vector q^k for the dissociating and ionizing air model in a multitemperature formulation can be expressed as follows:[10]

$$q^k = -(K_{\text{tr}}^* + K_{\text{rot}})\frac{\partial T}{\partial x^k} - K_{\text{vib}}\frac{\partial T_{\text{vib}}}{\partial x^k} - K_{\text{el}}\frac{\partial T_{\text{el}}}{\partial x^k} - K_e\frac{\partial T_e}{\partial x^k} + \sum_{i=1}^{\text{NS}} \rho_i h_i V_i^k \tag{A1}$$

where the various symbols are explained in the main text after equation (50a). For thermal equilibrium conditions, equation (A1) may be written as

$$q^k = -(K_{\text{tr}}^* + K_{\text{rot}} + K_{\text{vib}} + K_{\text{el}} + K_e)\frac{\partial T}{\partial x^k} + \sum_{i=1}^{\text{NS}} \rho_i h_i V_i^k \tag{A2}$$

or

$$q^k = -K_f\frac{\partial T}{\partial x^k} + \sum_{i=1}^{\text{NS}} \rho_i h_i V_i^k \tag{A3}$$

where

$$K_f = (K_{\text{tr}}^* + K_e) + K_{\text{int}} \tag{A4}$$

and

$$K_{\text{int}} = K_{\text{rot}} + K_{\text{vib}} + K_{\text{el}} \tag{A5}$$

Also, under thermal equilibrium conditions,

$$K_{\text{tr}} = K_{\text{tr}}^* + K_e \tag{A6}$$

where K_{tr} is given by equation (40a), K_{tr}^* is obtained from equation (49), and K_e is evaluated from equation (54). The last terms in equations (A1), (A2), and (A3) represent the diffusion contribution to the heat-flux vector. The diffusion mass flux of species i, J_i^k, is related to the diffusion velocity V_i^k through the relation

$$J_i^k = \rho_i V_i^k \tag{A7}$$

or, in terms of the concentration gradients, may be expressed (refs. 64 and 65) as

$$J_i^k = -\frac{\mu}{N_{Pr,f}}\left(Le_i\frac{\partial C_i}{\partial x^k} + \sum_{\substack{l=1 \\ l\neq i}}^{\text{NS}} \Delta b_{il}\frac{\partial C_l}{\partial x^k}\right) \tag{A8}$$

where pressure and thermal diffusion have been neglected and where

$$Le_i = \sum_{\substack{j=1 \\ j\neq i}}^{\text{NS}} \frac{C_j}{M_j} \left/ \sum_{\substack{j=1 \\ j\neq i}}^{\text{NS}} \frac{C_j}{M_j Le_{f,ij}}\right. \tag{A9}$$

$$\Delta b_{il} = Le_i - \left[\frac{M_i}{M}L_{f,il} + \left(1 - \frac{M_i}{M_l}\right)\sum_{\substack{j=1 \\ j\neq i}}^{\text{NS}} L_{f,ij}C_j\right] \tag{A10}$$

---

[10] The heat-flux vector is positive for heat flow in the positive coordinate direction.

33

The multicomponent Lewis number $L_{f,ij}$ and the binary Lewis number $Le_{f,ij}$ are defined, respectively, as

$$L_{f,ij} = \rho C_{p_f} \tilde{D}_{ij}/K_f \tag{A11}$$

and

$$Le_{f,ij} = \rho C_{p_f} D_{ij}/K_f \tag{A12}$$

where $\tilde{D}_{ij}$ is the multicomponent diffusion coefficient that can be obtained from the binary diffusion coefficient following the approach of reference 65.

For binary diffusion, equation (A8) may be simplified to (ref. 64)

$$J_i^k = -\rho D_{ij}\frac{\partial C_i}{\partial x^k} \tag{A13}$$

If the species j is assumed to be some effective mean species for the gas, then using equations (A7) and (A13) in equation (A3) gives

$$q^k = -K_f\frac{\partial T}{\partial x^k} - \rho\sum_{i=1}^{NS} D_{ij}h_i\frac{\partial C_i}{\partial x^k} \tag{A14}$$

or, for chemical equilibrium flow applications,

$$q^k = -K_f\frac{\partial T}{\partial x^k} - \left(\rho\sum_{i=1}^{NS} D_{ij}h_i\frac{\partial C_i}{\partial T}\right)\frac{\partial T}{\partial x^k} \tag{A15}$$

or

$$q^k = -K\frac{\partial T}{\partial x^k} \tag{A16}$$

where K is the total effective thermal conductivity defined as

$$K = K_f + \rho\sum_{i=1}^{NS} D_{ij}h_i\frac{\partial C_i}{\partial T} \tag{A17}$$

or

$$K = K_f + K_r \tag{A18}$$

with the reactive contribution to the thermal conductivity K_r defined as

$$K_r = \rho\sum_{i=1}^{NS} D_{ij}h_i\frac{\partial C_i}{\partial T} \tag{A19}$$

for chemical equilibrium conditions.

An alternate definition of the reactive thermal conductivity[11] K_r for a flow in chemical equilibrium is given in reference 7 as

$$K_r = k\sum_{l=1}^{NIR}\left\{\frac{(\Delta h_l/R_{univ}T)^2}{\sum_{i=1}^{NS}[(\beta_{i,l}-\alpha_{i,l})/x_i]\sum_{j=1}^{NS}[(\beta_{i,l}-\alpha_{i,l})x_j - (\beta_{j,l}-\alpha_{j,l})x_i]\Delta_{ij}^{(1)}}\right\} \tag{A20}$$

---

[11] The formula for K_r given here already includes the effects of ambipolar diffusion (ref. 66) on the reaction conductivity of an ionized gas.

34

where k is the Boltzmann constant, NIR is the total number of independent reactions in the system, NS is the total number of species in the system, $\Delta h_l = \sum_{i=1}^{NS} (\beta_{i,l} - \alpha_{i,l})h_i$ is the heat of reaction per g-mole for the lth reaction, x_i is the mole fraction of species i, $\Delta_{ij}^{(1)}$ is defined by equation (34), and $\alpha_{i,l}$ and $\beta_{i,l}$ are the stoichiometric coefficients for reactants and products in the reaction given by equation (1). The thermal conductivities K_r given by equations (A19) and (A20) are equivalent under conditions of chemical equilibrium.

Similar to relations (A17) and (A18), the total specific heat at constant pressure may be defined as

$$C_p = \left(\frac{\partial h}{\partial T}\right)_p \tag{A21}$$

or, from equation (9),

$$C_p = C_{p_f} + \left(\sum_{i=1}^{NS} h_i \frac{\partial C_i}{\partial T}\right)_p \tag{A22}$$

or

$$C_p = C_{p_f} + C_{p_r} \tag{A23}$$

with

$$C_{p_r} = \left(\sum_{i=1}^{NS} h_i \frac{\partial C_i}{\partial T}\right)_p \tag{A24}$$

where C_{p_r} is the total contribution to the specific heat at constant pressure.

The specific heat at constant volume C_v may be obtained from

$$C_v = \left(\frac{\partial e}{\partial T}\right)_v \tag{A25}$$

where

$$e = \sum_{i=1}^{NS} C_i(h_i - p_i/\rho_i) \tag{A26}$$

This equation may be used with equation (A21) to obtain the ratio of specific heats γ from

$$\gamma = C_p/C_v \tag{A27}$$

Using the various definitions for the thermal conductivity and the specific heats at constant pressure, the frozen and total Prandtl and Lewis numbers usually employed in dimensionless heat-flux calculations may now be defined.[12]

Generally, the frozen values of specific heat at constant pressure and thermal conductivities are employed in flow-field calculations. Associated heat flux from these calculations is, accordingly, expressed in terms of the frozen Prandtl and Lewis numbers. Alternatively, one may also use total values of specific heat at constant pressure and thermal conductivity in flow-field computations. In this case, the heat flux may be expressed in terms of the total Prandtl and Lewis numbers. However, the total values of C_p and K, as well as those of the total Prandtl and Lewis numbers, can be used only with calculations involving thermal equilibrium. This is obvious from the definitions of K and C_p given by equations (A18) and (A23), respectively.

The frozen Prandtl number and Lewis numbers are defined as

$$N_{Pr,f} = C_{p_f}\mu/K_f \tag{A28}$$

$$Le_{f,ij} = \rho C_{p_f} D_{ij}/K_f \tag{A29}$$

---

[12] Kenneth Sutton of NASA Langley Research Center provided some of these definitions in an unpublished memo.

where C_{p_f} and K_f are defined by equations (9) and (37), respectively. Generally, the subscript f is not used in the literature to denote the frozen Prandtl and Lewis numbers as is done here.

The total Prandtl and Lewis numbers (consisting of both frozen and reactive components) are defined by employing the total values of C_p and K as

$$N_{Pr} = C_p \mu / K \tag{A30}$$

$$Le_{ij} = \rho C_p D_{ij} / K \tag{A31}$$

where C_p and K are defined through equations (A22) and (A18), respectively. Reference 37 gives similar definitions of the total Prandtl and Lewis numbers. The frozen values defined by equations (A28) and (A29) are denoted as partial values in reference 37 and are denoted as Pr' and Le' therein.

Appendix B

Procedure For Obtaining the Heats of Formation at 298.15 K

As mentioned in the main text, various sources provide tabulated values of the species specific enthalpy and free energy based on a reference temperature of 0 K. To transform these thermodynamic values to the 298.15 K reference, the heat of reaction is required at the new reference temperature. The general method employed for this transformation involves calculation of the heat of formation for the reaction

$$\sum_{i=1}^{\text{Reactants}} \alpha_{i,r} X_i \longrightarrow \sum_{i=1}^{\text{Products}} \beta_{i,r} X_i \tag{B1}$$
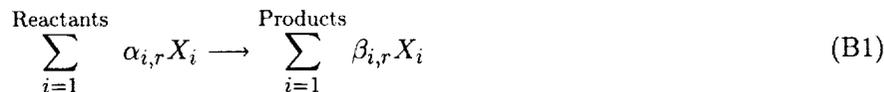
For illustration, the following reaction for the formation of atomic nitrogen, N, may be considered:

$$\frac{1}{2} N_2 \rightarrow N \tag{B2}$$

The heat of formation of a substance is defined as the change in enthalpy created by its production. Since the enthalpy is a point function of temperature and is independent of the path used to arrive at that point, the reactants may be cooled from the reference temperature of 298.15 K to 0 K, thus allowing the formation reaction to occur at the lower temperature. The products may then be heated to the reference temperature of 298.15 K. Through this process we can obtain the heat of formation of atomic nitrogen, N, at 298.15 K by the following relation:

$$(\Delta h_N^f)_{T=298.15} = (\Delta h_N^f)_{T=0} + \Delta h_1 + \Delta h_2 \tag{B3}$$

where

$$\Delta h_1 = \sum_{i=1}^{\text{Reactants}} \alpha_{i,r} \left[(h_i)_{T=0} - (h_i)_{T=298.15} \right] \tag{B4a}$$

$$= \frac{1}{2} \left[(h_{N_2})_{T=0} - (h_{N_2})_{T=298.15} \right] \tag{B4b}$$

$$\Delta h_2 = \sum_{i=1}^{\text{Products}} \beta_{i,r} \left[(h_i)_{T=298.15} - (h_i)_{T=0} \right] \tag{B5a}$$

$$= \left[(h_N)_{T=298.15} - (h_N)_{T=0} \right] \tag{B5b}$$

The reference species used here as reactants in the formation reactions are N_2, O_2, and e^-. Care should be taken in selecting the reaction for the formation of a particular compound. The reactions used for the formation of each substance, along with the heats of formation at 0 K and 298.15 K, are listed in table B1. The heats of formation at 0 K are taken from reference 38. The procedure for obtaining the heat of formation for any substance at 298.15 K from the corresponding value at 0 K is illustrated in figure B1.

Table B1. Reactions for the Formation of Various Substances With Heats of Formation

Substance	Reaction	$(\Delta h_i^f)_{T=298.15}$, kcal/g-mole	$(\Delta h_i^f)_{T=0}$, kcal/g-mole
N	$\frac{1}{2} N_2 \rightarrow N$	112.973	112.529 ± 0.024
O	$\frac{1}{2} O_2 \rightarrow O$	59.553	58.984 ± 0.024
N^+	$\frac{1}{2} N_2 \rightarrow N^+ + e^-$	449.840	447.694 ± 0.1
O^+	$\frac{1}{2} O_2 \rightarrow O^+ + e^-$	374.949	373.024 ± 0.024
NO	$\frac{1}{2} N_2 + \frac{1}{2} O_2 \rightarrow NO$	21.580	21.457 ± 0.04
NO^+	$\frac{1}{2} N_2 + \frac{1}{2} O_2 \rightarrow NO^+ + e^-$	236.660	235.180 ± 0.2
N_2^+	$N_2 \rightarrow N_2^+ + e^-$	360.779	359.298 ± 0.01
O_2^+	$O_2 \rightarrow O_2^+ + e^-$	279.849	278.370 ± 0.2
e^-		0.0	0.0

Reactants
at 298.15 K

$$\Delta h_1 = \sum_{i=1}^{\text{Reactants}} \alpha_{i,r} \, [(h_i)_{T=0} - (h_i)_{T=298.15}]$$

Reactants
at 0 K

$(\Delta h_i^f)_{T=298.15}$
is unknown

$(\Delta h_i^f)_0$
is known
from
tabulated
data

Products
at 298.15 K

$$\Delta h_2 = \sum_{i=1}^{\text{Products}} \beta_{i,r} \, [(h_i)_{T=298.15} - (h_i)_{T=0}]$$

Products
at 0 K
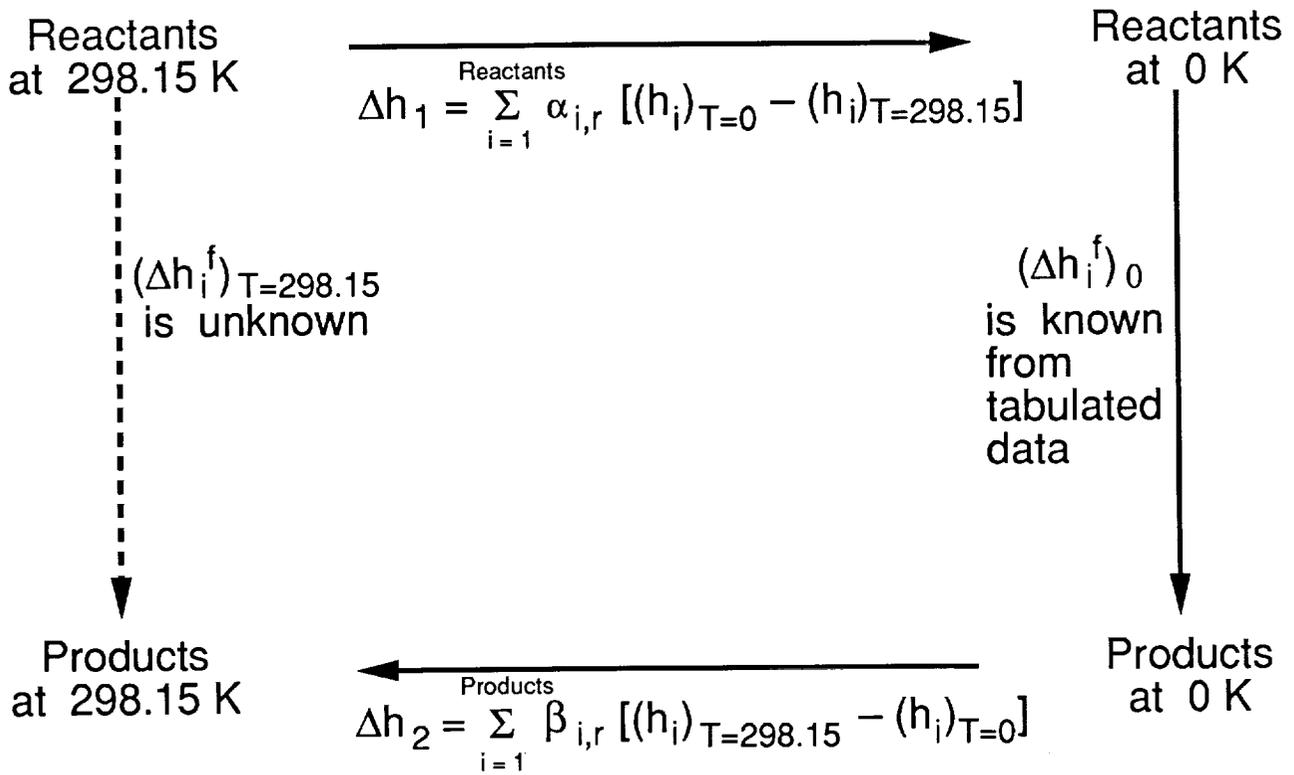
Figure B1. Flow chart for obtaining heat of formation at 298.15 K from corresponding value at 0 K.

Appendix C

Sample Program To Evaluate Thermodynamic Properties From Polynomial Curve Fits

This appendix is a sample Fortran subroutine which evaluates the species specific heats and enthalpies for an 11-species air model using polynomial curve fits as functions of temperature. Five temperature ranges are used for each species for temperatures between 300 K and 30 000 K. Properties evaluated near the temperature range boundaries are smoothed by linearly averaging the polynomial coefficients to assure continuous derivatives. The subroutine may be easily modified for different needs.

```
      SUBROUTINE THERMO(T,CPI,HI)
C  Computes enthalpy and specific heat for 11 species by
C  approximating polynomials.  Polynomial coefficients are stored in
C  arrays A1 to A6 and are linearly averaged at the temperature range
C  boundaries.
C
C  input: T    temperature, K
C  output: CPI  specific heats of the species, cal/g-mole-K
C          HI   enthalpies of the species, cal/g-mole
      DIMENSION A1(11,5),A2(11,5),A3(11,5),A4(11,5),A5(11,5),A6(11,5)
      DIMENSION P(6),COEF(11,5,6)
      DIMENSION CPI(11),HI(11)
      EQUIVALENCE (A1,COEF)
C  Universal gas constant, cal/g-mole-K
      DATA UNIR /1.987/
C
C  Coefficients are input for five temperature ranges
C
      K=4
      L=5
      IF(T.GT.15500.)GO TO 20
      K=3
      L=4
      IF(T.GT.6500)GO TO 30
      K=2
      L=3
      IF(T.GT.1200.)GO TO 40
      K=1
      L=2
      PA=1.0
      PB=0.0
      IF(T.LE.800.)GO TO 50
      PB=(1./400.)*(T-800.)
      PA=1.0-PB
      GO TO 50
   40 CONTINUE
      PA=1.0
      PB=0.0
      IF(T.LE.5500.)GO TO 50
      PB=(1./1000.)*(T-5500.)
      PA=1.0-PB
      GO TO 50
   20 CONTINUE
      PA=0.0
      PB=1.0
```

40

```
      IF(T.GE.25500.)GO TO 50
      PA=1.0
      PB=0.0
      IF(T.LE.24500.)GO TO 50
      PB=0.001*(T-24500.)
      PA=1.0-PB
      GO TO 50
30    CONTINUE
      PA=1.0
      PB=0.0
      IF(T.LE.14500.)GO TO 50
      PB=0.001*(T-14500.)
      PA=1.0-PB
50    CONTINUE
C
      T2=T*T
      T3=T2*T
      T4=T3*T
      TOV=1.0/T
C     Compute properties for 11 species
      DO 65 I=1,11
      DO 60 J=1,6
60    P(J)=PA*COEF(I,K,J)+PB*COEF(I,L,J)
      HI(I)=UNIR*T*(P(1)+0.5*P(2)*T+P(3)*T2/3.+0.25*P(4)*T3
     1 +0.2*P(5)*T4+P(6)*TOV)
      CPI(I)=UNIR*(P(1)+P(2)*T+P(3)*T2+P(4)*T3+P(5)*T4)
65    CONTINUE
      RETURN
      END
```

References

1. Howe, John T.: Introductory Aerothermodynamics of Advanced Space Transportation Systems. AIAA-83-0406, Jan. 1983.

2. Walberg, Gerald D.: A Survey of Aeroassisted Orbit Transfer. *J. Spacecr. & Rockets,* vol. 22, no. 1, Jan. Feb. 1985, pp. 3–18.

3. Williams, Robert M.: National Aero-Space Plane: Technology for America's Future. *Aerosp. America,* vol. 24, no. 11, Nov. 1986, pp. 18–22.

4. Martin, James A.: Orbit on Demand: In this Century If Pushed. *Aerosp. America,* vol. 23, no. 2, Feb. 1985, pp. 46–48.

5. Hansen, C. Frederick; and Heims, Steve P.: *A Review of the Thermodynamic, Transport, and Chemical Reaction Rate Properties of High-Temperature Air.* NACA TN 4359, 1958.

6. Bird, G. A.: *Molecular Gas Dynamics.* Oxford Univ. Press, 1976.

7. Yos, Jerrold M.: *Transport Properties of Nitrogen, Hydrogen, Oxygen, and Air to $30,000\,^oK$.* Tech. Memo. RAD-TM-63-7 (Contract AF33(616)-7578), AVCO Corp., Mar. 22, 1963.

8. Research and Advanced Development Div.: *Theoretical and Experimental Studies of High-Temperature Gas Transport Properties.* Tech. Rep. RAD-TR-65-7 (Contract NASw-916), AVCO Corp., May 1965. (Available as NASA CR-80649.)

9. Yos, J.: *Revised Transport Properties for High Temperature Air and Its Components.* Tech. Release, Dep. Z220, Avco Systems Div., Nov. 28, 1967.

10 Hilsenrath, Joseph; and Beckett, Charles W.: *Tables of Thermodynamic Properties of Argon-Free Air to $15,000^oK$.* AEDC-TN-56-12, Arnold Engineering Development Center, Sept. 1956. (Available from DTIC as AD 989 74.)

11. Gilmore, F. R.: *Equilibrium Composition and Thermodynamic Properties of Air to $24,000^oK$.* U.S. Air Force Proj. Rand Res. Memo. RM-1543, Rand Corp., Aug. 24, 1955. (Available from DTIC as AD 840 52.)

12. Predvoditelev, A. S.; Stupochenko, E. V.; Samuilov, E. V.; Stakhanov, I. P.; Pleshanov, A. S.; and Rozhdestvenskii, I. B.: *Tables of Thermodynamic Functions of Air for the Temperature Range 6,000 $12,000^oK$ and Pressure Range 0.001 1000 atm.* Infosearch, Ltd. (London), 1958.

13. Wilke, C. R.: A Viscosity Equation for Gas Mixtures. *J. Chem. Phys.,* vol. 18, no. 4. Apr. 1950, pp. 517 519.

14. Mason, E. A.; and Saxena, S. C.: Approximate Formula for the Thermal Conductivity of Gas Mixtures. *Phys. Fluids,* vol. 1, no. 5, Sept. Oct. 1958, pp. 361 369.

15. Armaly, Bassem F.; and Sutton, Kenneth: Viscosity of Multicomponent Partially Ionized Gas Mixtures. AIAA-80-1495, July 1980.

16. Thompson, Richard A.; Lee, Kam-Pui; and Gupta, Roop N.: *Computer Codes for the Evaluation of Thermodynamic Properties, Transport Properties, and Equilibrium Constants of an 11-Species Air Model.* NASA TM-102602, 1990.

17. Blottner, F. G.: Viscous Shock Layer at the Stagnation Point With Nonequilibrium Air Chemistry. *AIAA J.,* vol. 7, no. 12, Dec. 1969, pp. 2281 2288.

18. Moss, James N.: *Reacting Viscous-Shock-Layer Solutions With Multicomponent Diffusion and Mass Injection.* NASA TR R-411, 1974.

19. Gupta, Roop N.; and Simmonds, A. L.: Hypersonic Low-Density Solutions of the Navier-Stokes Equations With Chemical Nonequilibrium and Multicomponent Surface Slip. AIAA-86-1349, June 1986.

20. Bortner, M. H.: Suggested Standard Chemical Kinetics for Flow Field Calculations A Consensus Opinion. *AMRAC Proceedings,* Volume XIV, Part I, Doc. No. 4613-135-X (Contract SD-91), Inst. of Science and Technology, Univ. of Michigan, Apr. 18 19, 1966, pp. 569 581. (Available from DTIC as AD 372 900.)

21. Dunn, Michael G.; and Kang, Sang-Wook: *Theoretical and Experimental Studies of Reentry Plasmas.* NASA CR-2232, 1973.

22. Gupta, Roop N.: Navier-Stokes and Viscous Shock-Layer Solutions for Radiating Hypersonic Flows. AIAA-87-1576, June 1987.

23. Park, Chul: *Nonequilibrium Hypersonic Aerothermodynamics.* John Wiley & Sons, Inc., 1989.

24. Park, Chul: A Review of Reaction Rates in High Temperature Air. AIAA-89-1740, June 1989.

25. Park, Chul: Assessment of Two-Temperature Kinetic Model for Ionizing Air. AIAA-87-1574, June 1987.

26. Carlson, Leland A.; and Gally, Thomas A.: The Effect of Electron Temperature and Impact Ionization on Martian Return AOTV Flowfields. AIAA-89-1729, June 1989.

27. Gnoffo, Peter A.; Gupta, Roop N.; and Shinn, Judy L.: *Conservation Equations and Physical Models for Hypersonic Air Flows in Thermal and Chemical Nonequilibrium.* NASA TP-2867, 1989.

28. Treanor, Charles E.; and Marrone, Paul V.: Effect of Dissociation on the Rate of Vibrational Relaxation. *Phys. Fluids,* vol. 5, no. 9, Sept. 1962, pp. 1022–1026.

29. Marrone, Paul V.; and Treanor, Charles E.: Chemical Relaxation With Preferential Dissociation From Excited Vibrational Levels. *Phys. Fluids,* vol. 6, no. 9, Sept. 1963, pp. 1215 1221.

30. Jaffe, Richard L.: Rate Constants for Chemical Reactions in High-Temperature Nonequilibrium Air. Thermo-physical Aspects of Re-Entry Flows, James N. Moss and Carl D. Scott, eds., *Volume 103 of Progress in Astro-nautics and Aeronautics,* American Inst. of Aeronautics and Astronautics, Inc., 1985, pp. 123 151. (Available as AIAA-85-1038.)

31. Moss, James N.; Cuda, Vincent, Jr.; and Simmonds, Ann L.: Nonequilibrium Effects for Hypersonic Transitional Flows. AIAA-87-0404, Jan. 1987.

32. Sharma, Surendra P.; Huo, Winifred M.; and Park, Chul: The Rate Parameters for Coupled Vibration-Dissociation in a Generalized SSH Approximation. AIAA-88-2714, June 1988.

33. McBride, Bonnie J.; Heimel, Sheldon; Ehlers, Janet G.; and Gordon, Sanford: *Thermodynamic Properties to $6000^{\circ}K$ for 210 Substances Involving the First 18 Elements.* NASA SP-3001, 1963.

34. Browne, William G.: *Thermodynamic Properties of Some Atoms and Atomic Ions.* Eng. Phys. Tech. Memo # 2, Missile and Space Vehicle Dep., General Electric Co., May 14, 1962.

35. Browne, William G.: *Thermodynamic Properties of Some Diatoms and Diatomic Ions at High Temperatures.* Advanced Aerospace Phys. Tech. Memo. No. 8, Missile and Space Vehicle Dep., General Electric Co., May 14, 1962.

36. Hirschfelder, Joseph O.; Curtiss, Charles F.; and Bird, R. Byron: *Molecular Theory of Gases and Liquids, Corrected Printing With Notes Added.* John Wiley & Sons, Inc., 1967.

37. Hansen, C. Frederick: *Approximations for the Thermodynamic and Transport Properties of High-Temperature Air.* NASA TR R-50, 1959. (Supersedes NACA TN 4150.)

38. Chase, M. W., Jr.; Davies, C. A.; Downey, J. R., Jr.; Frurip, D. J.; McDonald, R. A.; and Syverud, A. N.: JANAF Thermochemical Tables, Third ed. Part II, Cr Zr. *J. Phys. & Chem.* Ref. Data, vol. 14, suppl. no. 1, 1985.

39. Bade, W. L.; and Yos, J. M.: *The NATA Code Theory and Analysis. Volume I.* NASA CR-2547, 1975.

40. Bade, W. L.; and Yos, J. M.: *The NATA Code Theory and Analysis. Volume 2: User's Manual.* NASA CR-141743, 1975.

41. Bade, W. L.; and Yos, J. M.: *The NATA Code Theory and Analysis. Volume 3: Programmer's Manual.* NASA CR-141744, 1975.

42. Monchick, Louis: Collision Integrals for the Exponential Repulsive Potential. *Phys. Fluids,* vol. 2, no. 6, Nov. Dec. 1959, pp. 695 700.

43. Yos, Jerrold M.: *Approximate Equations for the Viscosity and Translational Thermal Conductivity of Gas Mixtures.* AVSSD-0112-67-RM (Contract No. C404-000-Z100), Avco Missiles, Space and Electronics Group, Missile Systems Div., Apr. 1967.

44. Svehla, Roger A.: *Estimated Viscosities and Thermal Conductivities of Gases at High Temperatures.* NASA TR R-132, 1962.

45. Mason, E. A.; and Monchick, L.: Heat Conductivity of Polyatomic and Polar Gases. *J. Chem. Phys.,* vol. 36, no. 6, Mar. 15, 1962, pp. 1622 1639.

46. Monchick, L.; Pereira, A. N. G.; and Mason, E. A.: Heat Conductivity of Polyatomic and Polar Gases and Gas Mixtures. *J. Chem. Phys.,* vol. 42, no. 9, May 1, 1965, pp. 3241 3256.

47. Svehla, Roger A.; and McBride, Bonnie J.: *FORTRAN IV Computer Program for Calculation of Thermodynamic and Transport Properties of Complex Chemical Systems.* NASA TN D-7056, 1973.

48. Yun, Kwang-Sik; Weissman, Stanley; and Mason, E. A.: High-Temperature Transport Properties of Dissociating Nitrogen and Dissociating Oxygen. *Phys. Fluids,* vol. 5, no. 6, June 1962, pp. 672 678.

49. Spitzer, Lyman, Jr.: *Physics of Fully Ionized Gases, Second Revis. ed.* Interscience Publ., 1962.

50. Stebbings, R. F.; Smith, A. C. H.; and Ehrhardt, H.: Charge Transfer Between Oxygen Atoms and O^+ and H^+ Ions. *J. Geophys. Res.,* vol. 69, no. 11, June 1, 1964, pp. 2349 2355.

51. Chapman, Sydney; and Cowling, T. G.: *The Mathematical Theory of Non-Uniform Gases, Second ed.* Cambridge Univ. Press, 1952.

52. Peng, T. C.; and Pindroh, A. L.: *An Improved Calculation of Gas Properties at High Temperatures.* Doc. No. D2-11722, Boeing Airplane Co., Feb. 23, 1962.

53. Brokaw, Richard S.: Approximate Formulas for the Viscosity and Thermal Conductivity of Gas Mixtures. *J. Chem. Phys.,* vol. 29, no. 2, Aug. 1958, pp. 391 397.

54. Hirschfelder, Joseph O.: Heat Conductivity in Polyatomic or Electronically Excited Gases. II. *J. Chem. Phys.,* vol. 26, no. 2, Feb. 1957, pp. 282 285.

55. Buddenberg, J. W.; and Wilke, C. R.: Calculation of Gas Mixture Viscosities. *Ind. & Eng. Chem.,* vol. 41, no. 7, July 1949, pp. 1345 1347.

56. Armaly, Bassem F.; and Sutton, Kenneth: Thermal Conductivity of Partially Ionized Gas Mixtures. AIAA-81-1174, June 1981.

57. Hansen, C. Frederick: Interpretation of Linear Approximations for the Viscosity of Gas Mixtures. *Phys. Fluids,* vol. 4, no. 7, July 1961, pp. 926 927.

58. Kennard, Earle H.: *Kinetic Theory of Gases.* McGraw-Hill Book Co., Inc., 1938.

59. Morris, J. C.; Rudis, R. P.; and Yos, J. M.: Measurements of Electrical and Thermal Conductivity of Hydrogen, Nitrogen and Argon at High Temperatures. *Phys. Fluids,* vol. 13, no. 3, Mar. 1970, pp. 608–617.

60. Vanderslice, Joseph T.; Mason, Edward A.; and Lippincott, Ellis R.: Interactions Between Ground-State Nitrogen Atoms and Molecules. The N–N, N–N_2, and N_2–N_2 Interactions. *J. Chem. Phys.,* vol. 30, no. 1, Jan. 1959, pp. 129–136.

61. Esch, Donald D.; Pike, Ralph W.; Engel, Carl D.; Farmer, Richard C.; and Balhoff, John F.: *Stagnation Region Heating of a Phenolic-Nylon Ablator During Return From Planetary Missions.* NASA CR-112026, 1971.

62. Lee, Jong-Hun: Basic Governing Equations for the Flight Regimes of Aeroassisted Orbital Transfer Vehicles. *Thermal Design of Aeroassisted Transfer Vehicles,* H. F. Nelson, ed., Volume 96 of Progress in Astronautics and Aeronautics, American Inst. of Aeronautics and Astronautics, Inc., 1985, pp. 3–53.

63. Vincenti, Walter G.; and Kruger, Charles H., Jr.: *Introduction to Physical Gas Dynamics.* John Wiley & Sons, Inc., c.1965.

64. Gupta, Roop N.; Scott, Carl D.; and Moss, James N.: *Slip-Boundary Equations for Multicomponent Nonequilibrium Airflow.* NASA TP-2452, 1985.

65. Blottner, F. G.: Finite Difference Methods of Solution of the Boundary-Layer Equations. *AIAA J.,* vol. 8, no. 2, Feb. 1970, pp. 193–205.

66. Blottner, F. G.: Nonequilibrium Laminar Boundary-Layer Flow of Ionized Air. *AIAA J.,* vol. 2, no. 11, Nov. 1964, pp. 1921–1927.

67. Gupta, Roop N.; and Simmonds, Ann L.: Stagnation Flowfield Analysis for an Aeroassist Flight Experiment Vehicle. AIAA-88-2613, June 1988.

Table I. Third Body Efficiencies Relative to Argon*

Catalytic bodies	$Z_{(j-NS),i}$	Efficiencies relative to argon of—									
		O_2 $(i=1)$	N_2 $(i=2)$	O $(i=3)$	N $(i=4)$	NO $(i=5)$	NO^+ $(i=6)$	O_2^+ $(i=7)$	N_2^+ $(i=8)$	O^+ $(i=9)$	N^+ $(i=10)$
M_1	1,i	9	2	25	1	1	0	0	0	0	0
M_2	2,i	1	2.5	1	0	1	0	0	0	0	0
M_3	3,i	1	1	20	20	20	0	0	0	0	0
M_4	4,i	4	1	0	0	0	0	0	0	0	0
e^-	5,i	0	0	0	0	0	1	1	1	1	1

*Extension for the 11 species and 5 catalytic bodies is based on the work of reference 17.

Table II. Chemical Reactions and Rate Coefficients

Reaction number,[*] r	Reaction	Forward rate coefficient, $k_{f,r}$, cm³/mole-sec	Backward rate coefficient, $k_{b,r}$, cm³/mole-sec or cm⁶/mole²-sec	Third body M
1	$O_2 + M_1 \rightleftarrows 2O + M_1$	$3.61 \times 10^{18} T^{-1.0} \exp(-5.94 \times 10^4/T)$	$3.01 \times 10^{15} T^{-0.5}$	O, N, O₂, N₂, NO
2	$N_2 + M_2 \rightleftarrows 2N + M_2$	$1.92 \times 10^{17} T^{-0.5} \exp(-1.131 \times 10^5/T)$	$1.09 \times 10^{16} T^{-0.5}$	O, O₂, N₂, NO
3	$N_2 + N \rightleftarrows 2N + N$	$4.15 \times 10^{22} T^{-1.5} \exp(-1.131 \times 10^5/T)$	$2.32 \times 10^{21} T^{-1.5}$	
4	$NO + M_3 \rightleftarrows N + O + M_3$	$3.97 \times 10^{20} T^{-1.5} \exp(-7.56 \times 10^4/T)$	$1.01 \times 10^{20} T^{-1.5}$	O, N, O₂, N₂, NO
5	$NO + O \rightleftarrows O_2 + N$	$3.18 \times 10^{9} T^{1.0} \exp(-1.97 \times 10^4/T)$	$9.63 \times 10^{11} T^{0.5} \exp(-3.6 \times 10^3/T)$	
6	$N_2 + O \rightleftarrows NO + N$	$6.75 \times 10^{13} \exp(-3.75 \times 10^4/T)$	1.5×10^{13}	
7	$N + O \rightleftarrows NO^+ + e^-$	$9.03 \times 10^{9} T^{0.5} \exp(-3.24 \times 10^4/T)$	$1.80 \times 10^{19} T^{-1.0}$	
8	$O + e^- \rightleftarrows O^+ + e^- + e^-$	$(3.6 \pm 1.2) \times 10^{31} T^{-2.91} \exp(-1.58 \times 10^5/T)$	$(2.2 \pm 0.7) \times 10^{40} T^{-4.5}$	
9	$N + e^- \rightleftarrows N^+ + e^- + e^-$	$(1.1 \pm 0.4) \times 10^{32} T^{-3.14} \exp(-1.69 \times 10^5/T)$	$(2.2 \pm 0.7) \times 10^{40} T^{-4.5}$	
10	$O + O \rightleftarrows O_2^+ + e^-$	$(1.6 \pm 0.4) \times 10^{17} T^{-0.98} \exp(-8.08 \times 10^4/T)$	$(8.02 \pm 2.0) \times 10^{21} T^{-1.5}$	
11	$O + O_2^+ \rightleftarrows O_2 + O^+$	$2.92 \times 10^{18} T^{-1.11} \exp(-2.8 \times 10^4/T)$	$7.8 \times 10^{11} T^{0.5}$	
12	$N_2 + N^+ \rightleftarrows N + N_2^+$	$2.02 \times 10^{11} T^{0.81} \exp(-1.3 \times 10^4/T)$	$7.8 \times 10^{11} T^{0.5}$	
13	$N + N \rightleftarrows N_2^+ + e^-$	$(1.4 \pm 0.3) \times 10^{13} \exp(-6.78 \times 10^4/T)$	$(1.5 \pm 0.5) \times 10^{22} T^{-1.5}$	
14	$O_2 + N_2 \rightleftarrows NO + NO^+ + e^-$	$1.38 \times 10^{20} T^{-1.84} \exp(-1.41 \times 10^5/T)$	$1.0 \times 10^{24} T^{-2.5}$	
15	$NO + M_4 \rightleftarrows NO^+ + e^- + M_4$	$2.2 \times 10^{15} T^{-0.35} \exp(-1.08 \times 10^5/T)$	$2.2 \times 10^{26} T^{-2.5}$	O₂, N₂
16	$O + NO^+ \rightleftarrows NO + O^+$	$3.63 \times 10^{15} T^{-0.6} \exp(-5.08 \times 10^4/T)$	1.5×10^{13}	
17	$N_2 + O^+ \rightleftarrows O + N_2^+$	$3.4 \times 10^{19} T^{-2.0} \exp(-2.3 \times 10^4/T)$	$2.48 \times 10^{19} T^{-2.2}$	
18	$N + NO^+ \rightleftarrows NO + N^+$	$1.0 \times 10^{19} T^{-0.93} \exp(-6.1 \times 10^4/T)$	4.8×10^{14}	
19	$O_2 + NO^+ \rightleftarrows NO + O_2^+$	$1.8 \times 10^{15} T^{0.17} \exp(-3.3 \times 10^4/T)$	$1.8 \times 10^{13} T^{0.5}$	
20	$O + NO^+ \rightleftarrows O_2 + N^+$	$1.34 \times 10^{13} T^{0.31} \exp(-7.727 \times 10^4/T)$	1.0×10^{14}	

*Reactions and reaction rates for numbers 1 to 7 are from Blottner's (ref. 17) 7-species chemical model and those for numbers 8 to 20 are from reference 21.

46

Table III. Curve-fit Coefficients for Equilibrium Constant K_{eq} at Different Number Densities

Number density, particles/cm³	$A_{K_{eq,r}}$	$B_{K_{eq,r}}$	$C_{K_{eq,r}}$	$D_{K_{eq,r}}$	$E_{K_{eq,r}}$	$F_{K_{eq,r}}$
*Reaction 1: $O_2 + M_1 \rightleftharpoons 2\,O + M_1$						
10^{14}	$0.000000E+00$	$-0.828621E+00$	$-0.105568E+01$	$0.151416E+01$	$-0.107091E+02$	$-0.307176E+01$
10^{15}	$0.000000E+00$	$-0.719241E+00$	$-0.135815E+01$	$0.973802E+00$	$-0.913167E+01$	$-0.352942E+01$
10^{16}	$0.000000E+00$	$-0.616239E+00$	$-0.160998E+01$	$0.365775E+00$	$-0.768180E+01$	$-0.382001E+01$
10^{17}	$0.000000E+00$	$-0.538034E+00$	$-0.176687E+01$	$-0.214344E+00$	$-0.655629E+01$	$-0.394645E+01$
10^{18}	$0.000000E+00$	$-0.481290E+00$	$-0.183099E+01$	$-0.828353E+00$	$-0.562039E+01$	$-0.396649E+01$
10^{19}	$0.000000E+00$	$-0.466031E+00$	$-0.178672E+01$	$-0.124877E+01$	$-0.515926E+01$	$-0.392801E+01$
Reaction 2: $N_2 + M_2 \rightleftharpoons 2\,N + M_2$						
10^{14}	$0.000000E+00$	$-0.142518E+01$	$-0.179191E+01$	$-0.152245E+00$	$-0.172635E+02$	$-0.777060E+01$
10^{15}	$0.000000E+00$	$-0.131460E+01$	$-0.211364E+01$	$-0.655486E+00$	$-0.156315E+02$	$-0.831884E+01$
10^{16}	$0.000000E+00$	$-0.120533E+01$	$-0.240055E+01$	$-0.123908E+01$	$-0.140810E+02$	$-0.870302E+01$
10^{17}	$0.000000E+00$	$-0.111597E+01$	$-0.260376E+01$	$-0.181730E+01$	$-0.128199E+02$	$-0.890679E+01$
10^{18}	$0.000000E+00$	$-0.104068E+01$	$-0.273172E+01$	$-0.246330E+01$	$-0.116894E+02$	$-0.898864E+01$
10^{19}	$0.000000E+00$	$-0.100734E+01$	$-0.274128E+01$	$-0.293912E+01$	$-0.110496E+02$	$-0.897632E+01$
Reaction 3: $N_2 + N \rightleftharpoons 2\,N + N$						
10^{14}	$0.000000E+00$	$-0.142518E+01$	$-0.179191E+01$	$-0.152245E+00$	$-0.172635E+02$	$-0.777060E+01$
10^{15}	$0.000000E+00$	$-0.131460E+01$	$-0.211364E+01$	$-0.655486E+00$	$-0.156315E+02$	$-0.831884E+01$
10^{16}	$0.000000E+00$	$-0.120533E+01$	$-0.240055E+01$	$-0.123908E+01$	$-0.140810E+02$	$-0.870302E+01$
10^{17}	$0.000000E+00$	$-0.111597E+01$	$-0.260376E+01$	$-0.181730E+01$	$-0.128199E+02$	$-0.890679E+01$
10^{18}	$0.000000E+00$	$-0.104068E+01$	$-0.273172E+01$	$-0.246330E+01$	$-0.116894E+02$	$-0.898864E+01$
10^{19}	$0.000000E+00$	$-0.100734E+01$	$-0.274128E+01$	$-0.293912E+01$	$-0.110496E+02$	$-0.897632E+01$
Reaction 4: $NO + M_3 \rightleftharpoons N + O + M_3$						
10^{14}	$0.000000E+00$	$-0.102874E+01$	$-0.121018E+01$	$0.111429E+01$	$-0.131595E+02$	$-0.572854E+01$
10^{15}	$0.000000E+00$	$-0.918760E+00$	$-0.152228E+01$	$0.592488E+00$	$-0.115548E+02$	$-0.623150E+01$
10^{16}	$0.000000E+00$	$-0.812622E+00$	$-0.179165E+01$	$-0.332370E-02$	$-0.100546E+02$	$-0.656888E+01$
10^{17}	$0.000000E+00$	$-0.728842E+00$	$-0.197170E+01$	$-0.582492E+00$	$-0.886131E+01$	$-0.673398E+01$
10^{18}	$0.000000E+00$	$-0.662823E+00$	$-0.206774E+01$	$-0.121250E+01$	$-0.782813E+01$	$-0.678492E+01$
10^{19}	$0.000000E+00$	$-0.638527E+00$	$-0.205038E+01$	$-0.166061E+01$	$-0.727765E+01$	$-0.675953E+01$

* Reaction numbers given here correspond to those in table II, which also contains definitions for the third bodies, M_i ($i = 1, 2, 3, 4$).

Table III. Continued

Number density, particles/cm³	$A_{K_{eq,r}}$	$B_{K_{eq,r}}$	$C_{K_{eq,r}}$	$D_{K_{eq,r}}$	$E_{K_{eq,r}}$	$F_{K_{eq,r}}$
Reaction 5: NO + O ⇌ O₂ + N						
10^{14}	$0.000000E+00$	$-0.233168E+00$	$-0.225679E+00$	$-0.517639E+00$	$-0.278006E+01$	$-0.302215E+01$
10^{15}	$0.000000E+00$	$-0.232567E+00$	$-0.235307E+00$	$-0.499081E+00$	$-0.275280E+01$	$-0.306745E+01$
10^{16}	$0.000000E+00$	$-0.229430E+00$	$-0.252843E+00$	$-0.486866E+00$	$-0.270247E+01$	$-0.311424E+01$
10^{17}	$0.000000E+00$	$-0.223855E+00$	$-0.276009E+00$	$-0.485915E+00$	$-0.263469E+01$	$-0.315291E+01$
10^{18}	$0.000000E+00$	$-0.214580E+00$	$-0.307925E+00$	$-0.501912E+00$	$-0.253742E+01$	$-0.318381E+01$
10^{19}	$0.000000E+00$	$-0.205544E+00$	$-0.334842E+00$	$-0.529614E+00$	$-0.244806E+01$	$-0.319689E+01$
Reaction 6: N₂ + O ⇌ NO + N						
10^{14}	$0.000000E+00$	$-0.396440E+00$	$-0.581737E+00$	$-0.126653E+01$	$-0.410395E+01$	$-0.204206E+01$
10^{15}	$0.000000E+00$	$-0.395839E+00$	$-0.591364E+00$	$-0.124797E+01$	$-0.407669E+01$	$-0.208735E+01$
10^{16}	$0.000000E+00$	$-0.392703E+00$	$-0.608901E+00$	$-0.123576E+01$	$-0.402636E+01$	$-0.213415E+01$
10^{17}	$0.000000E+00$	$-0.387127E+00$	$-0.632066E+00$	$-0.123481E+01$	$-0.395858E+01$	$-0.217281E+01$
10^{18}	$0.000000E+00$	$-0.377852E+00$	$-0.663983E+00$	$-0.125081E+01$	$-0.386131E+01$	$-0.220371E+01$
10^{19}	$0.000000E+00$	$-0.368817E+00$	$-0.690900E+00$	$-0.127851E+01$	$-0.377195E+01$	$-0.221680E+01$
Reaction 7: N + O ⇌ NO⁺ + e⁻						
10^{14}	$-0.308374E+00$	$0.831634E+00$	$0.276168E+00$	$-0.715691E+00$	$-0.310632E+00$	$-0.114489E+02$
10^{15}	$-0.283546E+00$	$0.654679E+00$	$0.483584E+00$	$-0.641636E+00$	$-0.179311E+01$	$-0.110019E+02$
10^{16}	$-0.237256E+00$	$0.423671E+00$	$0.577781E+00$	$-0.541270E+00$	$-0.306540E+01$	$-0.107689E+02$
10^{17}	$-0.180028E+00$	$0.185513E+00$	$0.496540E+00$	$-0.432931E+00$	$-0.397692E+01$	$-0.107328E+02$
10^{18}	$-0.110967E+00$	$-0.668014E-01$	$0.301396E+00$	$-0.309083E+00$	$-0.467007E+01$	$-0.108375E+02$
10^{19}	$-0.636990E-01$	$-0.218605E+00$	$0.847459E-01$	$-0.222625E+01$	$-0.498783E+01$	$-0.109694E+02$
Reaction 8: O + e⁻ ⇌ O⁺ + e⁻ + e⁻						
10^{14}	$-0.454142E+00$	$0.169029E-01$	$-0.205312E+01$	$-0.105613E+02$	$-0.154030E+02$	$-0.215570E+02$
10^{15}	$-0.442619E+00$	$-0.930789E-01$	$-0.182913E+01$	$-0.103294E+02$	$-0.161706E+02$	$-0.213094E+02$
10^{16}	$-0.410741E+00$	$-0.261721E+00$	$-0.170184E+01$	$-0.984387E+01$	$-0.168396E+02$	$-0.212010E+02$
10^{17}	$-0.368429E+00$	$-0.445136E+00$	$-0.168076E+01$	$-0.923660E+01$	$-0.173180E+02$	$-0.212121E+02$
10^{18}	$-0.319211E+00$	$-0.634295E+00$	$-0.174946E+01$	$-0.852603E+01$	$-0.176715E+02$	$-0.213010E+02$
10^{19}	$-0.289041E+00$	$-0.737514E+00$	$-0.184624E+01$	$-0.805937E+01$	$-0.178217E+02$	$-0.213843E+02$

Table III. Continued

Number density, particles/cm³	$A_{K_{eq,r}}$	$B_{K_{eq,r}}$	$C_{K_{eq,r}}$	$D_{K_{eq,r}}$	$E_{K_{eq,r}}$	$F_{K_{eq,r}}$
Reaction 9: $N + e^- \rightleftharpoons N^+ + e^- + e^-$
10^{14}	$-0.474396E+00$	$0.614580E-02$	$-0.229468E+01$	$-0.114334E+02$	$-0.157101E+02$	$-0.213937E+02$
10^{15}	$-0.474831E+00$	$-0.654883E-01$	$-0.202828E+01$	$-0.113511E+02$	$-0.165058E+02$	$-0.210712E+02$
10^{16}	$-0.453275E+00$	$-0.204988E+00$	$-0.185082E+01$	$-0.109883E+02$	$-0.172377E+02$	$-0.208889E+02$
10^{17}	$-0.417456E+00$	$-0.373700E+00$	$-0.178585E+01$	$-0.104515E+02$	$-0.177927E+02$	$-0.208436E+02$
10^{18}	$-0.370274E+00$	$-0.564285E+00$	$-0.182040E+01$	$-0.975050E+01$	$-0.182364E+02$	$-0.208947E+02$
10^{19}	$-0.337233E+00$	$-0.682777E+00$	$-0.190692E+01$	$-0.923376E+01$	$-0.184523E+02$	$-0.209704E+02$
Reaction 10: $O + O \rightleftharpoons O_2^+ + e^-$
10^{14}	$-0.404633E+00$	$0.587134E+00$	$-0.944981E-01$	$-0.965358E+01$	$-0.601891E+01$	$-0.157055E+02$
10^{15}	$-0.374219E+00$	$0.395710E+00$	$0.797369E-01$	$-0.884526E+01$	$-0.744662E+01$	$-0.153164E+02$
10^{16}	$-0.322759E+00$	$0.153892E+00$	$0.114598E+00$	$-0.778383E+01$	$-0.864313E+01$	$-0.151418E+02$
10^{17}	$-0.262628E+00$	$-0.865210E-01$	$0.179512E-01$	$-0.667391E+01$	$-0.947258E+01$	$-0.151509E+02$
10^{18}	$-0.194432E+00$	$-0.327225E+00$	$-0.205459E+00$	$-0.545905E+01$	$-0.100727E+02$	$-0.152846E+02$
10^{19}	$-0.151657E+00$	$-0.457874E+00$	$-0.430084E+00$	$-0.466176E+01$	$-0.103232E+02$	$-0.154195E+02$
Reaction 11: $O + O_2^+ \rightleftharpoons O_2 + O^+$
10^{14}	$-0.238630E+00$	$0.672246E+00$	$-0.312986E+00$	$-0.443140E+01$	$-0.566846E+00$	$-0.341823E+01$
10^{15}	$-0.227108E+00$	$0.562265E+00$	$-0.890019E-01$	$-0.419943E+01$	$-0.133444E+01$	$-0.317067E+01$
10^{16}	$-0.195230E+00$	$0.393622E+00$	$0.382875E-01$	$-0.371395E+01$	$-0.200352E+01$	$-0.306225E+01$
10^{17}	$-0.152918E+00$	$0.210208E+00$	$0.593682E-01$	$-0.310667E+01$	$-0.248187E+01$	$-0.307338E+01$
10^{18}	$-0.103699E+00$	$0.210489E-01$	$-0.933321E-02$	$-0.239611E+01$	$-0.283537E+01$	$-0.316226E+01$
10^{19}	$-0.735291E-01$	$-0.821705E-01$	$-0.106106E+00$	$-0.192945E+01$	$-0.298555E+01$	$-0.324557E+01$
Reaction 12: $N_2 + N^+ \rightleftharpoons N + N_2^+$
10^{14}	$0.000000E+00$	$-0.454093E+00$	$0.710863E+00$	$0.878489E+00$	$-0.551525E+01$	$-0.128042E-01$
10^{15}	$0.000000E+00$	$-0.381287E+00$	$0.446289E+00$	$0.792372E+00$	$-0.472167E+01$	$-0.334316E+00$
10^{16}	$0.000000E+00$	$-0.299935E+00$	$0.177941E+00$	$0.619510E+00$	$-0.388369E+01$	$-0.565230E+00$
10^{17}	$0.000000E+00$	$-0.227847E+00$	$-0.380430E-01$	$0.398254E+00$	$-0.315226E+01$	$-0.691244E+00$
10^{18}	$0.000000E+00$	$-0.164537E+00$	$-0.202432E+00$	$0.112950E+00$	$-0.247625E+01$	$-0.746487E+00$
10^{19}	$0.000000E+00$	$-0.135176E+00$	$-0.255223E+00$	$-0.112672E+00$	$-0.209774E+01$	$-0.745209E+00$

Table III. Continued

Number density, particles/cm^3	$A_{K_{eq,r}}$	$B_{K_{eq,r}}$	$C_{K_{eq,r}}$	$D_{K_{eq,r}}$	$E_{K_{eq,r}}$	$F_{K_{eq,r}}$
Reaction 13: $N + N \rightleftharpoons N_2^+ + e^-$						
10^{14}	$-0.412910E+00$	$0.821758E+00$	$-0.287790E-01$	$-0.982394E+01$	$-0.355555E+01$	$-0.136596E+02$
10^{15}	$-0.393669E+00$	$0.659271E+00$	$0.211819E+00$	$-0.915117E+01$	$-0.509279E+01$	$-0.131548E+02$
10^{16}	$-0.352549E+00$	$0.439073E+00$	$0.325352E+00$	$-0.820528E+01$	$-0.644087E+01$	$-0.128633E+02$
10^{17}	$-0.298223E+00$	$0.203171E+00$	$0.299515E+00$	$-0.714841E+01$	$-0.743445E+01$	$-0.127819E+02$
10^{18}	$-0.228297E+00$	$-0.607538E-01$	$0.132638E+00$	$-0.588631E+01$	$-0.822061E+01$	$-0.128577E+02$
10^{19}	$-0.176536E+00$	$-0.233712E+00$	$-0.760369E-01$	$-0.495445E+01$	$-0.860561E+01$	$-0.129867E+02$
Reaction 14: $O_2 + N_2 \rightleftharpoons NO + NO^+ + e^-$						
10^{14}	$-0.231244E+00$	$-0.711962E+00$	$-0.192440E+01$	$-0.662339E+01$	$-0.158460E+02$	$-0.179580E+02$
10^{15}	$-0.231244E+00$	$-0.711962E+00$	$-0.192440E+01$	$-0.662339E+01$	$-0.158460E+02$	$-0.179580E+02$
10^{16}	$-0.231244E+00$	$-0.711962E+00$	$-0.192440E+01$	$-0.662339E+01$	$-0.158460E+02$	$-0.179580E+02$
10^{17}	$-0.231244E+00$	$-0.711962E+00$	$-0.192440E+01$	$-0.662339E+01$	$-0.158460E+02$	$-0.179580E+02$
10^{18}	$-0.231244E+00$	$-0.711962E+00$	$-0.192440E+01$	$-0.662339E+01$	$-0.158460E+02$	$-0.179580E+02$
10^{19}	$-0.231244E+00$	$-0.711962E+00$	$-0.192440E+01$	$-0.662339E+01$	$-0.158460E+02$	$-0.179580E+02$
Reaction 15: $NO + M_4 \rightleftharpoons NO^+ + e^- + M_4$						
10^{14}	$-0.167618E+00$	$-0.576804E+00$	$-0.152748E+01$	$-0.480246E+01$	$-0.127771E+02$	$-0.174947E+02$
10^{15}	$-0.167618E+00$	$-0.576804E+00$	$-0.152748E+01$	$-0.480246E+01$	$-0.127771E+02$	$-0.174947E+02$
10^{16}	$-0.167618E+00$	$-0.576804E+00$	$-0.152748E+01$	$-0.480246E+01$	$-0.127771E+02$	$-0.174947E+02$
10^{17}	$-0.167618E+00$	$-0.576804E+00$	$-0.152748E+01$	$-0.480246E+01$	$-0.127771E+02$	$-0.174947E+02$
10^{18}	$-0.167618E+00$	$-0.576804E+00$	$-0.152748E+01$	$-0.480246E+01$	$-0.127771E+02$	$-0.174947E+02$
10^{19}	$-0.167618E+00$	$-0.576804E+00$	$-0.152748E+01$	$-0.480246E+01$	$-0.127771E+02$	$-0.174947E+02$
Reaction 16: $O + NO^+ \rightleftharpoons NO + O^+$						
10^{14}	$-0.287924E+00$	$0.589931E+00$	$-0.536001E+00$	$-0.579812E+01$	$-0.270809E+01$	$-0.414258E+01$
10^{15}	$-0.276402E+00$	$0.479949E+00$	$-0.312017E+00$	$-0.556615E+01$	$-0.347569E+01$	$-0.389502E+01$
10^{16}	$-0.244524E+00$	$0.311307E+00$	$-0.184728E+00$	$-0.508067E+01$	$-0.414477E+01$	$-0.378660E+01$
10^{17}	$-0.202212E+00$	$0.127893E+00$	$-0.163647E+00$	$-0.447339E+01$	$-0.462312E+01$	$-0.379773E+01$
10^{18}	$-0.152993E+00$	$-0.612664E-01$	$-0.232348E+00$	$-0.376282E+01$	$-0.497662E+01$	$-0.388661E+01$
10^{19}	$-0.122823E+00$	$-0.164486E+00$	$-0.329121E+00$	$-0.329617E+01$	$-0.512679E+01$	$-0.396992E+01$

Table III. Concluded

Number density, particles/cm^3	$A_{K_{eq,r}}$	$B_{K_{eq,r}}$	$C_{K_{eq,r}}$	$D_{K_{eq,r}}$	$E_{K_{eq,r}}$	$F_{K_{eq,r}}$
Reaction 17: $N_2 + O^+ \rightleftharpoons O + N_2^+$						
10^{14}	$0.000000E+00$	$-0.510046E+00$	$0.404235E+00$	$0.218493E+00$	$-0.562846E+01$	$0.209226E+00$
10^{15}	$0.000000E+00$	$-0.431146E+00$	$0.131669E+00$	$0.880469E-01$	$-0.480413E+01$	$-0.643024E-01$
10^{16}	$0.000000E+00$	$-0.348496E+00$	$-0.130027E+00$	$-0.116570E+00$	$-0.397810E+01$	$-0.244581E+00$
10^{17}	$0.000000E+00$	$-0.279222E+00$	$-0.329509E+00$	$-0.351046E+00$	$-0.329143E+01$	$-0.328820E+00$
10^{18}	$0.000000E+00$	$-0.222833E+00$	$-0.468329E+00$	$-0.627963E+00$	$-0.269560E+01$	$-0.350877E+00$
10^{19}	$0.000000E+00$	$-0.200998E+00$	$-0.498762E+00$	$-0.828803E+00$	$-0.239688E+01$	$-0.335574E+00$
Reaction 18: $N + NO^+ \rightleftharpoons NO + N^+$						
10^{14}	$-0.306778E+00$	$0.582950E+00$	$-0.767203E+00$	$-0.663096E+01$	$-0.293297E+01$	$-0.389893E+01$
10^{15}	$-0.307212E+00$	$0.511315E+00$	$-0.500797E+00$	$-0.654867E+01$	$-0.372868E+01$	$-0.357644E+01$
10^{16}	$-0.285656E+00$	$0.371815E+00$	$-0.323335E+00$	$-0.618588E+01$	$-0.446054E+01$	$-0.339411E+01$
10^{17}	$-0.249838E+00$	$0.203103E+00$	$-0.258375E+00$	$-0.564904E+01$	$-0.501561E+01$	$-0.334883E+01$
10^{18}	$-0.202656E+00$	$0.125187E-01$	$-0.292918E+00$	$-0.494803E+01$	$-0.545932E+01$	$-0.339994E+01$
10^{19}	$-0.169615E+00$	$-0.105973E+00$	$-0.379439E+00$	$-0.443130E+01$	$-0.567515E+01$	$-0.347569E+01$
Reaction 19: $O_2 + NO^+ \rightleftharpoons NO + O_2^+$						
10^{14}	$0.000000E+00$	$-0.311598E+00$	$-0.638297E+00$	$-0.127561E+01$	$-0.285932E+01$	$-0.190026E+01$
10^{15}	$0.000000E+00$	$-0.311598E+00$	$-0.638297E+00$	$-0.127561E+01$	$-0.285932E+01$	$-0.190026E+01$
10^{16}	$0.000000E+00$	$-0.311598E+00$	$-0.638297E+00$	$-0.127561E+01$	$-0.285932E+01$	$-0.190026E+01$
10^{17}	$0.000000E+00$	$-0.311598E+00$	$-0.638297E+00$	$-0.127561E+01$	$-0.285932E+01$	$-0.190026E+01$
10^{18}	$0.000000E+00$	$-0.311598E+00$	$-0.638297E+00$	$-0.127561E+01$	$-0.285932E+01$	$-0.190026E+01$
10^{19}	$0.000000E+00$	$-0.311598E+00$	$-0.638297E+00$	$-0.127561E+01$	$-0.285932E+01$	$-0.190026E+01$
Reaction 20: $O + NO^+ \rightleftharpoons O_2 + N^+$						
10^{14}	$-0.337408E+00$	$0.464795E+00$	$-0.793976E+00$	$-0.730306E+01$	$-0.554075E+01$	$-0.649398E+01$
10^{15}	$-0.332256E+00$	$0.378693E+00$	$-0.560752E+00$	$-0.715299E+01$	$-0.628170E+01$	$-0.622937E+01$
10^{16}	$-0.305530E+00$	$0.228382E+00$	$-0.422626E+00$	$-0.673244E+01$	$-0.693777E+01$	$-0.610550E+01$
10^{17}	$-0.266808E+00$	$0.574151E-01$	$-0.393071E+00$	$-0.616907E+01$	$-0.741078E+01$	$-0.610542E+01$
10^{18}	$-0.220492E+00$	$-0.121559E+00$	$-0.455881E+00$	$-0.549169E+01$	$-0.776148E+01$	$-0.618548E+01$
10^{19}	$-0.191944E+00$	$-0.218897E+00$	$-0.550376E+00$	$-0.504223E+01$	$-0.791007E+01$	$-0.626419E+01$

Table IV. Constants for Polynomial Curve Fits of Thermodynamic Properties for a Reference State* of 298.15 K and 1 atm Pressure With N_2, O_2, and e^- as Reference Elements (300 K $\leq T \leq$ 30 000 K)†

Species	A_1	A_2	A_3	A_4	A_5	A_6	A_7
N_2	0.36748E + 01	−0.12081E − 02	0.23240E − 05	−0.63218E − 09	−0.22577E − 12	−0.10430E + 04	0.23580E + 01
	0.32125E + 01	0.10137E − 02	−0.30467E − 06	0.41091E − 10	−0.20170E − 14	−0.10430E + 04	0.43661E + 01
	0.31811E + 01	0.89745E − 03	−0.20216E − 06	0.18266E − 10	−0.50334E − 15	−0.10430E + 04	0.46264E + 01
	0.96377E + 01	−0.25728E − 02	0.33020E − 06	−0.14315E − 10	0.20333E − 15	−0.10430E + 04	−0.37587E + 02
	−0.51681E + 01	0.23337E − 02	−0.12953E − 06	0.27872E − 11	−0.21360E − 16	−0.10430E + 04	0.66217E + 02
O_2	0.36146E + 01	−0.18598E − 02	0.70814E − 05	−0.68070E − 08	0.21628E − 11	−0.10440E + 04	0.43628E + 01
	0.35949E + 01	0.75213E − 03	−0.18732E − 06	0.27913E − 10	−0.15774E − 14	−0.10440E + 04	0.38353E + 01
	0.38599E + 01	0.32510E − 03	−0.92131E − 08	−0.78684E − 12	0.29426E − 16	−0.10440E + 04	0.23789E + 01
	0.34867E + 01	0.52384E − 03	−0.39123E − 07	0.10094E − 11	−0.88718E − 17	−0.10440E + 04	0.48179E + 01
	0.39620E + 01	0.39446E − 03	−0.29506E − 07	0.73975E − 12	−0.64209E − 17	−0.10440E + 04	0.13985E + 01
N	0.25031E + 01	−0.21800E − 04	0.54205E − 07	−0.56476E − 10	0.20999E − 13	0.56130E + 05	0.41676E + 01
	0.24820E + 01	0.69258E − 04	−0.63065E − 07	0.18387E − 10	−0.11747E − 14	0.56130E + 05	0.42618E + 01
	0.27480E + 01	−0.39090E − 03	0.13380E − 06	−0.11910E − 10	0.33690E − 15	0.56130E + 05	0.28720E + 01
	−0.12280E + 01	0.19268E − 02	−0.24370E − 06	0.12193E − 10	−0.19918E − 15	0.56130E + 05	0.28469E + 02
	0.15520E + 02	−0.38858E − 02	0.32288E − 06	−0.96053E − 11	0.95472E − 16	0.56130E + 05	−0.88120E + 02
O	0.28236E + 01	−0.89478E − 03	0.83060E − 06	−0.16837E − 09	−0.73205E − 13	0.29150E + 05	0.35027E + 01
	0.25421E + 01	−0.27551E − 04	−0.31028E − 08	0.45511E − 11	−0.43681E − 15	0.29150E + 05	0.49203E + 01
	0.25460E + 01	−0.59520E − 04	0.27010E − 07	−0.27980E − 11	0.93800E − 16	0.29150E + 05	0.50490E + 01
	−0.97871E − 02	0.12450E − 02	−0.16154E − 06	0.80380E − 11	−0.12624E − 15	0.29150E + 05	0.21711E + 02
	0.16428E + 02	−0.39313E − 02	0.29840E − 06	−0.81613E − 11	0.75004E − 16	0.29150E + 05	−0.94358E + 02
NO	0.35887E + 01	−0.12479E − 02	0.39786E − 05	−0.28651E − 08	0.63015E − 12	0.97640E + 04	0.51497E + 01
	0.32047E + 01	0.12705E − 02	−0.46603E − 06	0.75007E − 10	−0.42314E − 14	0.97640E + 04	0.66867E + 01
	0.38543E + 01	0.23409E − 03	−0.21354E − 07	0.16689E − 11	−0.49070E − 16	0.97640E + 04	0.31541E + 01
	0.43309E + 01	−0.58086E − 04	0.28059E − 07	−0.15694E − 11	0.24104E − 16	0.97640E + 04	0.10735E + 00
	0.23507E + 01	0.58643E − 03	−0.31316E − 07	0.60495E − 12	−0.40557E − 17	0.97640E + 04	0.14026E + 02

Footnotes at end of table, page 54.

Table IV. Continued

Species	A_1	A_2	A_3	A_4	A_5	A_6	A_7
NO$^+$	$0.35294E+01$	$-0.30342E-03$	$0.38544E-06$	$0.10519E-08$	$-0.72777E-12$	$0.11840E+06$	$0.37852E+01$
	$0.32152E+01$	$0.99742E-03$	$-0.29030E-06$	$0.36925E-10$	$-0.15994E-14$	$0.11840E+06$	$0.51508E+01$
	$0.26896E+01$	$0.13796E-02$	$-0.33985E-06$	$0.33776E-10$	$-0.10427E-14$	$0.11840E+06$	$0.83904E+01$
	$0.59346E+01$	$-0.13178E-02$	$0.23297E-06$	$-0.11733E-10$	$0.18402E-15$	$0.11840E+06$	$-0.11079E+02$
	$-0.51595E+01$	$0.26290E-02$	$-0.16254E-06$	$0.39381E-11$	$-0.34311E-16$	$0.11840E+06$	$0.65896E+02$
e$^-$	$0.25000E+01$	$0.00000E+00$	$0.00000E+00$	$0.00000E+00$	$0.00000E+00$	$-0.74542E+03$	$-0.11734E+02$
	$0.25000E+01$	$0.00000E+00$	$0.00000E+00$	$0.00000E+00$	$0.00000E+00$	$-0.74542E+03$	$-0.11734E+02$
	$0.25000E+01$	$0.00000E+00$	$0.00000E+00$	$0.00000E+00$	$0.00000E+00$	$-0.74542E+03$	$-0.11733E+02$
	$0.25000E+01$	$0.00000E+00$	$0.00000E+00$	$0.00000E+00$	$0.00000E+00$	$-0.74542E+03$	$-0.11733E+02$
	$0.25000E+01$	$0.00000E+00$	$0.00000E+00$	$0.00000E+00$	$0.00000E+00$	$-0.74542E+03$	$-0.11733E+02$
N$^+$	$0.27270E+01$	$-0.28200E-03$	$0.11050E-06$	$-0.15510E-10$	$0.78470E-15$	$0.22540E+06$	$0.36450E+01$
	$0.27270E+01$	$-0.28200E-03$	$0.11050E-06$	$-0.15510E-10$	$0.78470E-15$	$0.22540E+06$	$0.36450E+01$
	$0.24990E+01$	$-0.37250E-05$	$0.11470E-07$	$-0.11020E-11$	$0.30780E-16$	$0.22540E+06$	$0.49500E+01$
	$0.23856E+01$	$0.83495E-04$	$-0.58815E-08$	$0.18850E-12$	$-0.16120E-17$	$0.22540E+06$	$0.56462E+01$
	$0.22286E+01$	$0.12458E-03$	$-0.87636E-08$	$0.26204E-12$	$-0.21674E-17$	$0.22540E+06$	$0.67811E+01$
O$^+$	$0.24985E+01$	$0.11411E-04$	$-0.29761E-07$	$0.32247E-10$	$-0.12376E-13$	$0.18790E+06$	$0.43864E+01$
	$0.25060E+01$	$-0.14464E-04$	$0.12446E-07$	$-0.46858E-11$	$0.65549E-15$	$0.18790E+06$	$0.43480E+01$
	$0.29440E+01$	$-0.41080E-03$	$0.91560E-07$	$-0.58480E-11$	$0.11900E-15$	$0.18790E+06$	$0.17500E+01$
	$0.12784E+01$	$0.40866E-03$	$-0.21731E-07$	$0.33252E-12$	$0.63160E-18$	$0.18790E+06$	$0.12761E+02$
	$0.12889E+01$	$0.43343E-03$	$-0.26758E-07$	$0.62159E-12$	$-0.45131E-17$	$0.18790E+06$	$0.12604E+02$
N$_2^+$	$0.35498E+01$	$-0.60810E-03$	$0.14690E-05$	$-0.65091E-10$	$-0.35649E-12$	$0.18260E+06$	$0.36535E+01$
	$0.33970E+01$	$0.45250E-03$	$0.12720E-06$	$-0.38790E-10$	$0.24590E-14$	$0.18260E+06$	$0.42050E+01$
	$0.33780E+01$	$0.86290E-03$	$-0.12760E-06$	$0.80870E-11$	$-0.18800E-15$	$0.18260E+06$	$0.40730E+01$
	$0.43942E+01$	$0.18868E-03$	$-0.71272E-08$	$-0.17511E-12$	$0.67176E-17$	$0.18260E+06$	$-0.23693E+01$
	$0.39493E+01$	$0.36795E-03$	$-0.26910E-07$	$0.67110E-12$	$-0.58244E-17$	$0.18260E+06$	$0.65472E+00$

Table IV. Concluded

Species	A_1	A_2	A_3	A_4	A_5	A_6	A_7
	$0.32430E+01$	$0.11740E-02$	$-0.39000E-06$	$0.54370E-10$	$-0.23920E-14$	$0.14000E+06$	$0.59250E+01$
	$0.32430E+01$	$0.11740E-02$	$-0.39000E-06$	$0.54370E-10$	$-0.23920E-14$	$0.14000E+06$	$0.59250E+01$
O_2^+	$0.51690E+01$	$-0.86200E-03$	$0.20410E-06$	$-0.13000E-10$	$0.24940E-15$	$0.14000E+06$	$-0.52960E+01$
	$-0.28017E+00$	$0.16674E-02$	$-0.12107E-06$	$0.32113E-11$	$-0.28349E-16$	$0.14000E+06$	$0.31013E+02$
	$0.20445E+01$	$0.10313E-02$	$-0.74046E-07$	$0.19257E-11$	$-0.17461E-16$	$0.14000E+06$	$0.14310E+02$

*The specific enthalpy for a reference state of 0 K and 1 atm pressure can be obtained from the relation

$$[h_i] \underset{\text{to } 0 \text{ K}}{\text{referenced}} = [h_i] \underset{\text{to } 298.15 \text{ K}}{\text{referenced}} + (\Delta h_i^f)_{T=0} - (\Delta h_i^f)_{T=298.15} + 298.15\, C_{p,i}$$

where the first term on the right-hand side is obtained from the curve fits given here and the second and third terms (which are the heats of formation at 0 K and 298.15 K, respectively) are provided in table B1. Various values of $C_{p,i}$ needed in the above equation are provided in the second footnote.

†There are five rows of constants provided for each species, which correspond to the following five temperature ranges, respectively:

$$300 \text{ K} \leq T \leq 1000 \text{ K}$$
$$1000 \text{ K} \leq T \leq 6000 \text{ K}$$
$$6000 \text{ K} \leq T \leq 15\,000 \text{ K}$$
$$15\,000 \text{ K} \leq T \leq 25\,000 \text{ K}$$
$$25\,000 \text{ K} \leq T \leq 30\,000 \text{ K}$$

For temperatures less than 300 K (which may arise in the free stream for certain flight trajectories (refs. 19 and 67)), the specific heats of O, O_2, N, and N_2 are practically constant. For such cases, the specific enthalpy may be obtained from the relation

$$h_i = C_{p,i}(T - T_{\text{ref}}) + (\Delta h_i^f)_{T_{\text{ref}}}$$

with $T_{\text{ref}} = 298$ K, $C_{p,O} = 5.44$ cal/g-mole-K, $C_{p,O_2} = 7.00$ cal/g-mole-K, $C_{p,N} = 4.97$ cal/g-mole-K, and $C_{p,N_2} = 6.96$ cal/g-mole-K.

Table V. Constants for Viscosity* Curve Fits
$(1000 \text{ K} \leq T \leq 30\,000 \text{ K})^\dagger$

Species[‡]	A_{μ_i}	B_{μ_i}	C_{μ_i}
N_2	0.0203	0.4329	-11.8153
O_2	.0484	$-.1455$	-8.9231
N	.0120	.5930	-12.3805
O	.0205	.4257	-11.5803
NO	.0452	$-.0609$	-9.4596
NO^+	0	2.5	-32.0453
e^-			-37.4475
N^+			-32.4285
O^+			-32.3606
N_2^+			-32.0827
O_2^+	↓	↓	-32.0148

* Viscosity is obtained in g/cm-sec.

† For temperatures less than 1000 K, Sutherland's viscosity law for air may be used for all species.

‡ The charged species viscosities given here are for the limiting electron pressure p_{em} (eq. (23g)). For different electron pressures, these values should be corrected by the formula given in equation (24a) in the main text.

Table VI. Constants for Frozen Thermal Conductivity* Curve Fits
$(1000 \text{ K} \leq T \leq 30\,000 \text{ K})^{\dagger}$

Species[‡]	$A_{K_{f,i}}$	$B_{K_{f,i}}$	$C_{K_{f,i}}$	$D_{K_{f,i}}$	$E_{K_{f,i}}$
N_2	0.03607	-1.07503	11.95029	-57.90063	93.21782
O_2	.07987	-2.58428	31.25959	-166.76267	321.69820
N	0	0	.01619	.55022	-12.92190
O	0	0	.03310	.22834	-11.58116
NO	.02792	$-.87133$	10.17967	-52.03466	88.67060
NO^+	$-.06836$	2.57829	-35.72737	219.09215	-519.00261
e^-	0	0	.00032	2.49375	-27.89805
N^+	0	0	.03088	2.06339	-31.51368
O^+	$-.04013$	1.32468	-16.22091	89.96782	-208.57442
N_2^+	0	$-.03723$	.84192	-3.59040	-18.65620
O_2^+	$-.08373$	2.75459	-33.74529	185.13274	-401.50753

* Thermal conductivity is obtained in cal/cm-sec-K.

† For temperatures lower than 1000 K, Sutherland's law for thermal conductivity of air may be used for each species.

‡ The charged species frozen thermal conductivities given here are for the limiting electron pressure p_{em} (eq. (23g)). For different electron pressures, these values should be corrected by the formula given in equation (24a) in the main text.

Table VII. Constants for Diffusion Coefficient* Curve Fits

Pair number[†]	Interaction pair $(i-j)$	$A_{\overline{D}_{ij}}$	$B_{\overline{D}_{ij}}$	$C_{\overline{D}_{ij}}$	$D_{\overline{D}_{ij}}$	Temperature range, K[‡]
1	N_2-N_2	0	0.0112	1.6182	-11.3091	
2	O_2-N_2		.0465	.9271	-8.1137	
3	O_2-O_2		.0410	1.0023	-8.3597	
4	$N-N_2$		.0195	1.4880	-10.3654	
5	$N-O_2$		.0179	1.4848	-10.2810	
6	$N-N$ [§]		.0033	1.5572	-11.1616	
7	$O-N_2$		.0140	1.5824	-10.8819	
8	$O-O_2$		.0226	1.3700	-9.6631	
9	$O-N$		$-.0048$	1.9195	-11.9261	
10	$O-O$ [§]		.0034	1.5572	-11.1729	
11	$NO-N_2$		.0291	1.2676	-9.6878	
12	$NO-O_2$		.0438	.9647	-8.2380	
13	$NO-N$		.0185	1.4882	-10.3301	
14	$NO-O$		.0179	1.4848	-10.3155	
15	$NO-NO$		.0364	1.1176	-8.9695	
16	NO^+-N_2		0	1.9000	-13.3343	
17	NO^+-O_2			1.9001	-13.3677	
18	NO^+-N			1.8999	-13.1254	
19	NO^+-O			1.9000	-13.1701	
20	NO^+-NO		.0047	1.5552	-11.3713	

Footnotes at end of table, page 60.

Table VII. Continued

Pair number[†]	Interaction pair $(i-j)$	$A_{\overline{D}_{ij}}$	$B_{\overline{D}_{ij}}$	$C_{\overline{D}_{ij}}$	$D_{\overline{D}_{ij}}$	Temperature range, K[‡]
21	$NO^+ - NO^+$	0	0	3.5000	-30.3210	
22	$e^- - N_2$	-.1147	2.8945	-23.0085	65.9815	
23	$e^- - O_2$	-.0241 -.0029	.3464 .0856	.1136 .6655	-1.3848 -.8205	1000 to 9000 9000 to 30 000
24	$e^- - N$	0	0	1.5000	-2.9987	
25	$e^- - O$	.0581	-1.5975	15.4508	-40.7370	
26	$e^- - NO$	.2202 .2871	-5.2261 -8.3759	42.0630 82.8802	-106.0937 -267.0227	1000 to 8000 8000 to 30 000
27	$e^- - NO^+$	0	0	3.5000	-25.2128	
28	$e^- - e^-$			3.5000	-24.8662	
29	$N^+ - N_2$			1.9000	-13.1144	
30	$N^+ - O_2$			1.9000	-13.1357	
31	$N^+ - N$		.0033	1.5572	-11.1616	
32	$N^+ - O$		0	1.9000	-13.0028	
33	$N^+ - NO$			1.8999	-13.1254	
34	$N^+ - NO^+$			3.5000	-30.0951	
35	$N^+ - e^-$			3.5000	-25.2128	
36	$N^+ - N^+$			3.5000	-29.9401	
37	$O^+ - N_2$			1.9000	-13.1578	
38	$O^+ - O_2$			1.9000	-13.1810	
39	$O^+ - N$			1.9000	-13.0028	
40	$O^+ - O$		.0034	1.5572	-11.1729	

Footnotes at end of table, page 60.

Table VII. Continued

Pair number[†]	Interaction pair $(i-j)$	$A_{\overline{D}_{ij}}$	$B_{\overline{D}_{ij}}$	$C_{\overline{D}_{ij}}$	$D_{\overline{D}_{ij}}$	Temperature range, K[‡]
41	$O^+ - NO$	0	0	1.9000	−13.1701	
42	$O^+ - NO^+$			3.5000	−30.1395	
43	$O^+ - e^-$				−25.2128	
44	$O^+ - N^+$				−29.9722	
45	$O^+ - O^+$			↓	−30.0066	
46	$N_2^+ - N_2$			1.9000	−13.3173	
47	$N_2^+ - O_2$				−13.3495	
48	$N_2^+ - N$				−13.1144	
49	$N_2^+ - O$				−13.1578	
50	$N_2^+ - NO$			↓	−13.3343	
51	$N_2^+ - NO^+$			3.5000	−30.3036	
52	$N_2^+ - e^-$				−25.2128	
53	$N_2^+ - N^+$				−30.0839	
54	$N_2^+ - O^+$				−30.1273	
55	$N_2^+ - N_2^+$			↓	−30.2867	
56	$O_2^+ - N_2$			1.9000	−13.3173	
57	$O_2^+ - O_2$				−13.3495	
58	$O_2^+ - N$				−13.1144	
59	$O_2^+ - O$	↓	↓	↓	−13.1578	

Table VII. Concluded

Pair number[†]	Interaction pair $(i-j)$	$A_{\overline{D}_{ij}}$	$B_{\overline{D}_{ij}}$	$C_{\overline{D}_{ij}}$	$D_{\overline{D}_{ij}}$	Temperature range, K[‡]
60	$O_2^+ - NO$	0	0	1.9000	-13.3343	
61	$O_2^+ - NO^+$			3.5000	-30.3036	
62	$O_2^+ - e^-$				-25.2128	
63	$O_2^+ - N^+$				-30.0839	
64	$O_2^+ - O^+$				-30.1273	
65	$O_2^+ - N_2^+$				-30.2867	
66	$O_2^+ - O_2^+$	↓	↓	↓	-30.2867	

*Diffusion coefficients are obtained in cm^2-atm/sec. Diffusion coefficients obtained from these curve fits are for the limiting electron pressure p_{em} (eq. (23g)). For different electron pressures, the cross sections should be corrected by the formula given in the main text when the interacting pair of species are both ions or electrons or a combination of the two. Diffusion coefficients for N_2^+ and O_2^+ are taken to be the same.

[†]Cross sections 1 to 15 are used in a 5-species air model and 1 to 28 in a 7-species model.

[‡]The temperature range for all curve fits is $1000 \leq T \leq 30\,000$ K, except where noted.

[§]Coefficient for diffusion of internal excitation energy (see p. 20).

Table VIII. Curve-Fit Constants for Collision Cross-Section $\overline{\Omega}_{ij}^{(1,1)}{}_*$

Pair number[†]	Interaction pair $(i-j)$	$A_{\overline{\Omega}_{ij}^{(1,1)}}$	$B_{\overline{\Omega}_{ij}^{(1,1)}}$	$C_{\overline{\Omega}_{ij}^{(1,1)}}$	$D_{\overline{\Omega}_{ij}^{(1,1)}}$	Temperature range, K[‡]
1	$N_2 - N_2$	0	−0.0112	−0.1182	4.8464	
2	$O_2 - N_2$		−.0465	.5729	1.6185	
3	$O_2 - O_2$		−.0410	.4977	1.8302	
4	$N - N_2$		−.0194	.0119	4.1055	
5	$N - O_2$		−.0179	.0152	3.9996	
6	$N - N$		−.0033	−.0572	5.0452	
7	$O - N_2$		−.0139	−.0825	4.5785	
8	$O - O_2$		−.0226	.1300	3.3363	
9	$O - N$		.0048	−.4195	5.7774	
10	$O - O$		−.0034	−.0572	4.9901	
11	$NO - N_2$		−.0291	.2324	3.2082	
12	$NO - O_2$		−.0438	.5352	1.7252	
13	$NO - N$		−.0185	.0118	4.0590	
14	$NO - O$		−.0179	.0152	3.9996	
15	$NO - NO$		−.0364	.3825	2.4718	
16	$NO^+ - N_2$		0	−.4000	6.8543	
17	$NO^+ - O_2$					
18	$NO^+ - N$					
19	$NO^+ - O$					
20	$NO^+ - NO$		−.0047	−.0551	4.8737	
21	$NO^+ - NO^+$		0	−2.0000	23.8237	

Footnotes at end of table, page 64.

Table VIII. Continued

Pair number[†]	Interaction pair $(i-j)$	$A_{\overline{\Omega}_{ij}^{(1,1)}}$	$B_{\overline{\Omega}_{ij}^{(1,1)}}$	$C_{\overline{\Omega}_{ij}^{(1,1)}}$	$D_{\overline{\Omega}_{ij}^{(1,1)}}$	Temperature range, K[‡]
22	$e - N_2$	.1147	−2.8945	24.5080	−67.3691	
23	$e - O_2$	.0241 .0025	−.3467 −.0742	1.3887 .7235	−0.0110 −0.2116	1000 to 9000 9000 to 30 000
24	$e - N$	0	0	0	1.6094	
25	$e - O$	.0164 −.2027	−.2431 5.6428	1.1231 −51.5646	−1.5561 155.6091	1000 to 9000 9000 to 30 000
26	$e - NO$	−.2202 −.2871	5.2265 8.3757	−40.5659 −81.3787	104.7126 265.6292	1000 to 8000 8000 to 30 000
27	$e - NO^+$	0	0	−2.0000	23.8237	
28	$e^- - e^-$			−2.0000	23.8237	
29	$N^+ - N_2$			−.4000	6.8543	
30	$N^+ - O_2$			−.4000	6.8543	
31	$N^+ - N$		−.0033	−.0572	5.0452	
32	$N^+ - O$		0	−.4000	6.8543	
33	$N^+ - NO$			−.4000	6.8543	
34	$N^+ - NO^+$			−2.0000	23.8237	
35	$N^+ - e^-$			−2.0000	23.8237	
36	$N^+ - N^+$			−2.0000	23.8237	
37	$O^+ - N_2$			−.4000	6.8543	
38	$O^+ - O_2$			−.4000	6.8543	
39	$O^+ - N$			−.4000	6.8543	
40	$O^+ - O$		−.0034	−0.0572	4.9901	

Footnotes at end of table, page 64.

Table VIII. Continued

Pair number[†]	Interaction pair $(i-j)$	$A_{\overline{\Omega}_{ij}^{(1,1)}}$	$B_{\overline{\Omega}_{ij}^{(1,1)}}$	$C_{\overline{\Omega}_{ij}^{(1,1)}}$	$D_{\overline{\Omega}_{ij}^{(1,1)}}$	Temperature range, K[‡]
41	$O^+ - NO$	0	0	$-.4000$	6.8543	
42	$O^+ - NO^+$			-2.0000	23.8237	
43	$O^+ - e$			-2.0000	23.8237	
44	$O^+ - N^+$			-2.0000	23.8237	
45	$O^+ - O^+$			-2.0000	23.8237	
46	$N_2^+ - N_2$			$-.4000$	6.8543	
47	$N_2^+ - O_2$					
48	$N_2^+ - N$					
49	$N_2^+ - O$					
50	$N_2^+ - NO$			$\downarrow$	$\downarrow$	
51	$N_2^+ - NO^+$			-2.0000	23.8237	
52	$N_2^+ - e$					
53	$N_2^+ - N^+$					
54	$N_2^+ - O^+$					
55	$N_2^+ - N_2^+$			$\downarrow$	$\downarrow$	
56	$O_2^+ - N_2$			$-.4000$	6.8543	
57	$O_2^+ - O_2$					
58	$O_2^+ - N$					
59	$O_2^+ - O$					
60	$O_2^+ - NO$	$\downarrow$	$\downarrow$	$\downarrow$	$\downarrow$	

Footnotes at end of table, page 64.

Table VIII. Concluded

Pair number[†]	Interaction pair $(i-j)$	$A_{\overline{\Omega}_{ij}^{(1,1)}}$	$B_{\overline{\Omega}_{ij}^{(1,1)}}$	$C_{\overline{\Omega}_{ij}^{(1,1)}}$	$D_{\overline{\Omega}_{ij}^{(1,1)}}$	Temperature range, K[‡]
61	$O_2^+ - NO^+$	0	0	-2.0000	23.8237	
62	$O_2^+ - e^-$					
63	$O_2^+ - N^+$					
64	$O_2^+ - O^+$					
65	$O_2^+ - N_2^+$					
66	$O_2^+ - O_2^+$					

* Cross sections are obtained in Å^2, $1\ \text{Å}^2 = 10^{-16}\text{cm}^2$. Collision cross sections obtained from these curve fits are for the limiting electron pressure p_{em} (eq. (23g)). For different electron pressures, the cross sections should be corrected by the formula given in the main text when the interacting pair of species are both ions or electrons or a combination of the two. Cross sections for N_2^+ and O_2^+ are taken to be the same.

[†] Cross sections 1 to 15 are used in a 5-species air model and 1 to 28 in a 7-species model.

[‡] The temperature range for all curve fits is $1000 \le T \le 30\,000$ K, except where noted.

Table IX. Curve-Fit Constants for Collision Cross-Section $\overline{\Omega}_{ij}^{(2,2)^*}$

Pair number[†]	Interaction pair $(i-j)$	$A_{\overline{\Omega}_{ij}^{(2,2)}}$	$B_{\overline{\Omega}_{ij}^{(2,2)}}$	$C_{\overline{\Omega}_{ij}^{(2,2)}}$	$D_{\overline{\Omega}_{ij}^{(2,2)}}$	Temperature range, K[‡]
1	$N_2 - N_2$	0	-0.0203	0.0683	4.0900	
2	$O_2 - N_2$		$-.0558$	.7590	.8955	
3	$O_2 - O_2$		$-.0485$	.6475	1.2607	
4	$N - N_2$		$-.0190$	.0239	4.1782	
5	$N - O_2$		$-.0203$	.0730	3.8818	
6	$N - N$		$-.0118$	$-.0960$	4.3252	
7	$O - N_2$		$-.0169$	$-.0143$	4.4195	
8	$O - O_2$		$-.0247$	.1783	3.2517	
9	$O - N$		.0065	$-.4467$	6.0426	
10	$O - O$		$-.0207$	.0780	3.5658	
11	$NO - N_2$		$-.0385$	.4226	2.4507	
12	$NO - O_2$		$-.0522$	.7045	1.0738	
13	$NO - N$		$-.0196$	.0478	4.0321	
14	$NO - O$		$-.0203$	.0730	3.8818	
15	$NO - NO$		$-.0453$	.5624	1.7669	
16	$NO^+ - N_2$		0	$-.4000$	6.7760	
17	$NO^+ - O_2$					
18	$NO^+ - N$					
19	$NO^+ - O$					
20	$NO^+ - NO$					
21	$NO^+ - NO^+$			-2.0000	24.3602	
22	$e^- - N_2$	.1147	-2.8945	24.5080	-67.3691	

Footnotes at end of table, page 68.

Table IX. Continued

Pair number[†]	Interaction pair $(i-j)$	$A_{\overline{\Omega}_{ij}^{(2,2)}}$	$B_{\overline{\Omega}_{ij}^{(2,2)}}$	$C_{\overline{\Omega}_{ij}^{(2,2)}}$	$D_{\overline{\Omega}_{ij}^{(2,2)}}$	Temperature range, K[‡]
23	e^- O_2	.0241 .0025	−.3467 −.0742	1.3887 .7235	−.0110 −.2116	1000 to 9000 9000 to 30 000
24	e N	0	0	0	1.6094	
25	$e - O$	.0164 −.2027	−.2431 5.6428	1.1231 −51.5646	−1.5561 155.6091	1000 to 9000 9000 to 30 000
26	e – NO	−.2202 −.2871	5.2265 8.3757	−40.5659 −81.3787	104.7126 265.6292	1000 to 8000 8000 to 30 000
27	$e - NO^+$	0	0	−2.0000	24.3061	
28	$e^- - e^-$			−2.0000	24.3061	
29	N^+ N_2			−.4000	6.7760	
30	N^+ O_2			−.4000	6.7760	
31	N^+ N			−.4146	6.9078	
32	N^+ O			−.4000	6.7760	
33	N^- NO			−.4000	6.7760	
34	N^+ – NO^+			−2.0000	24.3602	
35	$N^+ - e$			−2.0000	24.3061	
36	$N^+ - N^+$			−2.0000	24.3602	
37	O^+ N_2			−.4000	6.7760	
38	O^+ O_2			−.4000	6.7760	
39	$O^+ - N$			−.4000	6.7760	
40	O^+ O			−.4235	6.7787	
41	O^+ NO			−.4000	6.7760	

Footnotes at end of table, page 68.

Table IX. Continued

Pair number[†]	Interaction pair $(i-j)$	$A_{\overline{\Omega}_{ij}^{(2.2)}}$	$B_{\overline{\Omega}_{ij}^{(2.2)}}$	$C_{\overline{\Omega}_{ij}^{(2.2)}}$	$D_{\overline{\Omega}_{ij}^{(2.2)}}$	Temperature range, K[‡]
42	$O^+ - NO^+$	0	0	-2.0000	24.3602	
43	$O^+ - e^-$				24.3061	
44	$O^+ - N^+$				24.3602	
45	$O^+ - O^-$			↓	24.3602	
46	$N_2^+ - N_2$			$-.4000$	6.7760	
47	$N_2^+ - O_2$					
48	$N_2^+ - N$					
49	$N_2^+ - O$					
50	$N_2^+ - NO$			↓	↓	
51	$N_2^+ - NO^+$			-2.0000	24.3602	
52	$N_2^+ - e^-$				24.3061	
53	$N_2^+ - N^+$				24.3602	
54	$N_2^+ - O^+$				24.3602	
55	$N_2^+ - N_2^+$			↓	24.3602	
56	$O_2^+ - N_2$			$-.4000$	6.7760	
57	$O_2^+ - O_2$					
58	$O_2^+ - N$					
59	$O_2^+ - O$	↓	↓	↓	↓	

Footnotes at end of table, page 68.

Table IX. Concluded

Pair number[†]	Interaction pair $(i-j)$	$A_{\overline{\Omega}_{ij}^{(2,2)}}$	$B_{\overline{\Omega}_{ij}^{(2,2)}}$	$C_{\overline{\Omega}_{ij}^{(2,2)}}$	$D_{\overline{\Omega}_{ij}^{(2,2)}}$	Temperature range, K[‡]
60	$O_2^+ - NO$	0	0	$-.4000$	6.7760	
61	$O_2^+ - NO^+$			-2.0000	24.3602	
62	$O_2^+ - e^-$				24.3061	
63	$O_2^+ - N^+$				24.3602	
64	$O_2^+ - O^+$	$\downarrow$	$\downarrow$	$\downarrow$	$\downarrow$	
65	$O_2^+ - N_2^+$					
66	$O_2^+ - O_2^+$					

* Cross sections are obtained in Å^2; $1\text{Å}^2 = 10^{-16}\text{cm}^2$. Collision cross sections obtained from these curve fits are for the limiting electron pressure p_{em} (eq. (23g)). For different electron pressures, the cross sections should be corrected by the formula given in the main text when the interacting pair of species are both ions or electrons or a combination of the two. Cross sections for N_2^+ and O_2^+ are taken to be the same.

† Cross sections 1 to 15 are used in a 5-species air model and 1 to 28 in a 7-species model.

‡ The temperature range for all curve fits is $1000 \leq T \leq 30\,000$ K, except where noted.

$$(1000 \text{ K} \leq T \leq 30\,000 \text{ K})$$

Pair number[†]	Interaction pair $(i-j)$	$A_{B_{ij}^{*}}$	$B_{B_{ij}^{*}}$	$C_{B_{ij}^{*}}$
1	$N_2 - N_2$	-0.0073	0.1444	-0.5625
2	$O_2 - N_2$	$-.0019$	$.0602$	$-.2175$
3	$O_2 - O_2$	$.0001$	$.0181$	$-.0306$
4	$N - N_2$	$.0043$	$-.0494$	$.2850$
5	$N - O_2$	$.0033$	$-.0366$	$.2332$
6	$N - N$	$.0002$	$.0002$	$.0537$
7	$O - N_2$	$.0042$	$-.0471$	$.2747$
8	$O - O_2$	$.0024$	$-.0245$	$.1808$
9	$O - N$	$.0147$	$-.2628$	1.2943
10	$O - O$	$.0002$	0	$.0549$
11	$NO - N_2$	$-.0045$	$.1010$	$-.3872$
12	$NO - O_2$	$-.0010$	$.0410$	$-.1312$
13	$NO - N$	$.0038$	$-.0425$	$.2574$
14	$NO - O$	$.0033$	$-.0366$	$.2332$
15	$NO - NO$	$-.0027$	$.0700$	$-.2553$
16	$NO^+ - N_2$	0	0	$.1933$
17	$NO^+ - O_2$	$\downarrow$	$\downarrow$	$\downarrow$
18	$NO^+ - N$			
19	$NO^+ - O$			
20	$NO^+ - NO$	$.0003$	$-.0006$	$.0632$

Footnotes at end of table, page 72.

Table X. Continued

Pair number[†]	Interaction pair $(i-j)$	$A_{B_{ij}^*}$	$B_{B_{ij}^*}$	$C_{B_{ij}^*}$
21	NO$^+$ – NO$^+$	0	0	.4463
22	e$^-$ – N$_2$			0
23	e$^-$ – O$_2$			
24	e$^-$ – N			
25	e$^-$ – O			
26	e$^-$ – NO			
27	e$^-$ – NO$^+$			.4463
28	e$^-$ – e$^-$			.4463
29	N$^+$ – N$_2$			.1933
30	N$^+$ – O$_2$			.1933
31	N$^+$ – N	.0002	.0002	.0537
32	N$^+$ – O	0	0	.1933
33	N$^+$ – NO			.1933
34	N$^+$ – NO$^+$			.4463
35	N$^+$ – e$^-$			.4463
36	N$^+$ – N$^+$			.4463
37	O$^+$ – N$_2$			.1933
38	O$^+$ – O$_2$			.1933
39	O$^+$ – N			.1933

Footnotes at end of table, page 72.

Table X. Continued

Pair number[†]	Interaction pair $(i-j)$	$A_{B^*_{ij}}$	$B_{B^*_{ij}}$	$C_{B^*_{ij}}$
40	O^+ O	.0002	0	.0549
41	O^+ NO	0		.1933
42	O^+ NO^+			.4463
43	$O^+ - e^-$			
44	$O^+ - N^+$			
45	O^+ O^+			↓
46	$N_2^+ - N_2$			.1933
47	$N_2^+ - O_2$			
48	$N_2^+ - N$			
49	$N_2^+ - O$			
50	$N_2^+ - NO$			↓
51	$N_2^+ - NO^+$			.4463
52	$N_2^+ - e^-$			
53	$N_2^+ - N^+$			
54	$N_2^+ - O^+$			
55	$N_2^+ - N_2^+$			↓
56	$O_2^+ - N_2$			.1933
57	$O_2^+ - O_2$			
58	$O_2^+ - N$	↓	↓	↓
59	$O_2^+ - O$			

Table X. Concluded

Pair number[†]	Interaction pair $(i - j)$	$A_{B_{ij}^*}$	$B_{B_{ij}^*}$	$C_{B_{ij}^*}$
60	O_2^+–NO	0	0	.1933
61	O_2^+–NO$^+$			.4463
62	O_2^+–e$^-$			
63	O_2^+–N$^+$			
64	O_2^+–O$^+$			
65	O_2^+–N$_2$$^+$			
66	O_2^+–O$_2$$^+$	↓	↓	↓

* The collision cross-section ratios are dimensionless parameters and are valid as given for all electron pressures.
† Cross sections 1 to 15 are used in a 5-species air model and 1 to 28 in a 7-species model.

Regions with chemical and thermal nonequilibrium	
Region	Aerothermal phenomenon
(A)	Chemical and thermal equilibrium
(B)	Chemical nonequilibrium with thermal equilibrium
(C)	Chemical and thermal nonequilibrium

Chemical species in high-temperature air		
Region	Air chemical model	Species present
(I)	2 species	O_2, N_2
(II)	5 species	O_2, N_2, O, N, NO
(III)	7 species	$O_2, N_2, O, N, NO, NO^+, e^-$
(IV)	11 species	$O_2, N_2, O, N, NO, O_2^+, N_2^+, O^+, N^+, NO^+, e^-$
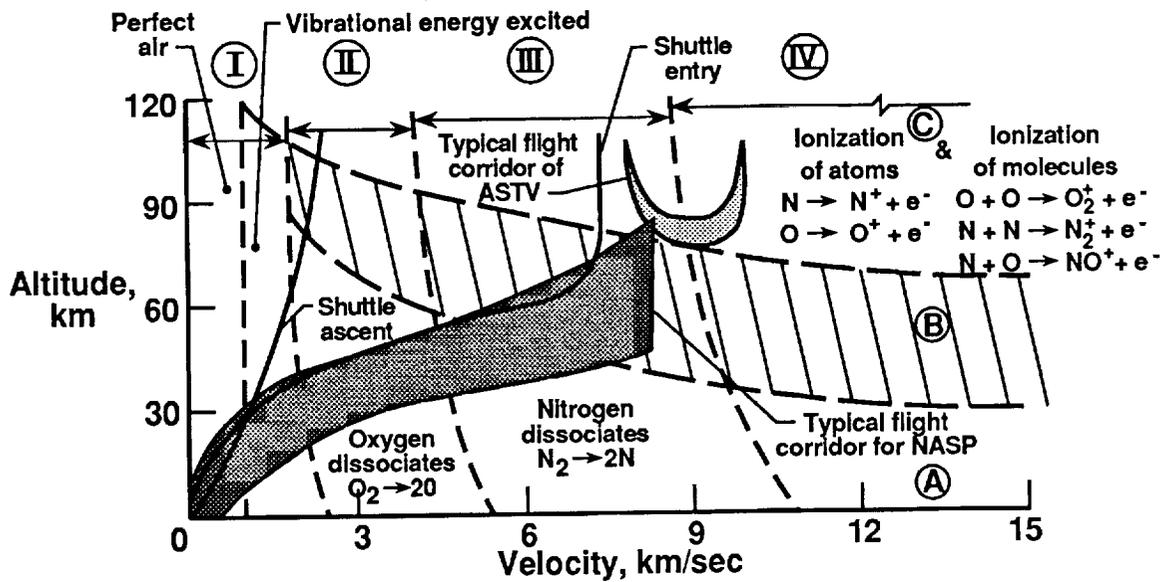
Figure 1. Flight stagnation region air chemistry for a 30.5-cm radius sphere (adapted from ref. 5).
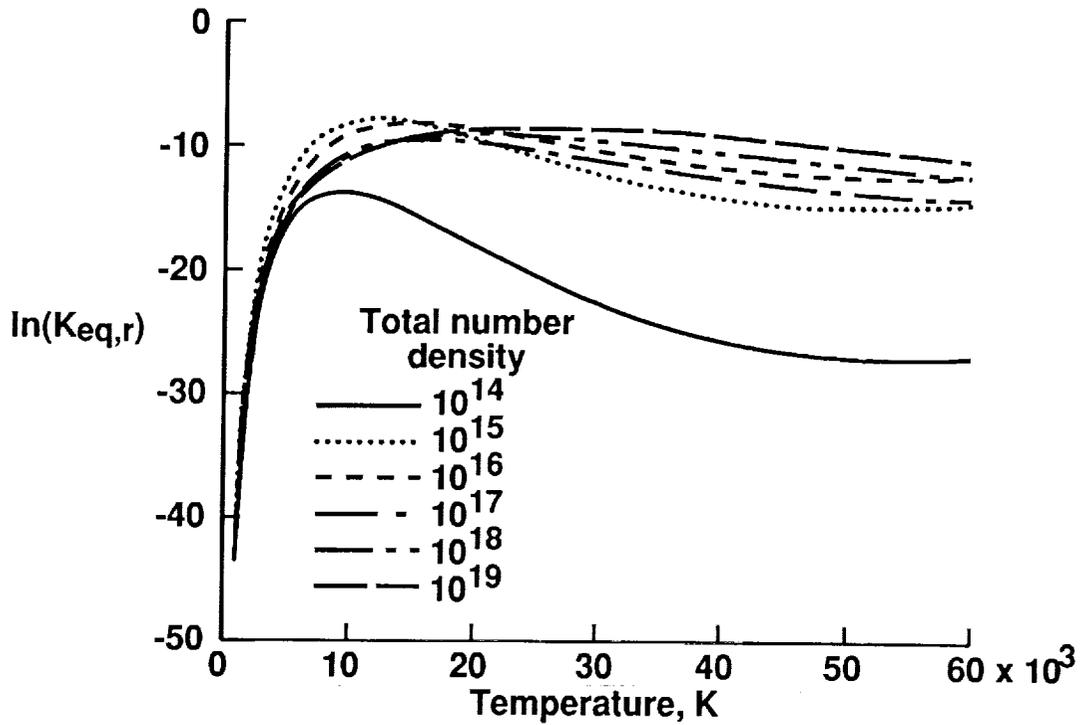
(a) For different values of total number density.
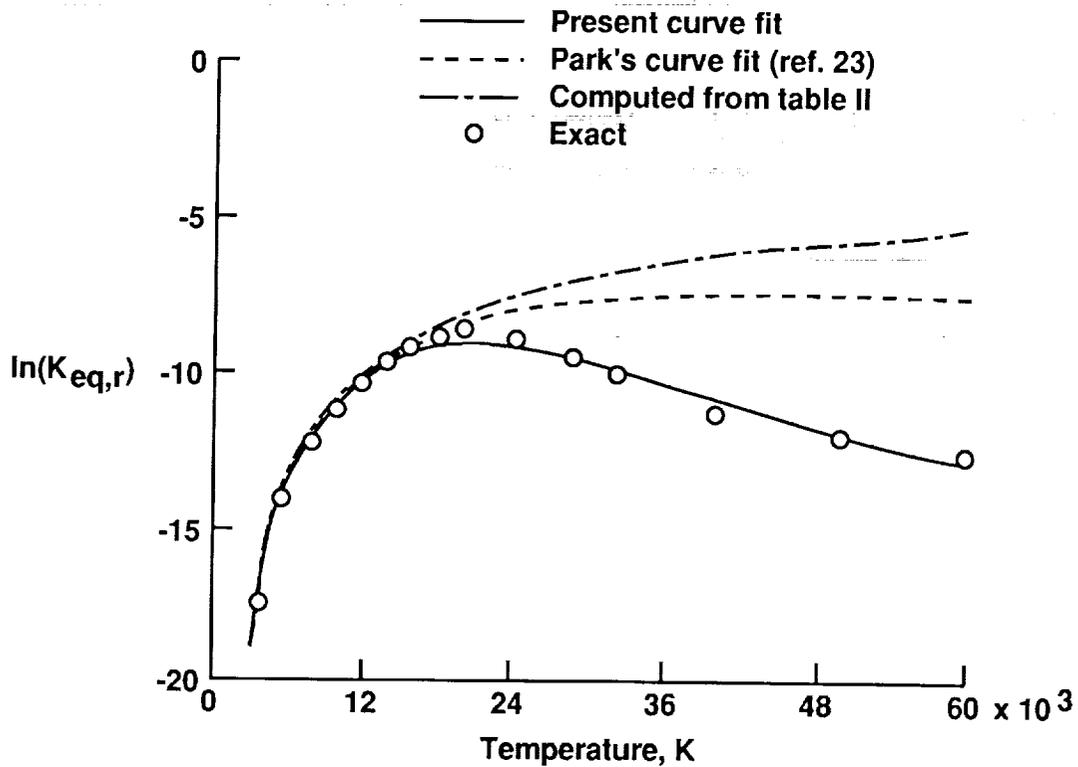
(b) For total number density of 10^{18} particles/cm^3.

Figure 2. Variation of equilibrium constant with temperature for reaction $N + O \rightleftharpoons NO^+ + e^-$.
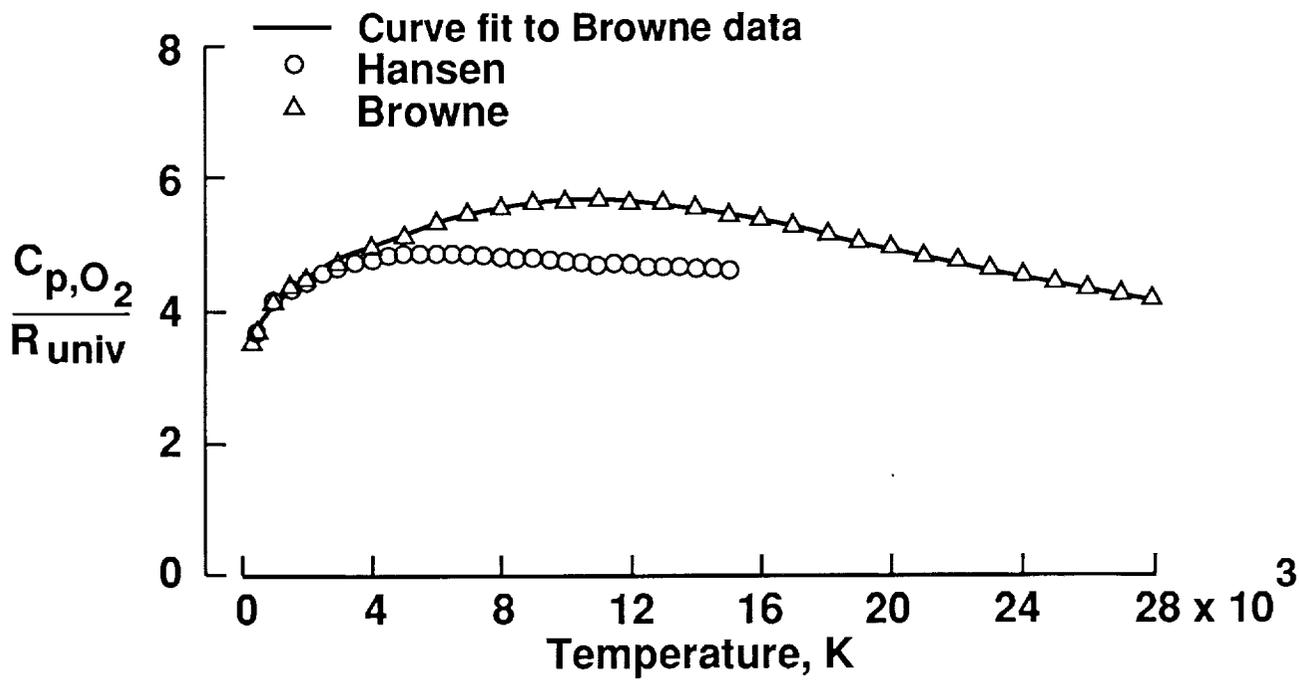
(a) Diatomic oxygen.
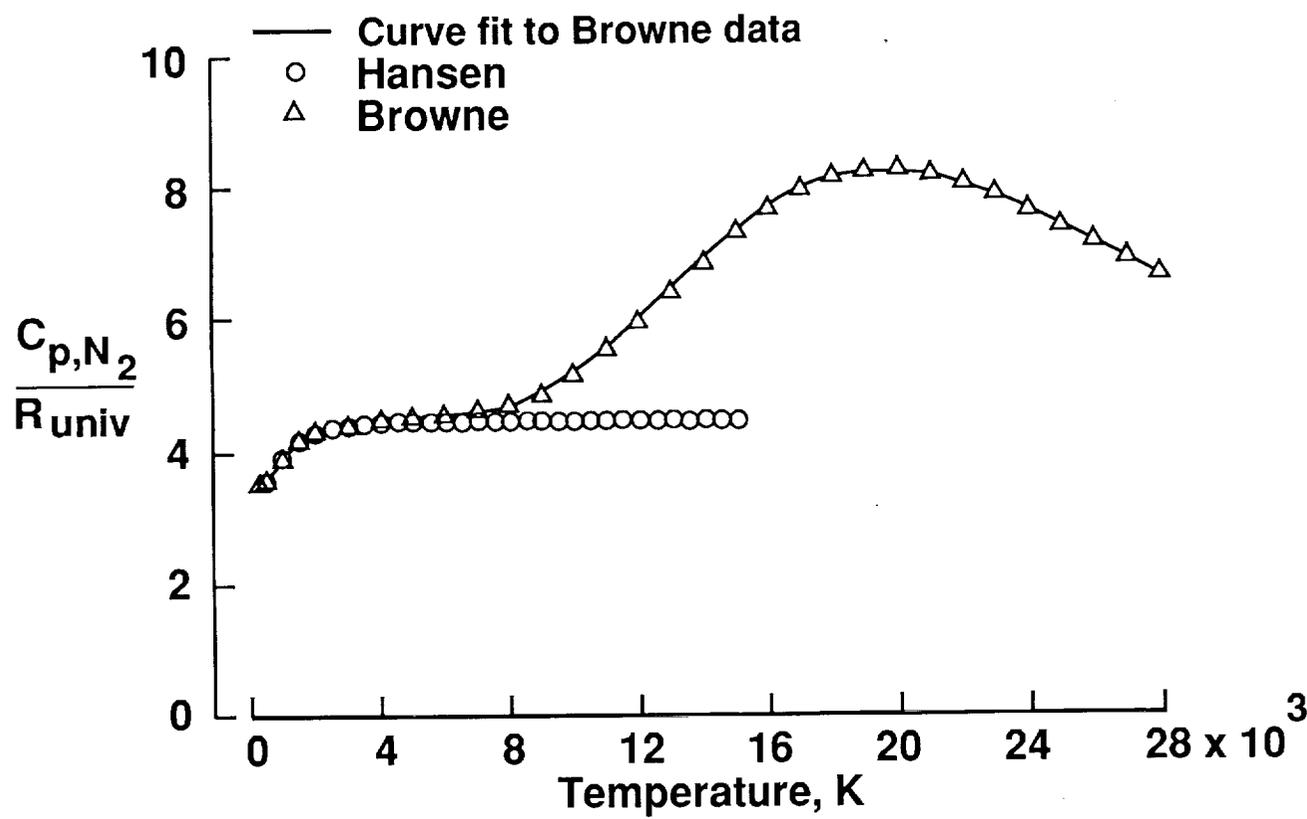
(b) Diatomic nitrogen.

Figure 3. Curve fit to specific-heat values obtained by Browne (ref. 35) and comparison with Hansen's values (ref. 37).
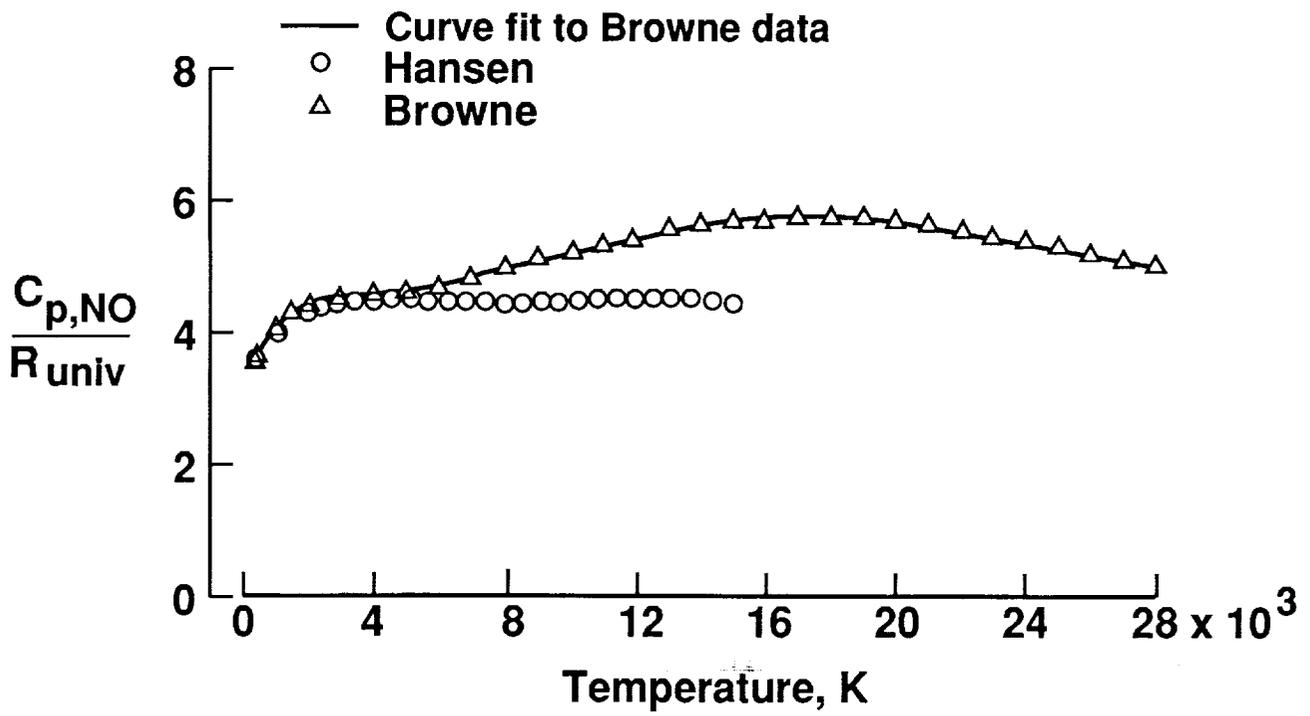
(c) Nitric oxide.

Figure 3. Concluded.
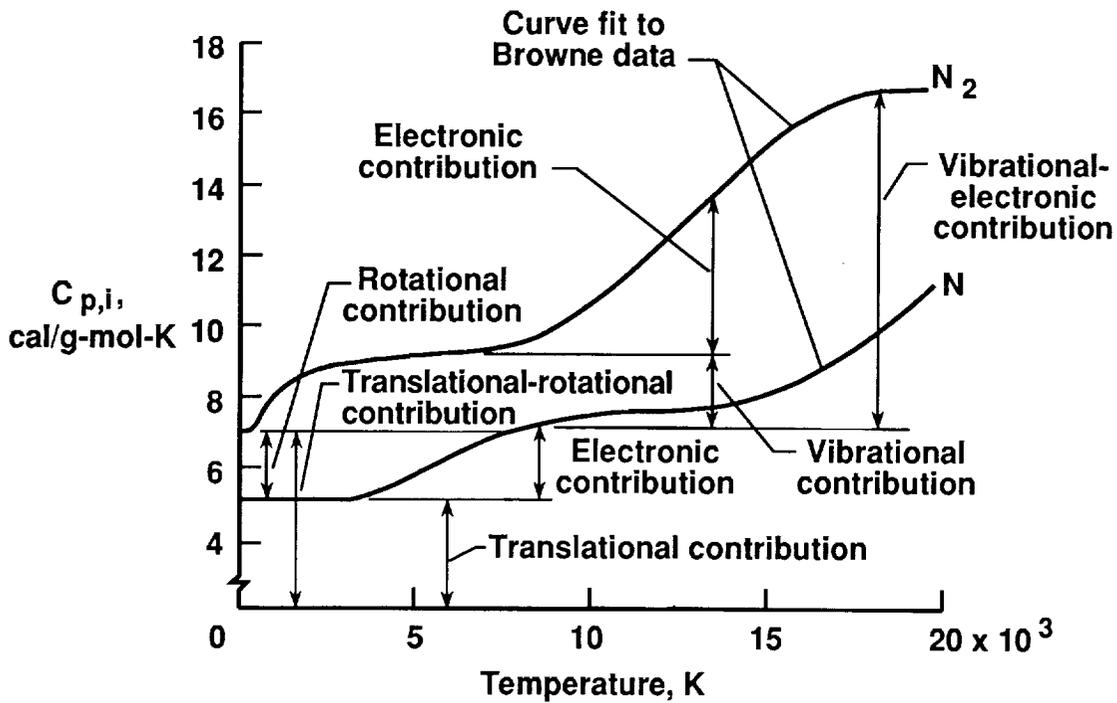
Figure 4. Specific heats of monatomic and diatomic nitrogen with contributions from excitation of different energy modes.
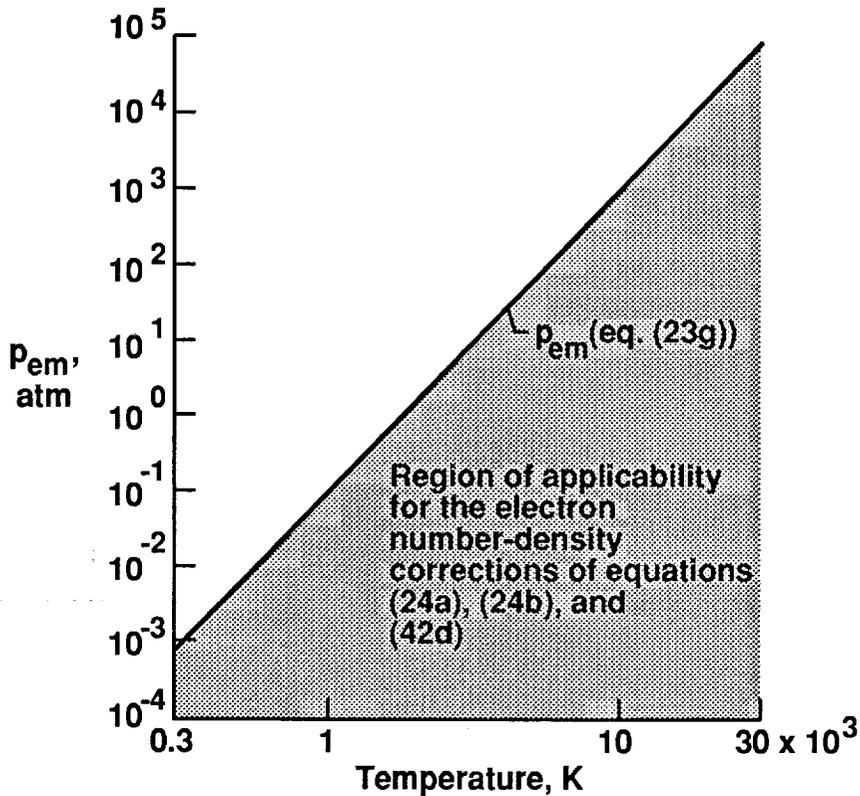
Figure 5. Limiting electron pressure for transport properties of ionic species. The present formulation is applicable only for electron pressure below this limit.
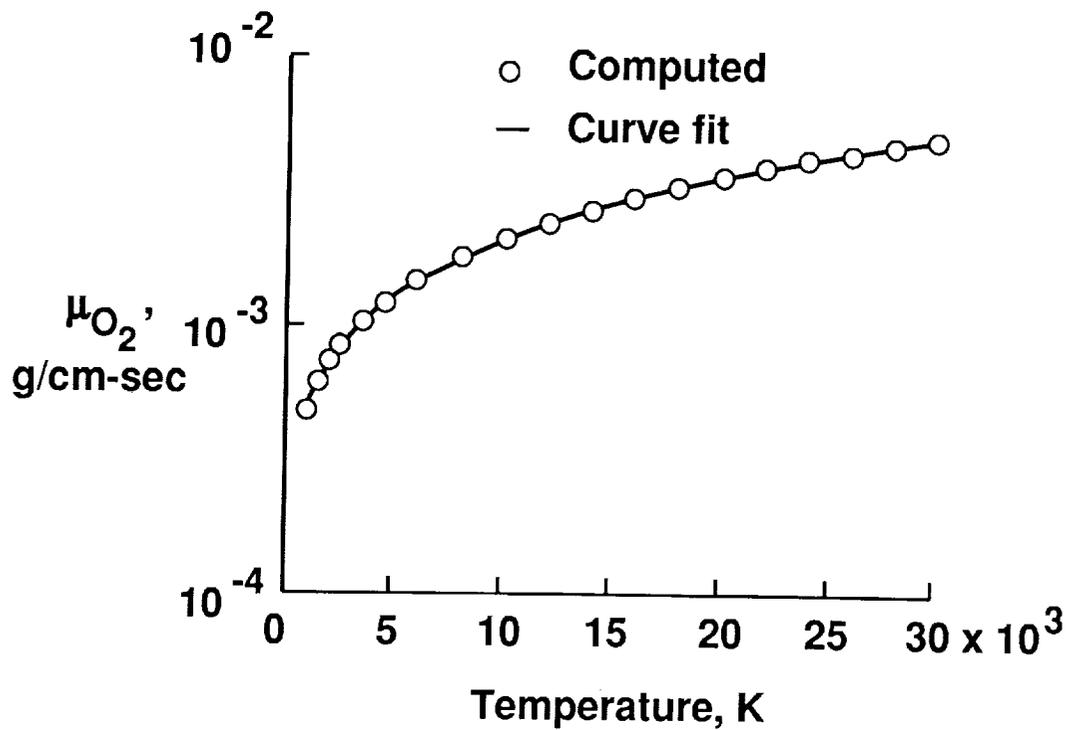
(a) Diatomic oxygen.
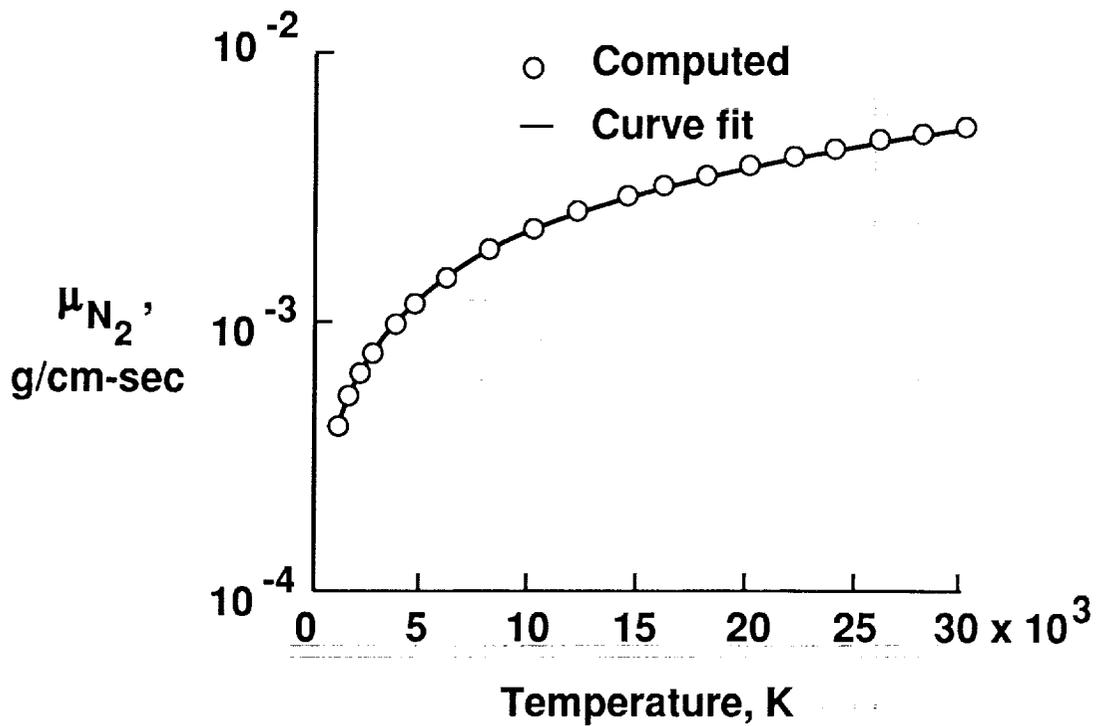
(b) Diatomic nitrogen.

Figure 6. Curve fit to viscosity values obtained by employing collision cross sections based on data of reference 40.
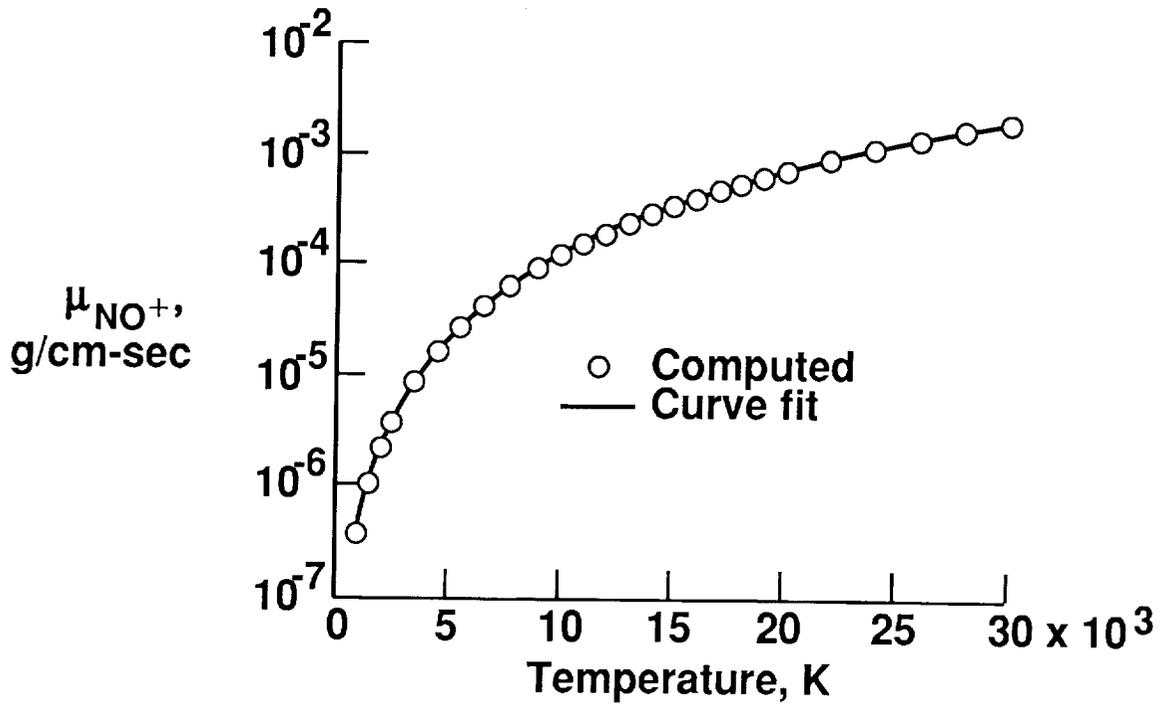
(c) Ionized nitric oxide ($p_e = p_{em}$).
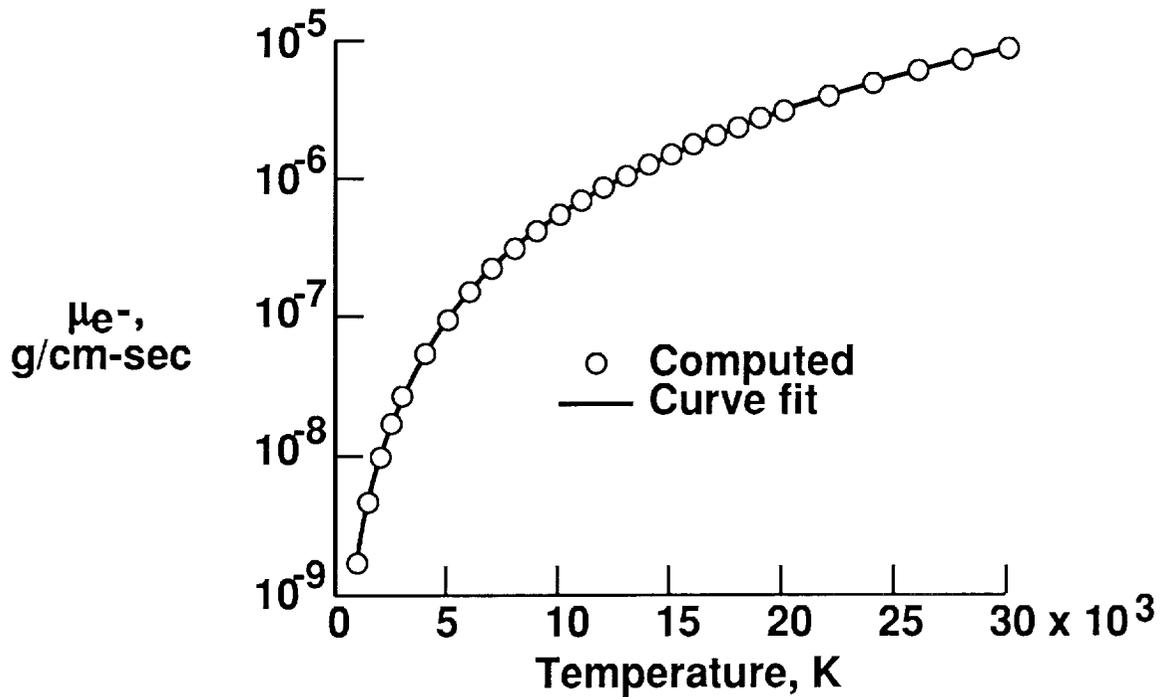
(d) Electron ($p_e = p_{em}$).

Figure 6. Concluded.
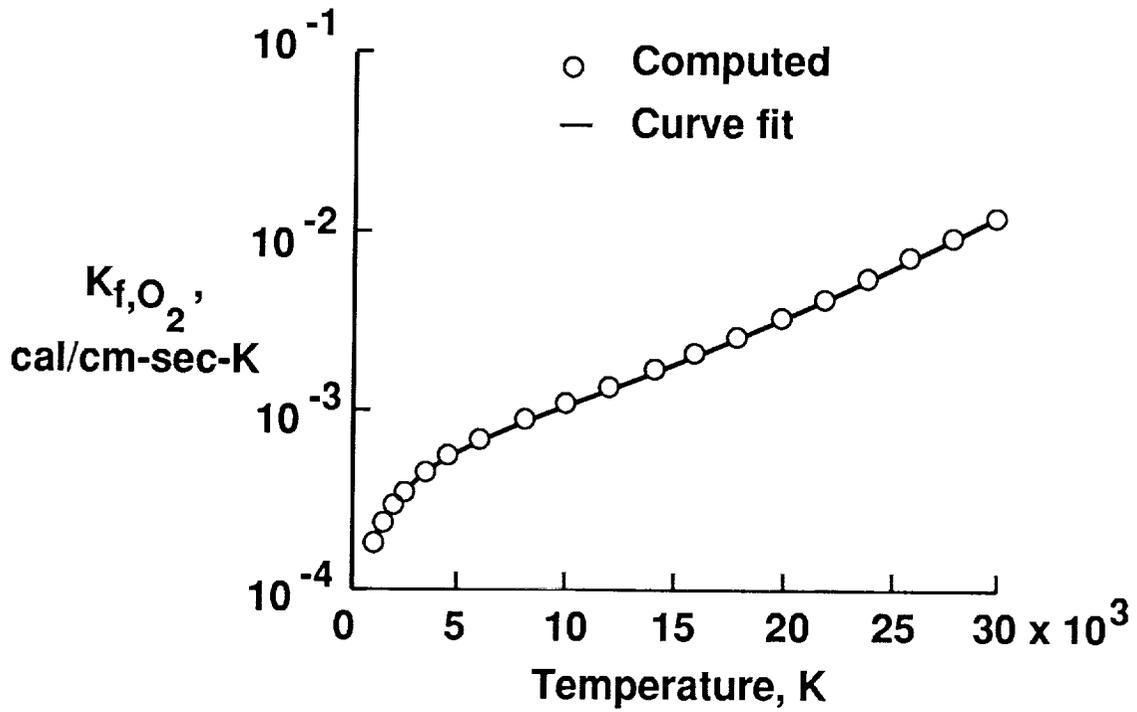
(a) Diatomic oxygen.
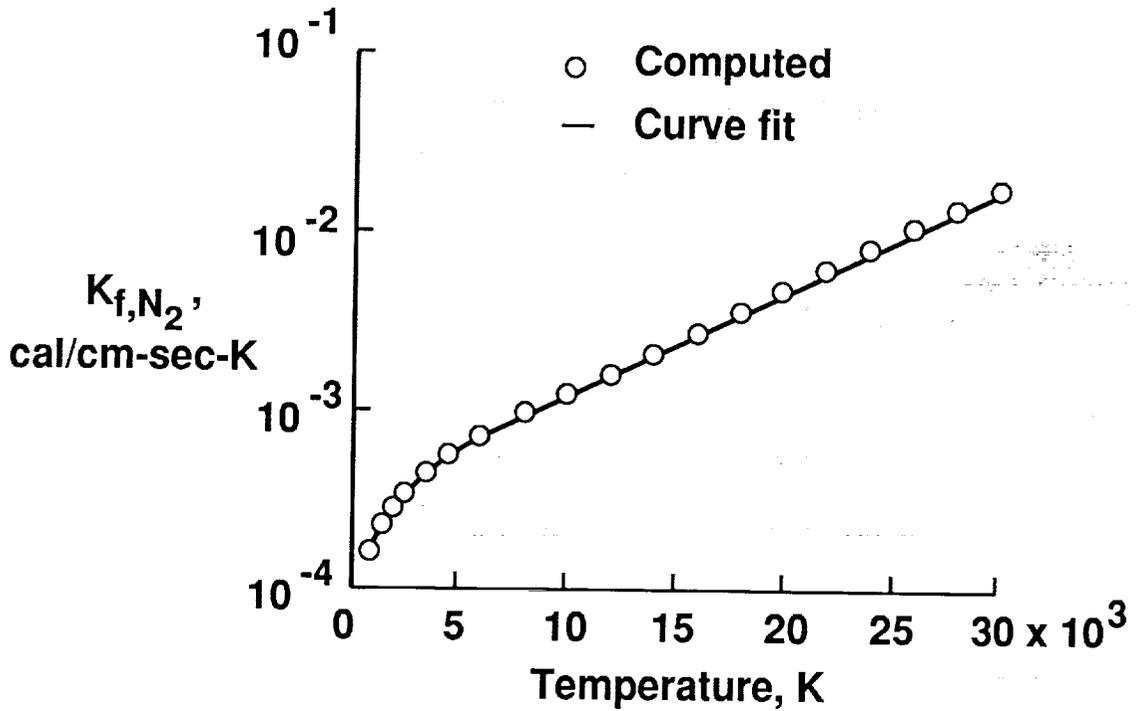
(b) Diatomic nitrogen.

Figure 7. Curve fit to frozen thermal conductivity values obtained by employing collision cross sections based on data of reference 40.
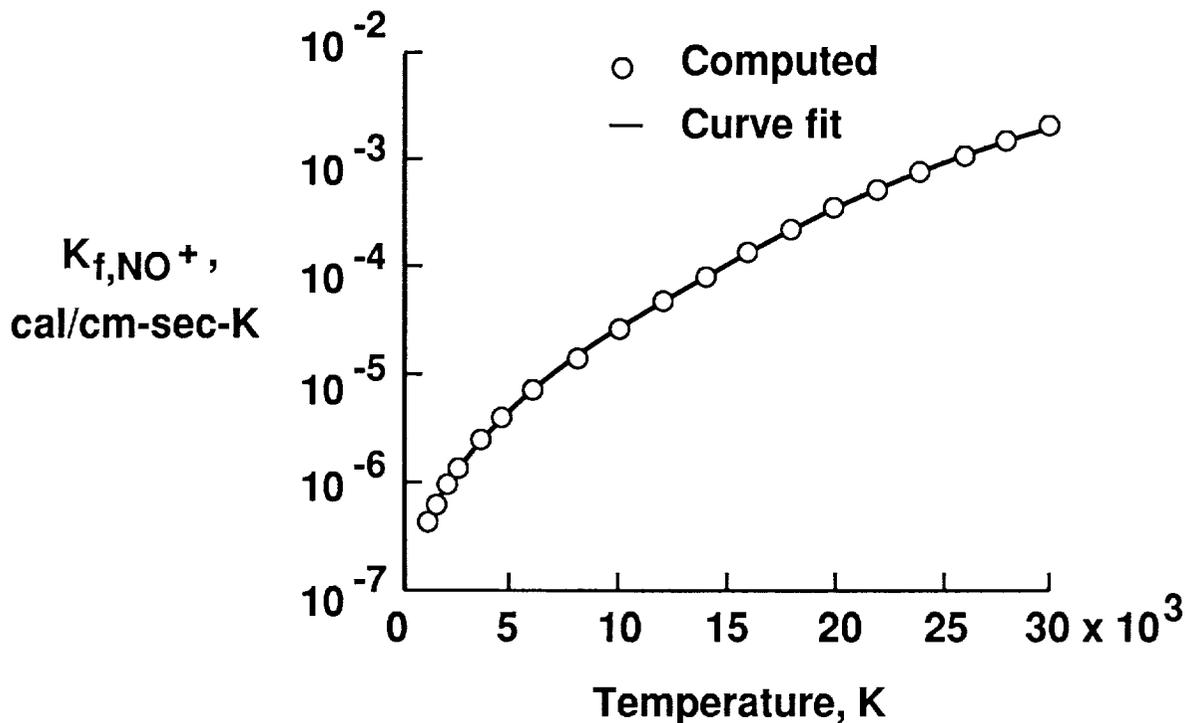
(c) Ionized nitric oxide ($p_e = p_{em}$).
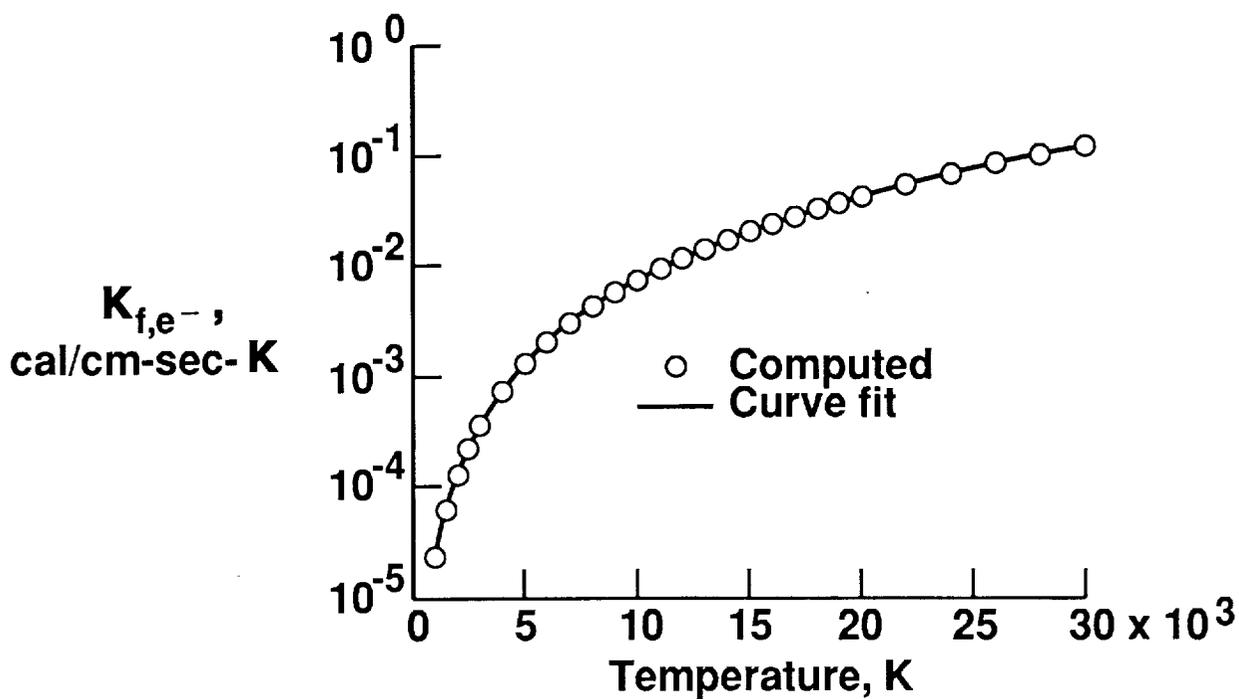
(d) Electron ($p_e = p_{em}$).

Figure 7. Concluded.
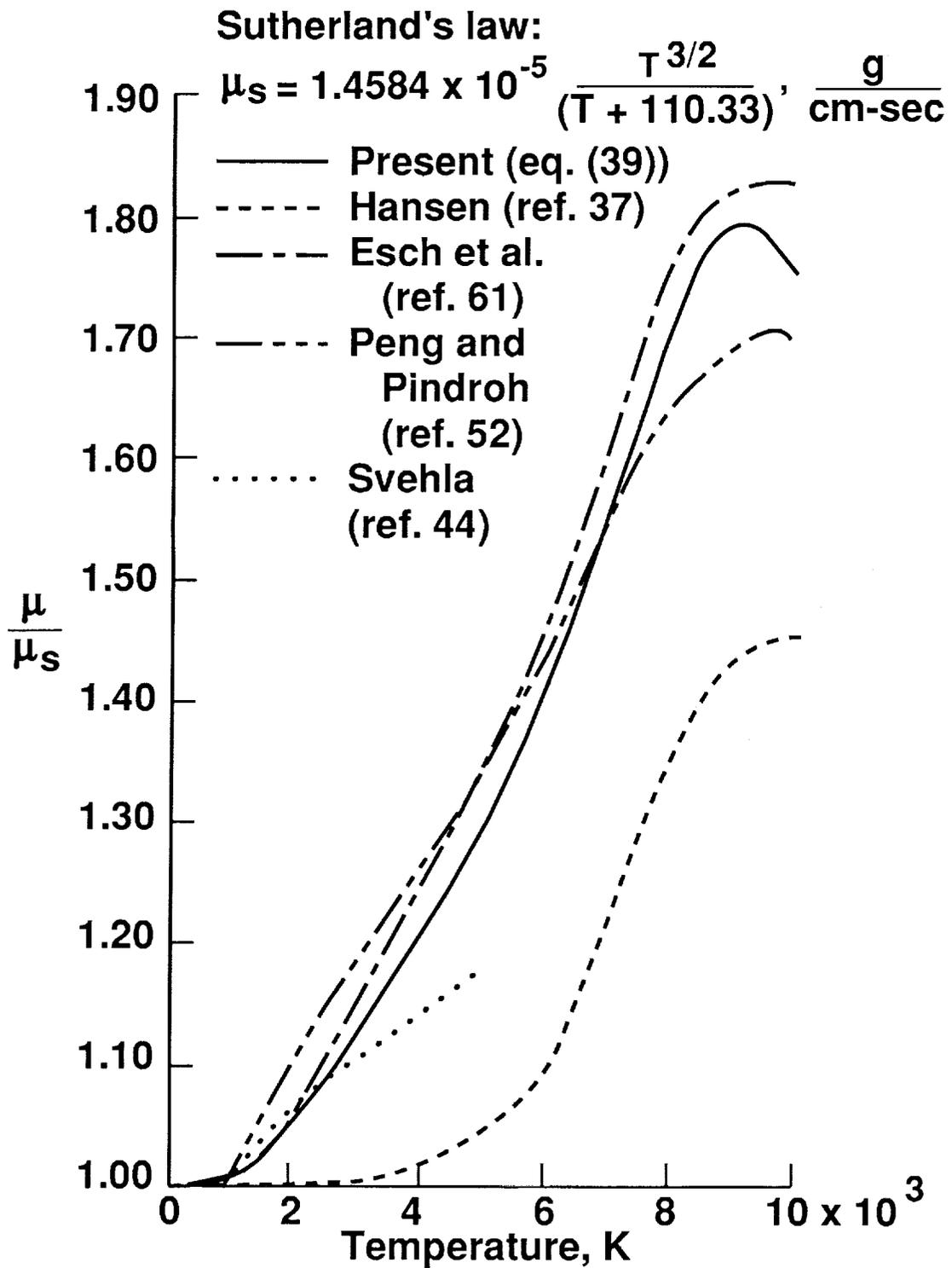
Figure 8. Viscosity of equilibrium air at 1 atm.
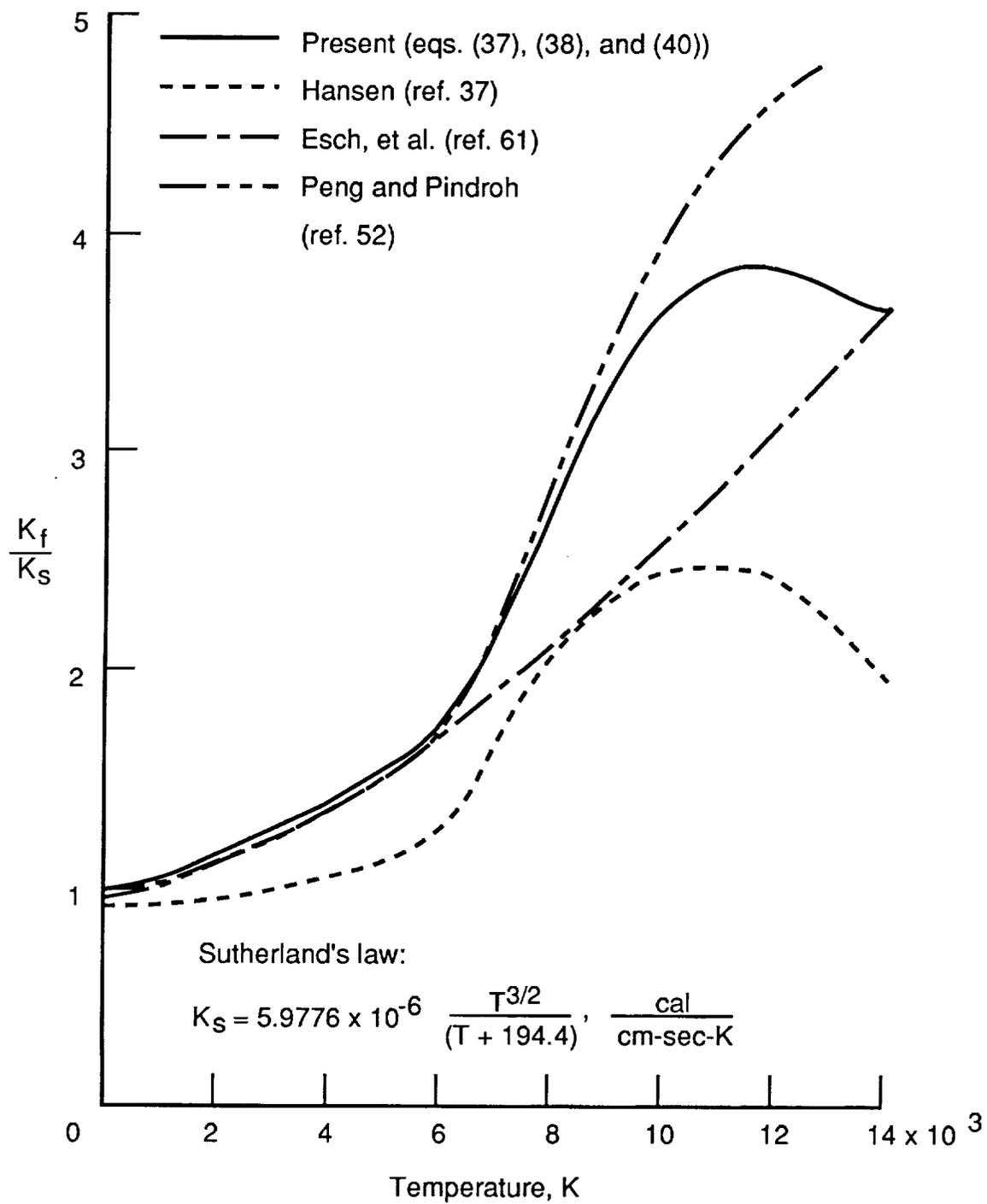
Figure 9. Frozen thermal conductivity of equilibrium air at 1 atm.
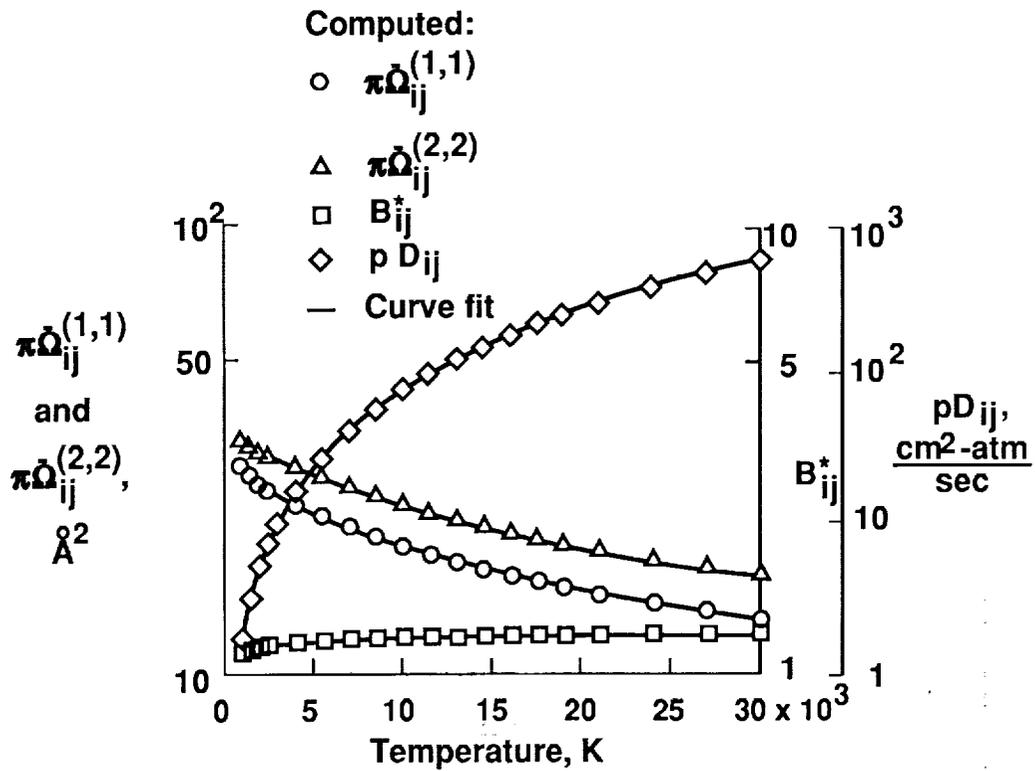
(a) Neutral-neutral molecular interaction: $O_2 \leftrightarrow O_2$.
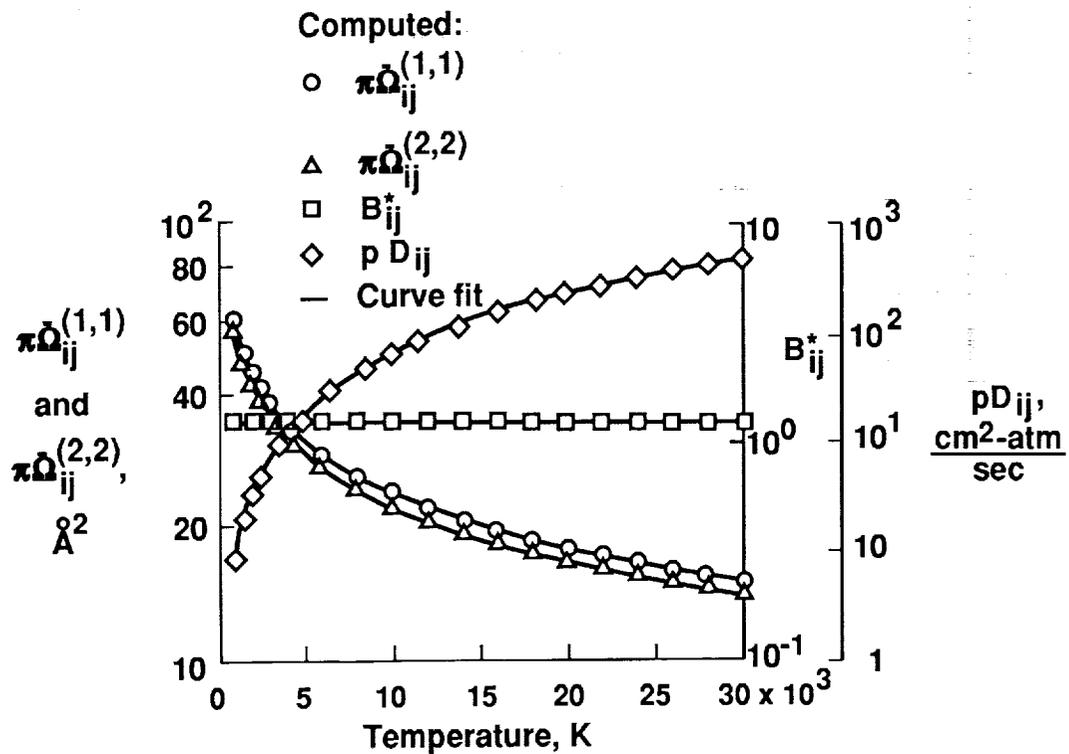
(b) Ion-neutral molecular interaction: $NO^+ \leftrightarrow O_2$.

Figure 10. Curve fit to computed values of collision integrals, collision-integral ratio, and binary diffusion coefficient obtained by using data of reference 40.
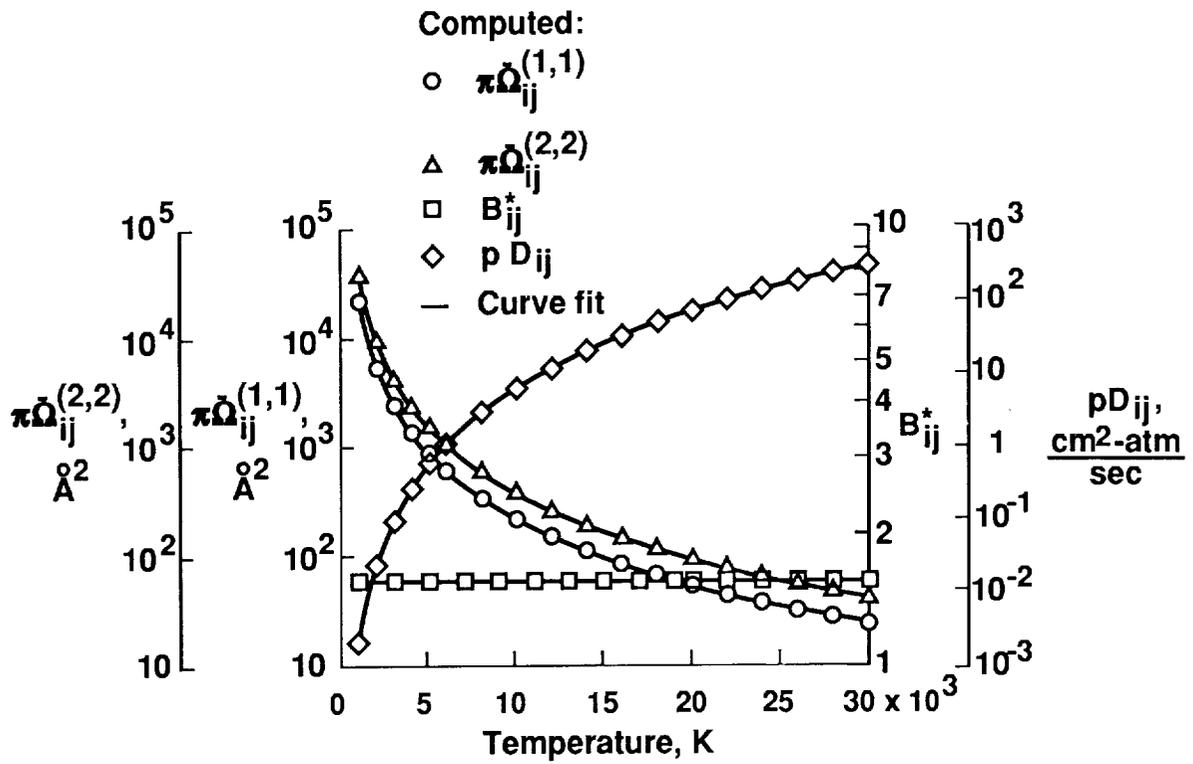
(c) Ion-ion molecular interaction $NO^+ \leftrightarrow NO^+ (p_e = p_{em})$.
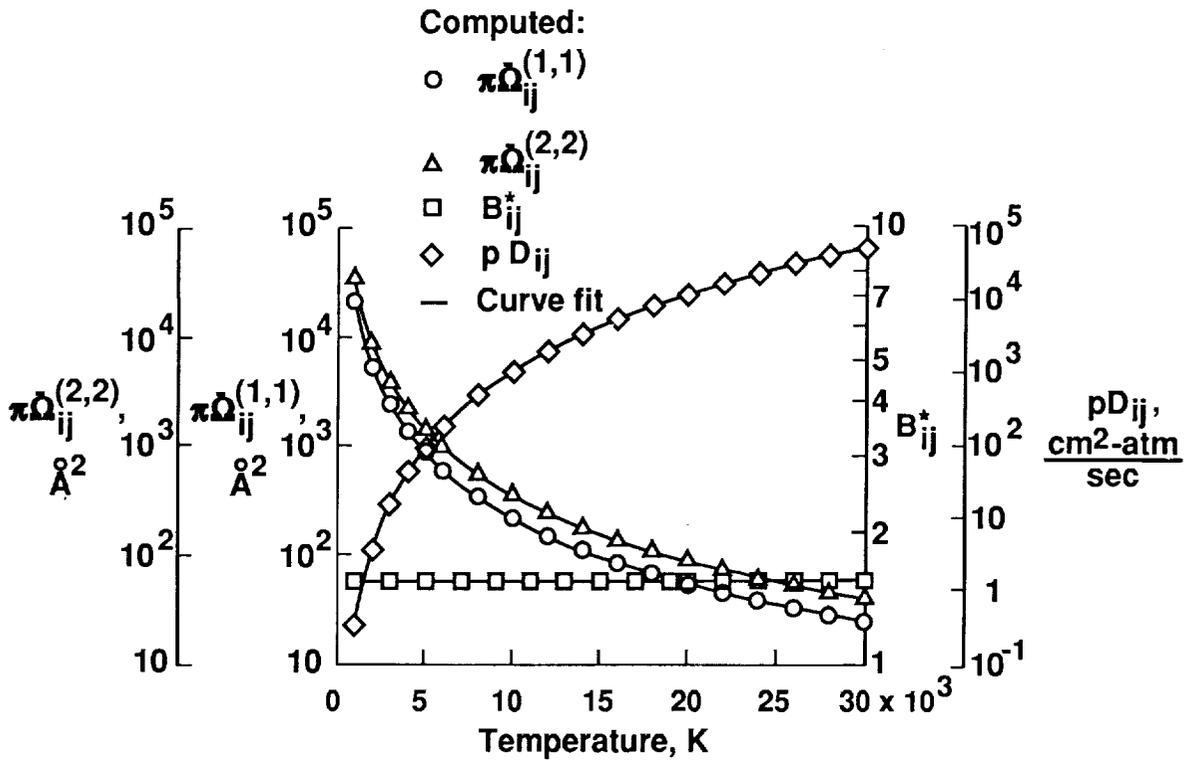
(d) Electron-ionized-molecule interaction: $NO^+ \leftrightarrow e^- (p_e = p_{em})$.

Figure 10. Continued.

85
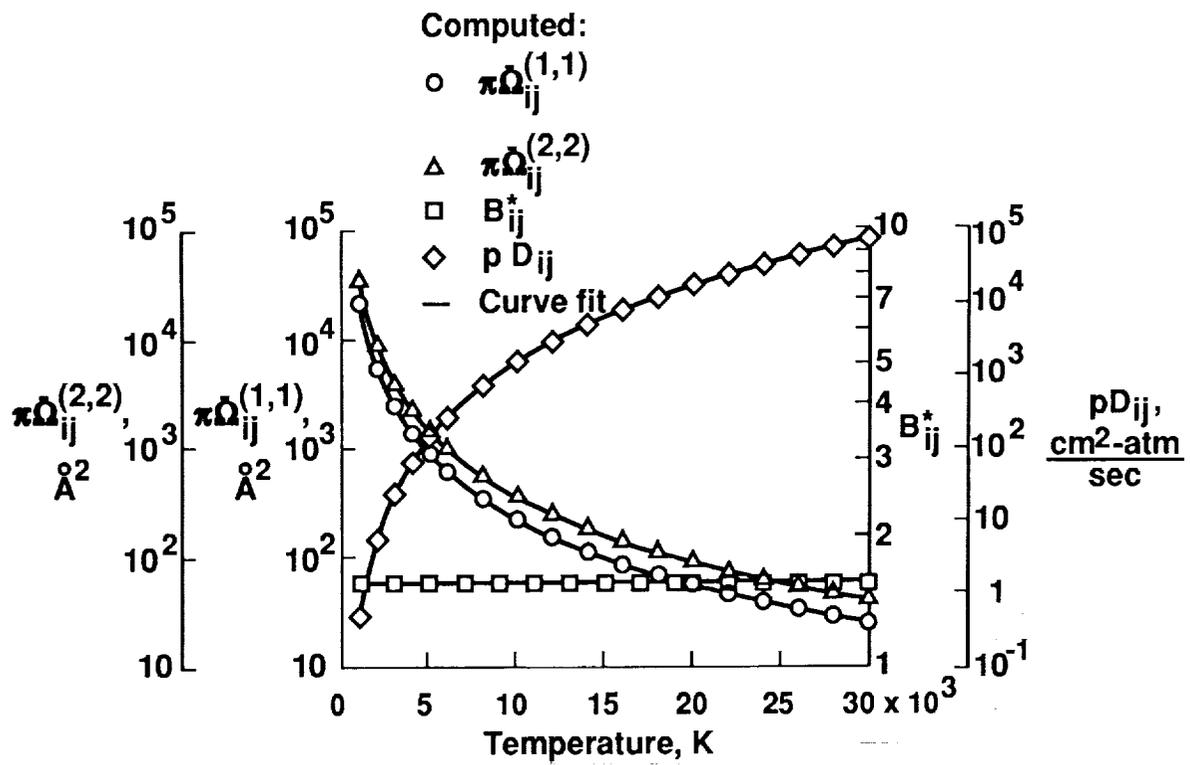
(e) Electron-electron interaction: $e^- \leftrightarrow e^- (p_e = p_{em})$.

Figure 10. Concluded.

Report Documentation Page

1. Report No. NASA RP-1232	2. Government Accession No.	3. Recipient's Catalog No.

4. Title and Subtitle	5. Report Date
A Review of Reaction Rates and Thermodynamic and Transport Properties for an 11-Species Air Model for Chemical and Thermal Nonequilibrium Calculations to 30 000 K	August 1990
	6. Performing Organization Code

7. Author(s)	8. Performing Organization Report No.
Roop N. Gupta, Jerrold M. Yos, Richard A. Thompson, and Kam-Pui Lee	L-16634

9. Performing Organization Name and Address	10. Work Unit No.
NASA Langley Research Center Hampton, VA 23665-5225	506-40-91-02
	11. Contract or Grant No.

12. Sponsoring Agency Name and Address	13. Type of Report and Period Covered
National Aeronautics and Space Administration Washington, DC 20546-0001	Reference Paper
	14. Sponsoring Agency Code

15. Supplementary Notes

This report is an updated version of NASA TM-101528.
Roop N. Gupta: Scientific Research and Technology, Inc., Tabb, Virginia.
Jerrold M. Yos: Textron Defense Systems, Subsidiary of Textron, Inc., Wilmington, Massachusetts.
Richard A. Thompson: Langley Research Center, Hampton, Virginia.
Kam-Pui Lee: Scientific Research and Technology, Inc., Tabb, Virginia.

16. Abstract

Reaction-rate coefficients and thermodynamic and transport properties are reviewed and supplemented for an 11-species air model. This model can be used for analyzing flows in chemical and thermal nonequilibrium up to temperatures of 30 000 K. Such flows will likely occur around currently planned and future hypersonic vehicles. Guidelines for determining the state of the surrounding environment are provided. Curve fits are given for the various species properties for their efficient computation in flow-field codes. Approximate and more exact formulas are provided for computing the properties of partially ionized air mixtures in a high-energy environment. Limitations of the approximate mixing laws are discussed for a mixture of ionized species. An electron number-density correction for the transport properties of the charged species is given. This correction has generally been ignored in the aerospace literature.

17. Key Words (Suggested by Authors(s))	18. Distribution Statement
Chemical and thermal nonequilibrium Species and mixture properties Chemical reacting rates Thermodynamic and transport properties 11-species air model	Unclassified—Unlimited Subject Category 34

19. Security Classif. (of this report)	20. Security Classif. (of this page)	21. No. of Pages	22. Price
Unclassified	Unclassified	89	A05